

# **An Experimental Study of the Influence of Major Damage of Flame Gap Surfaces in Flameproof Apparatus on the Ability of the Gaps to Prevent Gas Explosion Transmission**

*Arild Grov*

A thesis submitted in partial fulfilment of the requirements  
for the degree of Master of Science in the subject of Physics;  
Process Safety Technology



Department of Physics and Technology  
University of Bergen  
Bergen Norway  
June 2010



# Preface

The present work is a master thesis which all graduating students from the master programme process technology, at the University of Bergen (UoB), Department of Physics and Technology, have to submit as a part of their Master Science degree. The experimental work has been performed in the Gas Explosion Laboratory at the UoB.

Many persons have contributed and been of great help and inspiration throughout the completion of this thesis. First I want to thank my supervisors Professor Rolf K. Eckhoff and Associate Professor Bjørn J. Arntzen for help and good discussions throughout the work with this thesis. Thanks to Leif Egil Sandnes, Roald Langøen and Kåre Slettebakken at the Mechanical workshop at the University of Bergen who always were helpful and provided invaluable help for designing and building the different experimental parts used in the experimental work. Chief engineer at the Section of Microelectronic at UoB Werner Olsen have provided help when problems related to electronic in the experimental apparatuses have failed. I would also like to thank the Science Library at UoB for good help and quick delivery of literature from other libraries, even from libraries abroad. Other contributors who have provided service and help: Prototech, for help with roughness measurements and Trainor A.S, for allowing me to follow an "Ex" course free of charge.

I am grateful to Jean-Claude Raemy and Eli Drange Vee who has been proofreading parts of this thesis in their spare time.

A special thanks goes to fellow master student Harald E. Z. Opsvik, who introduced me to the subject of damage of flame gaps of flameproof enclosures, and gave me the opportunity to continue the work he started. He has given invaluable backing and help throughout the work with this thesis. The present work is a continuation of the work he did in his master thesis.

Finally thanks to my parents Per Grov and Torunn V. Grov, for encouragement and financial support in hard times through the whole five year study period. And to Randi Vee who has been of great support and kept up with me even though the hours at UoB in some periods have been longer than the hours at home.

**Bergen, 10. June 2010**

---

**Arild Grov**



Department of Physics and Technology  
University of Bergen  
Norway



# Abstract

Electrical apparatuses for use in the presence of explosive gas atmospheres have to be specially designed to prevent them from igniting the explosive gas. Flameproof design implies that electrical components producing incendiary electrical sparks, e.g. relays and switches, be contained in enclosures that not only withstand the maximum pressure of an internal gas explosion. In addition any holes or slits in the enclosure wall have to be designed in such a way that they will not transmit a gas explosion inside the enclosure to an explosive gas atmosphere outside it.

Designs of a variety of flameproof enclosure joints, including plane flanged joints, are specified in detail in international standards (IEC) requiring that the maximum permissible average roughness of any flame gap surface has to be  $< 6.3 \mu\text{m}$ . The standards also require that any damaged joint surface has to be restored to the original quality prescribed in standards (IEC). However, the standards do not provide any guidance as to what level of damage is considered significant. As a result even minor mechanical or corrosive damage of flame path surfaces gives rise to expensive overhaul and repair of flame proof apparatuses. In fact, this is mandatory in spite of the fact that a generous safety factor is included in the requirements to maximum permissible gap widths. For example, for the plane-flange configuration and explosive gas (propane) used in the present investigation, the maximum permissible width in a practical apparatus is only 0.4 mm, whereas the real limiting value is 0.92 mm.

The purpose of the present investigation has been to obtain some experimental guidance as to what level of damage of flame gap surfaces is required to significantly reduce the flameproofing effect of flame gaps in flameproof electrical apparatuses.

The maximum experimental safe gap (MESG) of an explosive gas mixture is the largest gap width between the two parts of a circular plane joint of 25 mm breadth in a standardized test, which prevents transmission of a gas explosion on the inside of the gap to an outside explosive gas mixtures. Normally the purpose of MESG experiments is to compare MESGs of different gases and vapours, using the same smooth flame gap surface in all experiments. However, in the present investigation MESG has been used as a parameter for judging whether various kinds of significant damage of the gap surface had any noticeable effect on the ability of the flame gap to prevent flame transmission. A significant reduction of MESG compared with that obtained with a standard undamaged surface (standard roughness of  $< 6.3 \mu\text{m}$ ) would mean that the particular type of damage under test had destroyed the gap efficiency significantly. On the other hand a significant increase of MESG compared with that for the undamaged surface would mean the damage had in fact significantly increased the gap efficiency.

In the experiments performed in the present work premixed 4.2 vol. % propane in air was used as the test gas mixture in all the experiments. Two different apparatuses were used, viz. a plane circular-flange apparatus (PCFA) and a plane rectangular-slit apparatus (PRSA). For both apparatuses the optimal distance between the ignition point and the gap entrance for flame transmission was 14 mm. Consequently this distance was used in all the experiments.

The flame gap surfaces were damaged mechanically by milling grooves of various depths and widths, either lengthwise or crosswise in relation to the flow direction of the gas through the

gap. In one test series the gap surface (steel) was exposed to severe outdoor rusting before being exposed to explosion experiments. In another test series the steel surface was sandblasted. In one single test series gap surfaces of Plexiglas was used.

Three main series of experiments were conducted, viz. a first series using the plane circular-flange apparatus (PCFA), a second series of similar experiments using the plane rectangular-slit apparatus (PRSA), and finally a third series using the PRSA only.

The overall conclusion from this investigation is that even very significant mechanical damage of surfaces of flame gaps in flameproof apparatus may not reduce the gap efficiency at all. In fact, in some cases significant improvement of gap performance was observed. This in particular applies to crosswise grooves (e.g. crosswise accidental scratches). It is expected that these findings may urge a discussion of possible revision of national and international standards for both design and maintenance of flameproof enclosures. A paper of the highlights from this thesis will be submitted for presentation at the Eighth International Symposium on Hazards, Prevention, and Mitigation of Industrial Explosions at the Keio University in Japan.

# Table of contents

<b>Preface</b> .....	<b>I</b>
<b>Abstract</b> .....	<b>III</b>
<b>1 Introduction</b> .....	<b>1 -</b>
1.1 Background .....	1 -
1.2 Motivation and aim of present research .....	2 -
<b>2 Review of relevant literature</b> .....	<b>5 -</b>
2.1 The gas explosion problem - A general overview .....	5 -
2.1.1 Explosion protection .....	6 -
2.2 Flameproof enclosures (Ex "d") .....	7 -
2.2.1 History of flameproof equipment .....	7 -
2.2.2 Flameproof enclosure (Ex "d") - A description of the concept .....	8 -
2.2.3 Basic mechanisms for flameproof enclosures (Ex "d") .....	9 -
2.2.4 Damage and requirements for inspection, maintenance and repair of flameproof equipment (Ex "d") given in the IEC standard .....	11 -
2.3 Basic theory of explosion transmission through narrow gaps of relevance to the present work .....	12 -
2.3.1 Quenching distance ( $Q_D$ ) .....	12 -
2.3.2 Maximum Experimental Safe Gap (MESG) .....	12 -
2.3.3 Ignition by a jet of hot combustion products .....	13 -
2.3.4 Cooling of the jet of hot combustion products .....	15 -
2.4 Literature review of previous work in relation to explosion transmission through narrow gaps and flameproof protection .....	20 -
2.4.1 H. Phillips' work on describing the mechanisms of MESG and flameproof protection .....	20 -
2.4.2 Ballal and Lefebvre's work on examining the influence of different flow parameters on flowing combustible mixtures .....	27 -
2.4.3 Classification of flammable gases and vapours by the flameproof safe gap and the incendivity of electrical sparks .....	28 -
2.4.4 Transmission of an explosion through an orifice .....	32 -
2.4.5 A Study of Critical Dimensions of Holes for Transmission of Gas Explosions and development & Testing of a Schlieren System for studying Jets of Hot Combustion Products .....	32 -
2.4.6 Experimental determination of holes and slits in flameproof enclosures, for preventing transmission to external explosive gas clouds. ....	34 -
2.4.7 Investigation of ignition by hot gas jets .....	36 -
2.4.8 Experimental investigation of the influence of mechanical and corrosion damage of gap surfaces on the efficiency of flame gaps in flameproof apparatus .....	39 -

<b>3</b>	<b>Experimental apparatuses and procedures .....</b>	<b>41 -</b>
3.1	Overall experimental approach .....	41 -
3.2	Different flame gap surfaces examined in experiments in the present work .....	41 -
3.3	Crosswise or lengthwise grooves .....	43 -
3.4	The Plane Circular Flange Apparatus (PCFA).....	46 -
3.4.1	Specifications of the Plane Circular Flange Apparatus.....	46 -
3.4.2	Adjustment of ignition position in the Plane Circular Flange Apparatus ....	47 -
3.4.3	Flow from primary chamber in the Plane Circular Flange Apparatus .....	48 -
3.4.4	Flame gap surfaces tested in the Plane Circular Flange Apparatus .....	49 -
3.4.5	Flame gap surfaces with grooves tested in the Plane Circular Flange Apparatus .....	53 -
3.4.6	Slightly modified Plane circular Flange Apparatus (MPCFA) .....	56 -
3.4.7	Flame gap surfaces tested in the Modified Plane Circular Flange Apparatus .....	57 -
3.5	The Plane Rectangular Slit Apparatus (PRSA).....	60 -
3.5.1	Specifications of the Plane Rectangular Slit Apparatus .....	62 -
3.5.2	Adjustment of ignition position in the Plane Rectangular Slit Apparatus ...	63 -
3.5.3	Flow from primary chamber in the Plane Rectangular Slit Apparatus .....	63 -
3.5.4	Flame gap surfaces tested in the Plane Rectangular Slit Apparatus.....	64 -
3.6	Gas mixture preparation, analysis and filling.....	75 -
3.7	Measurement and data logging system .....	76 -
3.7.1	Data acquisition system.....	76 -
3.7.2	Control system.....	77 -
3.7.3	Pressure measurements .....	77 -
3.8	Sources of error .....	78 -
3.8.1	Data Acquisition System .....	78 -
3.8.2	Gas concentration measurements .....	78 -
3.8.3	Atmospheric pressure and temperature .....	78 -
3.8.4	Air humidity .....	79 -
3.8.5	Pressure .....	79 -
3.8.6	Condensed water .....	79 -
3.8.7	Experiments.....	79 -
<b>4</b>	<b>Experimental results and discussion .....</b>	<b>81 -</b>
4.1	Results and discussion from experiments for finding the ignition point most favourable for re-ignition in the secondary chamber in the PRSA .....	82 -
4.2	Results and discussion from experiments with similar gap surface configurations in the PCFA and PRSA .....	84 -
4.2.1	Results and discussion from experiments with reference flame gap surface, undamaged gap surface .....	84 -
4.2.2	Results and discussion from sandblasted flame gap surfaces.....	88 -
4.2.3	Results and discussion from experiments on rusted flame gap surfaces.....	90 -
4.2.4	Results and discussion from experiments on Plexiglas flame gap surfaces.-	92 -



4.2.5	Results and discussion from experiments on gap surfaces with crosswise grooves on the flame gap surfaces .....	- 94 -
4.2.6	Results and discussion from experiments on slits with lengthwise grooves on the flame gap surfaces .....	- 98 -
4.3	Results and discussion from experiments with single lengthwise grooves performed in the PRSA .....	- 100 -
<b>5</b>	<b>Conclusions .....</b>	<b>- 103 -</b>
<b>6</b>	<b>Recommendations for further work .....</b>	<b>- 105 -</b>
	<b>References .....</b>	<b>- 107 -</b>
	<b>APPENDIX .....</b>	<b>i</b>
	<b>Appendix A – Experimental apparatuses and procedures .....</b>	<b>ii</b>
A.1	Equipment list .....	ii
A.2	Experimental Procedures .....	ii
A 2.1	Adjusting Procedure - gap opening in the Plane Circular Flange Apparatus .....	ii
A 2.2	Experimental procedure - The Plane Circular Flange Apparatus (PCFA) .....	iv
A 2.3	Checklist .....	vii
A 2.4	Adjusting Procedure - gap opening in the PRSA .....	viii
A 2.5	Experimental procedure – The Plane Rectangular Slit Apparatus (PRSA) .....	x
A 2.6	Calibration procedure - Gas Analyzer .....	xii
A 2.7	Data Acquisition System .....	xiv
	<b>Appendix B – Spark Generator .....</b>	<b>xvi</b>
	<b>Appendix C – Measurement data from experiments .....</b>	<b>xix</b>
	<b>Appendix D – Surface roughness measurements .....</b>	<b>xxxi</b>
	<b>Scope of inspection .....</b>	<b>xxxiii</b>
	<b>General theory .....</b>	<b>xxxiv</b>
	<b>Measurement equipment .....</b>	<b>xxxv</b>
	<b>Summary of results .....</b>	<b>xxxvi</b>
	<b>Appendix E – Certificates / Specifications .....</b>	<b>xxxix</b>
E.1	Calibration gas .....	xl
E.2	Test gas .....	xli
E.3	Pressure transducers .....	xlii
E.4	Pressure transducers .....	xliii
E.5	Charge amplifier .....	xliv
	<b>References .....</b>	<b>xlvi</b>



# 1 Introduction

## 1.1 Background

A gas explosion constitutes a risk to all industries where an explosive atmosphere can be formed. An explosive atmosphere can be the result of mixing of flammable gases, vapours, mists or dusts with air. Examples of industries where explosion hazards have to be taken into special consideration include:

- Gas and oil industries, offshore and onshore, including transportation of gas.
- Petrochemical, chemical, and metallurgical process industries.
- Mechanical processing.
- Industries which produces and handles explosives, pyrotechnics, and propellants.
- Nuclear industries.

Understanding of the explosion phenomena are necessary not only to prevent loss of life, but also to keep the production going. There are numerous examples of companies that had to declare bankruptcy due to damage on plant and operation equipment following explosions.

In Norway, there is a lot of activity related to production and handling of gas and oil. This is an industry where the risks of explosions are high, and there have been several serious accidents throughout history, where the Piper Alpha accident was one of the worst. Piper Alpha was a North Sea oil production platform. On July 6, 1988 an explosion and resulting fire completely destroyed the platform, killing 167 persons.

Studies of the mechanisms involved in gas explosions have provided the industries with knowledge that enables them to reduce the risk of such accidents. Increased focus on training of personnel and development of standards and guidelines for equipment has also had a great effect in this direction. But despite all the measures being taken to increase the safety, there is always a risk of gas leakage and consecutive explosions in the industries that handles oil and flammable gases, and serious accidents still happen. The latest large accident in the oil industry happened on April 21, 2010 on Deepwater Horizon, which was a semi-submersible mobile offshore drilling platform, drilling in the Gulf of Mexico. The accident is still being investigated, but it is believed that a blowout from the well filled the platform with flammable methane gas, which then was ignited. The platform sank killing 11 persons, and there is a large ongoing oil spill that can have serious environmental consequences.

Figure 1-1 shows leak frequency of hydrocarbon gases on Norwegian oil and gas installations from 1996 to 2009. The graph shows that there are over 10 leakages each year. Note that there were over 40 leakages in 2000 and 2002.

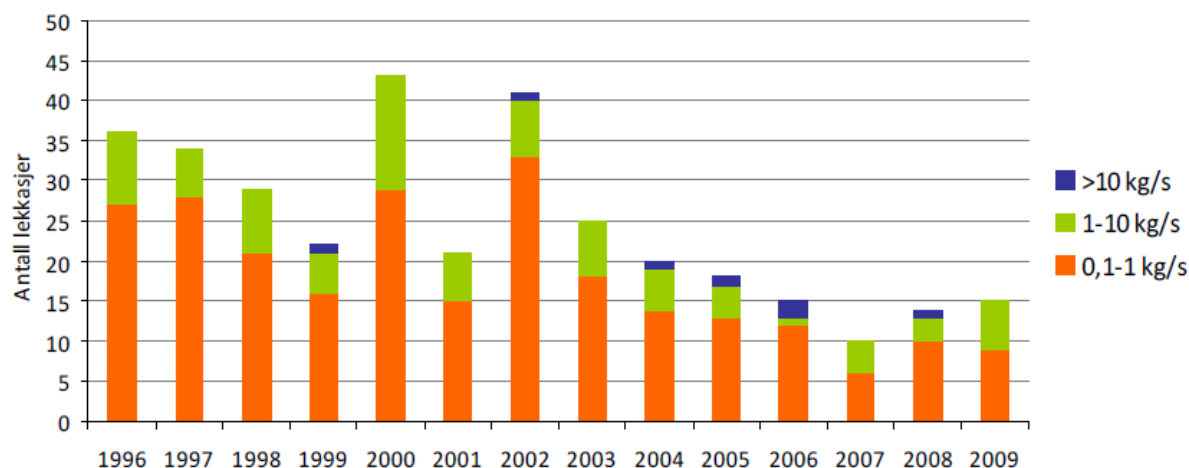


**Figure 1-1** Hydrocarbon leaks on Norwegian installations above 0.1 Kg/s, in the period 1996 to 2009. From (Petroleum Safety Authority Norway 2009)

Due the continued danger of leaks, it is important to continue the work to increase the understanding of the mechanisms related to explosions, and to develop equipment that will further reduce the risk of accidental gas explosions. If a leakage occurs, it is of great importance to have control over possible ignition sources, e.g. electrical equipment. The use of electrical equipment in potentially explosive environments demands special protection in order to avoid accidental ignition of possible explosive surrounding atmospheres. Equipment which uses different methods and protection principles is commercially available; the safety requirements for the equipment are regulated by international standards. There are different requirements according to which hazard zone the equipment is to be used in.

One type of protection method used is flameproof enclosures (Ex "d"). This design implies that potential electrical ignition sources such as switches, relays etc. are kept in strong enclosures that can withstand a possible gas explosion inside the enclosure, at the same time as any holes or slits in the enclosure wall are designed in such a way that they will not transmit a gas explosion inside the enclosure to an explosive gas atmosphere outside it.

## 1.2 Motivation and aim of present research

The concept of flameproof enclosure (Ex "d") is one of the oldest protection methods for electrical apparatuses; the concept is described in Section 2.2.2. Requirements for design and maintenance for Ex "d" equipment are given in (IEC 2007a), according to which joint surfaces shall have an average surface roughness of  $< 6.3 \mu m$ .

Ex "d" equipment is widely used in the offshore industry where the surrounding environment is highly corrosive (due to the presence and probability for contact with seawater); rust formation in the flame gap surfaces is therefore a potential damage that can occur on this type of equipment. (IEC 2007b) requires that any damaged joint surface is restored to the original quality described in (IEC 2007a). Damage on the flame joints can also occur by poor handling under inspection of Ex "d" equipment where grooves from tools used for dismounting and mounting the enclosure can cause damage of the flame gap. The standard does not provide guidance as to what degree of damage is considered to be significant enough to affect the efficiency of the gap in a negative way and to make Ex "d" equipment to be considered as

defect. The only parameter is that the joint surfaces shall have an average surface roughness of  $< 6.3 \mu m$ . As a result of this, even minor mechanical or corrosive damage of flame gap surfaces has often prompted expensive overhaul and repair of flameproof apparatuses.

The aim of the experimental research in the present work has been to study the influence of significant damage of gap surfaces on the efficacy of flame gaps in Ex "d" equipment. This research is a continuation of the work done by (Opsvik 2010), who built an experimental apparatus that made it possible to inflict various damage of flame gap surfaces. Opsvik also tested the effect of sandblasting of the surface, to create a roughness well above the permitted value of  $6.3 \mu m$ . Furthermore, a rusted surface was tested to see the effect this had upon the efficiency of the gap. Quite surprisingly, the rusted surface showed a better ability to prevent explosion transmission than an undamaged gap surface, some of the experiments were done in corporation with Grov, and these results are also given in (Opsvik et.al 2010)

The experimental work described in this thesis consists of a large amount of experiments; the aim was to provide some answers to the following questions:

- How significant must the damage of a flame gap be before it constitutes a danger for reducing the efficiency of the flame gap in Ex "d" equipment?
- Is there a limiting value of width and depth of grooves on gap surfaces before they affect the MESH value and efficiency of the gap negatively? If such a limit is found, can it be used to distinguish between damage that is critical for the efficiency of a flame gap in Ex "d" equipment, and damage that are not? Should this be included in the existing standards?
- Is there any difference in the influence on the flame gap efficiency depending on the different direction of a groove on the gap surface?
- How do gap surfaces with considerably rougher surfaces influence the efficiency of the flame gap? Do the experimental results found in this thesis support the requirement in the standard for only allowing a maximum average surface roughness of  $6.3 \mu m$ ?
- Could frequent inspections cause more harm than good when considering the possibility for damaging the equipment under inspection, if the experimental results show that the damage has to be of considerably degree before it influences the efficiency of the flame gap?
- How do flame gap with different materials with different thermal properties influence the efficiency of the flame gap?

Another objective was to further investigating the surprising results found by (Opsvik 2010) that showed that a rusted surface had better ability to prevent explosion transmission than an undamaged gap surface.

All the experimental results shall be thoroughly explained, and hopefully the work with testing different damages of flame gap surfaces will increase the understanding of the mechanisms involved in gas explosion transmission, and be used to further improve the design of flameproof equipment.



## 2 Review of relevant literature

### 2.1 The gas explosion problem - A general overview

There are a number of different definitions to the term explosion. Some definitions emphasize on the effect on the surroundings (sound, pressure wave and damage on surroundings), while others describe the physical phenomenon that occurs. Definition from (Eckhoff 2005): “*An explosion is an exothermal chemical process which, when occurring at constant volume, gives rise to a sudden and significant pressure rise*”.

The same mechanisms as in an ordinary fire will be at play in an explosion, and one can say that an explosion is a rapid fire out of control. The Fire Triangle (see figure 2-1) can also be used to explain the main events leading to an explosion; it could also be extended to take into account that there is a given air/oxygen to fuel ratio (explosion limits) needed to initiate an explosion. It exist an upper and lower explosion limit for all gases, above or below these limits it is either too much fuel gas or insufficient air/oxygen, and the mixture is not explosive and can not be ignited. Different gases have different ignition temperatures, and ignition energies needed to ignite the gas.

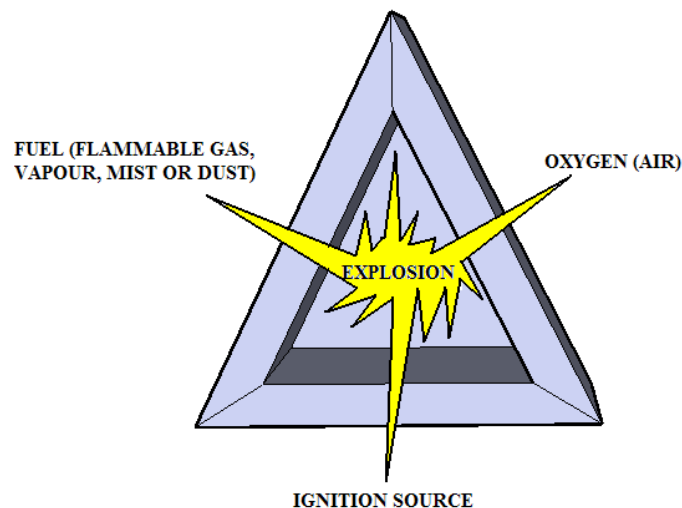


**Figure 2-1** *The explosion triangle.*

The definition above describes an explosion as an exothermal process. This is a chemical reaction that releases/produces energy in the form of heat. For instance can the combustion process of propane burning in oxygen be described by:



Gas explosions can occur inside process equipment or outside the equipment as a result of a leakage. The consequences from an explosion are determined according to where the explosion occurs. From the definition above, the combustion reaction in an explosion will increase the pressure and if an explosion occurs inside process equipment, the increased

pressure can destroy the equipment (if the equipment is not dimensioned for the resulting explosion pressure).

### 2.1.1 Explosion protection

The efforts to minimize the risk of accidental explosions in the industry are of high priority, and much work and money are spent on preventing and mitigating accidental gas and vapour cloud explosions.

Explosion protection can be divided into three parts, shown in figure 2-2.

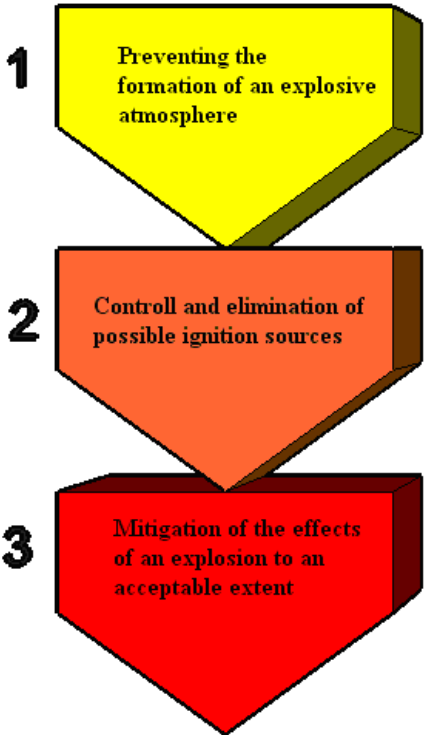


**Figure 2-2** *Basic principle of explosion protection*

In industries where an explosive atmosphere can be created, protection methods and systems need to be designed to take into account all the three steps shown in figure 2-2. It is for example not enough to only have systems that prevent formation of an explosive atmosphere. This is because one can never be entirely sure that an explosive atmosphere won't build up, for example by failure in one of the protection systems. The experimental work presented in the present thesis examines damage of Ex "d" equipment, which is a protection method for electrical equipment, and hence a way to control and eliminate possible ignition sources, which is step two in figure 2-2. In the present work there is not given any information on other types of explosion protection, because this is not of relevance to the present work, for more information about explosion protection it can be referred to (Groh 2004).



## 2.2 Flameproof enclosures (Ex "d")

The concept of flameproof enclosure (Ex "d") is one of the oldest protection methods for electrical apparatuses; in this chapter the history of the development and the mechanisms which influences on the way this protection method works is given. The requirements for inspection, maintenance and repair from the standard are also discussed.

### 2.2.1 History of flameproof equipment

It was in the developing mining industry, during the 17<sup>th</sup> century, that one first became aware of explosive atmospheres. The discovery was particularly pertinent in coal mines, where the process of mining coal produce methane gas, and *"in fact gassy coal could take as long as 1000 hours in a well ventilated location to become completely free of methane"* (Toney, Griffith et al. 2000). The miners open flame candles used for lighting would occasionally ignite the methane gas. When the methane gas was ignited, the pressure wave whirled up coal dust, which then was ignited and produced a more violent secondary explosion. For a long time, the reason for the explosions remained a mystery for the workers. This led to new routines to eliminate the hazards for the workers, but it lead to new routines to eliminate the hazards for the workers where a "volunteer" from the mine crew, wrapped in wet blankets, crawled through the mine with a flaming torch. When the workers understood the danger involved in this they refused to do the job. The job was then offered to prisoners, but soon they also refused to risk their lives to secure the mine. It was realized that research was needed in order to be able to making mining safe for the workers and thus continue expanding mining activities.

In 1815, Sir Humphrey Davy invented the Davy lamp. This lamp was a kerosene lantern with fine gauze that separated the open flame from the surroundings. The mesh of the fine gauze emitted light but it was fine enough to not support flame propagation (through the gauze). This would later lead to the concept of Maximum Experimental Safe Gap (MESG) (see section 2.31).

When electrical equipment, like electrical motors used to drive elevators, ventilators and mining equipment, where introduced in the mines, the electrical sparking in the motors would lead to explosions. To increase safety, a motor that was totally enclosed was developed (see figure 2-3). This was the start of flameproof enclosures for electrical equipment.

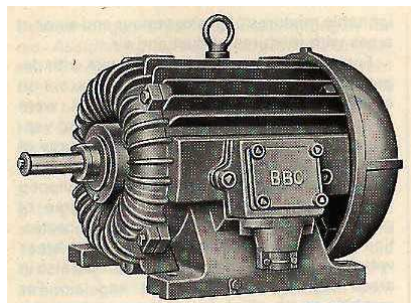


**Figure 2-3** An illustration of an early version of an enclosed electrical motor

During the 1940s and 1950s, the use of electrical instruments grew rapidly, and as the quantity of electrical instruments installed increased, so did the safety problem and the need for standardized equipment and guidelines for use in hazardous locations.

The first standard for electrical equipment in hazardous locations was published in 1935 by the German Verband der Elektrotechnik (VDE), which is the German association for electrical, electronic and information technologies(VDE 1935).

The requirements for Ex equipment are based upon international standards from IEC (International Electrotechnical Commission). In 1957, several countries in Europe founded the European Union (EU). This led to the development of technical standards, which all the countries had to follow in order to be allowed to sell their equipment within the EU. As a result, the European Organization for Electrotechnical Standardization (CENELEC) was created, and standards for electrical equipment for use in explosive atmospheres were established. The international rules from IEC is further adapted for the European marked by CENELEC. In Norway, NEK (Norwegian electro technical comity) administers the standards from CENELEC and to a large extent uses the CENELEC standards as Norwegian Electro technical norms.

### **2.2.2 Flameproof enclosure (Ex "d") - A description of the concept**

The concept of flameproof enclosure (Ex "d") is one of the oldest protection methods for electrical apparatuses. Detailed descriptions for design and maintenance of Ex "d" equipment are given in (IEC 2007a), according to which joint surfaces shall have an average surface roughness of  $< 6.3 \mu m$ . This design implies that potential electrical ignition sources such as switches, relays etc. are kept in strong enclosures that can withstand a possible gas explosion, at the same time as any holes or slits in the enclosure wall are designed in such a way that they will not transmit a gas explosion inside the enclosure to an explosive gas atmosphere outside it. Requirements for the maximum surface temperature for the enclosure are also given; this temperature should not exceed the minimum ignition temperature for the gas that may be present and develop in and around the enclosure. The test gas used in the present experimental work is Propane, which has a minimum ignition temperature of  $470^{\circ}C$ .

It would be desirable to construct all flameproof equipment to meet the most stringent requirements with regard to ignition temperature, explosive force and ignition capability of the gases, but this would not be economical. Due to this, the apparatuses are divided into explosion groups and temperature classes based on the environment where the equipment is to be used. Equipment with Ex "d" protection is approved for Zone 1 and 2. Examples for the application of equipment protection Ex "d":

- Motors.
- Switchgear.
- Transformers.
- Heating equipment.
- Light fittings etc.

Type of joint		Minimum width of joint L mm	Maximum gap mm													
			For a volume cm <sup>3</sup> V ≤ 100			For a volume cm <sup>3</sup> 100 < V ≤ 500			For a volume cm <sup>3</sup> 500 < V ≤ 2 000			For a volume cm <sup>3</sup> V > 2 000				
			I	IIA	IIB	I	IIA	IIB	I	IIA	IIB	I	IIA	IIB		
Flanged, cylindrical or spigot joints		6	0,30	0,30	0,20	–	–	–	–	–	–	–	–	–	–	
		9,5	0,35	0,30	0,20	0,35	0,30	0,20	0,08	0,08	0,08	–	–	–		
		12,5	0,40	0,30	0,20	0,40	0,30	0,20	0,40	0,30	0,20	0,40	0,20	0,15		
		25	0,50	0,40	0,20	0,50	0,40	0,20	0,50	0,40	0,20	0,50	0,40	0,20		
Cylindrical joints for shaft glands of rotating electrical machines with:		Sleeve bearings	6	0,30	0,30	0,20	–	–	–	–	–	–	–	–	–	
			9,5	0,35	0,30	0,20	0,35	0,30	0,20	–	–	–	–	–	–	
			12,5	0,40	0,35	0,25	0,40	0,30	0,20	0,40	0,30	0,20	0,40	0,20	–	
			25	0,50	0,40	0,30	0,50	0,40	0,25	0,50	0,40	0,25	0,50	0,40	0,20	
			40	0,60	0,50	0,40	0,60	0,50	0,30	0,60	0,50	0,30	0,60	0,50	0,25	
		Rolling-element bearings	6	0,45	0,45	0,30	–	–	–	–	–	–	–	–	–	–
			9,5	0,50	0,45	0,35	0,50	0,40	0,25	–	–	–	–	–	–	–
			12,5	0,60	0,50	0,40	0,60	0,45	0,30	0,60	0,45	0,30	0,60	0,30	0,20	
			25	0,75	0,60	0,45	0,75	0,60	0,40	0,75	0,60	0,40	0,75	0,60	0,30	
			40	0,80	0,75	0,60	0,80	0,75	0,45	0,80	0,75	0,45	0,80	0,75	0,40	

NOTE Constructional values rounded according to ISO 31-0 should be taken when determining the maximum gap.

**Figure 2-4** Minimum width of joint and maximum gap opening for enclosures of groups I, IIA and IIB. From (IEC 2007a)

Flameproof enclosures are, as mentioned above, not necessarily vapour-tight. In many cases, it is desirable to have gaps and openings in the flameproof enclosures to be able to inspect and perform routine maintenance of the components inside the enclosure. In motors with revolving shafts, there has to be a distance for the shaft to be able to move. The openings in Ex "d" equipment are referred to as flame gaps. In flameproof enclosures, gas or vapour can enter the enclosures and be ignited, but the resulting inner explosion must not be able to ignite the surrounding atmosphere. There are strictly defined requirements for the maximum allowed opening, and for the minimum width or length of these flame gaps, as shown in figure 2-4. The allowed values are based on MESH values (see Section 2.3.1) for the actual gas, provided with a safety factor.

### 2.2.3 Basic mechanisms for flameproof enclosures (Ex "d")

When an explosion is initiated within the internal enclosure, the flame front and the pressure wave propagates towards the enclosure walls and reaches the gap opening. These gap openings are < MESH (see Section 2.3.1), the flame front gets "quenched" (see Section 2.3.1) hence no flame is transmitted through the gap. The pressure wave "pushes" hot combustion products through the gap opening and into the unburned explosive external atmosphere without igniting it (illustrated in figure 2-5).

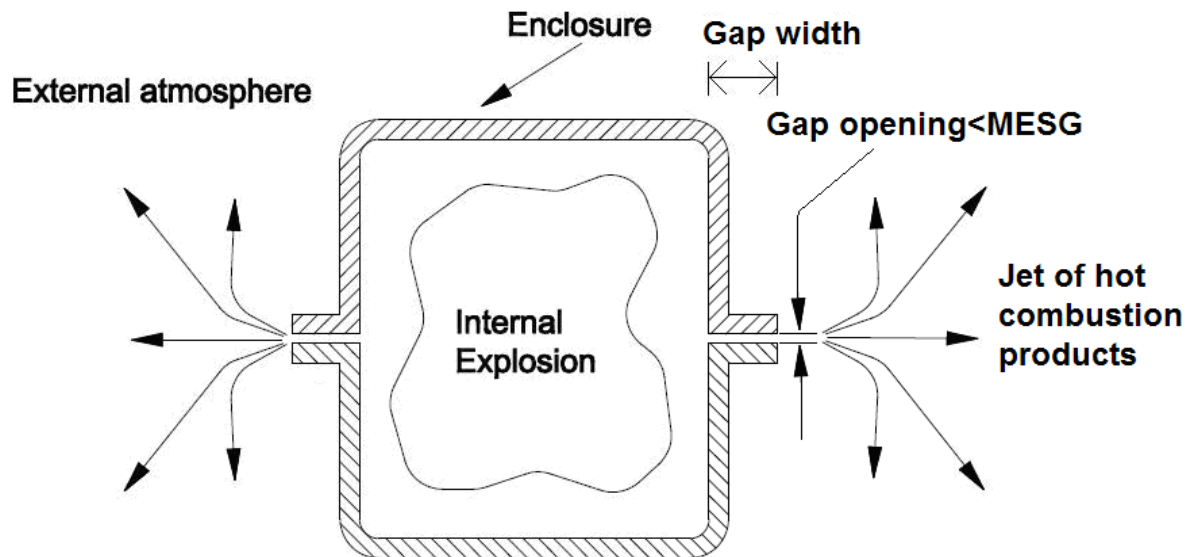


**Figure 2-5** Illustration of flameproof enclosure with an internal explosion. From (Opsvik 2010)

There has been some discussion as to what mechanisms that is of greatest importance for preventing the explosion to be transmitted to the external explosive atmosphere when the gap is at MESH.

In Section 2.3 different literature on the subject has been reviewed. One aspect in which all literature on the subject is concordant is that the process involves a complex interplay of physical and chemical processes and that further research is needed to fully understand all the mechanisms involved in this process. Some important mechanisms involved are listed below:

- "Cooling" of the hot exhaust gases inside the flame gap.
- The influence of mixing and entrainment of "cold" unburned gas, and the competition with the rate of heat generation by combustion reaction, on the ignition process in the external surroundings.
- The internal explosion pressure and hence the velocity of the hot combustion jet through the flame gap and into the external surroundings.
- Cooling from adiabatic expansion when the hot exhaust gas leaves the flame gap.
- The air-gas ratio inside and outside the gap.
- The degree of turbulence outside the flame gap.

To continue the research of the mechanisms involved for preventing explosions through narrow gaps is important to be able to design safer protection methods for electrical equipment used in explosive atmospheres. Hopefully, can the results from the experimental work in this thesis increase the understanding of the mechanisms involved in gas explosion transmission, and be used to further improve the design of flameproof equipment.

## **2.2.4 Damage and requirements for inspection, maintenance and repair of flameproof equipment (Ex "d") given in the IEC standard**

To guarantee a safe operation in hazardous areas it is strict requirements for inspection, maintenance and repair of Ex "d" equipment to ensure safe operation during the total lifetime of this type of equipment, requirements for Ex "d" equipment are given in (IEC 2007b) and (IEC 2007c).

### **2.2.4.1 Maintenance and inspection**

In (IEC 2007c) it is stated that Ex "d" equipment require initial inspection before it is brought into service and it should be carried out regular periodic inspections thereafter, or continuous supervision by skilled personnel. When inspection that requires to dismounting covers of Ex "d" equipment is to be carried out, the equipment need to be de-energized first. Most plants require that a "hot permit" be obtained before work on Ex "d" equipment is permitted. During inspection special care has to be taken so the equipment is not damaged. As described in Section 2.2.3, the protection by flameproof enclosure depends on quenching of flames by flame gaps. Therefore special care has to be taken so that the flame gaps are not damaged. Inspections should only be carried out by qualified personnel. The enclosures should be handled in clean conditions so that foreign materials will not be trapped between the flanges in the flame gap.

Typical damage that can occur on Ex "d" equipment during operation:

- Corrosion on the enclosure and in flame gaps, e.g. in offshore industries seawater is used for fire water and the environment is highly corrosive.
- High pressure hosing with water can cause water ingress in the enclosure, this can lead to failure of the electrical components and stagnant water in the flame gap can give rust formation in the flame gap.
- Drilling sludge consists of chemicals, acids and it is hygroscopic which means that it will absorb water, these factors gives a highly corrosive effect on equipment.
- Sand blasting can destroy equipment.
- Deformation of the enclosure as a result of "collisions" with other types of equipment.
- Damage as a result of glowing particles from welding, cutting and other hot work.
- Damage from poor handling during inspection, e.g. formation of a groove or scratch by a screwdriver.

### **2.2.4.2 When does a flame gap need repair?**

Some doubt exists when dealing with repair of flame gaps; this is because the standard does not provide any guidance as to what degree of damage is considered to be significant enough

to affect the efficiency of the gap in a negative way and to make Ex "d" equipment to be considered as defect and not safe anymore. The only parameter is that of the joint surfaces shall have an average surface roughness of  $< 6.3 \mu\text{m}$ . From (IEC 2007b): *"Damaged or corroded flameproof joint faces should be machined, after consultation with the manufacturer wherever possible, only if the resultant joint gap and flange dimensions are not affected in such a way that they contravene the certification documents."* This means in general that all damage of surfaces of flame gaps must be brought back to the original state as the equipment were when it was certified, which means that the surface must have an average surface roughness of  $< 6.3 \mu\text{m}$ . As a result of this, even minor mechanical or corrosive damage of flame path surfaces has often prompted expensive overhaul and repair of flame proof apparatuses.

Hopefully will the experiments carried out in the present work provide some more knowledge to what degree of damage that is significant enough to have a negative effect on the efficiency of the flame gaps in Ex "d" enclosures.

## **2.3 Basic theory of explosion transmission through narrow gaps of relevance to the present work**

This chapter is provided to explain some of the most important physical mechanisms involved in explosion transmission, and to give the reader a basic insight of expressions used further in this thesis for discussion of the experimental results.

### **2.3.1 Quenching distance ( $Q_D$ )**

In gaps and tubes, critical dimensions for flame propagation for different fuel compositions exist. These have been experimentally tested in a series of different studies, e.g. by (Friedman and Johnston 1950) who showed that different fuel to air ratios had influence on the ability to propagate a flame in narrow channels. This critical dimension is called "quenching distance" ( $Q_D$ ) and is defined as *"the smallest tube diameter (or gap) through which a laminar flame can propagate"*. To successfully propagate a self-sustained flame through a tube or gap, the rate of heat production in the flame zone must exceed the rate of heat loss to the tube wall (see Section 2.3.2).

### **2.3.2 Maximum Experimental Safe Gap (MESG)**

An explosion in a vessel vented through narrow gaps can be transmitted through gap openings below the quenching distance. The re-ignition outside the gap is then not initiated by a flame, but from a jet of hot combustion gases "pushed" out by the pressure rise (see Section 2.2.3, figure 2-5). A maximum value which is the highest gap opening giving no re-ignition outside the gap opening is eventually reached, this is called the Maximum Experimental Safe Gap (MESG).

MESG is defined as: *"The maximum gap between the two parts of the interior chamber which, under specified test conditions, that prevents ignition of the external gas mixture through a 25 mm long flame path when the internal mixture is ignited, for all concentrations"*

of the tested gas or vapour in air” from (IEC 2002). A standardized method for determining the MESG value is developed and used to classify different gases after their ignition sensitivity and how reactive the gases are. A standard test apparatus is shown in figure 2-6. The aperture consists of a spherical primary chamber with volume 20 ml where the gas is ignited. The primary chamber is connected to a secondary chamber with a 25 mm equatorial flange gap. Adjusting the gap-opening in steps of 0.02 mm, the largest opening giving 10 following trials with no ignition of the external gas, is the MESG of the tested gas mixture.

The MESG value is the parameter used when designing and building electrical apparatuses for use in specific flammable atmospheres (e.g. Ex "d" equipment). The maximum allowed gap opening of Ex "d" equipment from figure 2-4, is based on MESG value for the actual gas, provided with a safety factor, which then gives the maximum allowed gap opening.

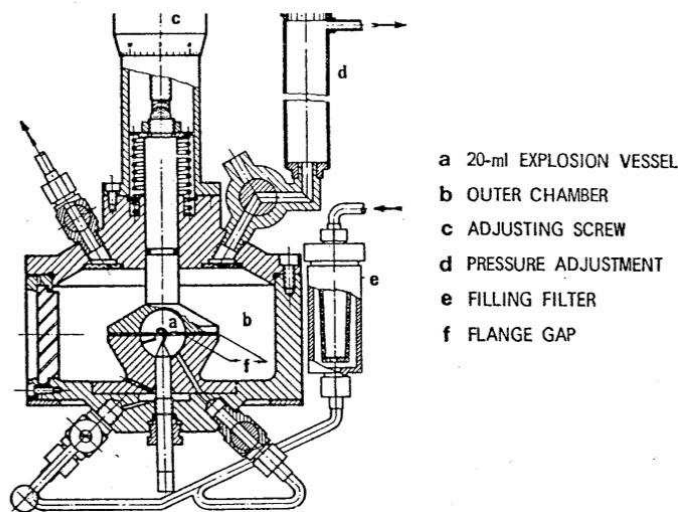


**Figure 2-6** MESG test apparatus. From (IEC 2002)

In the present experimental work, MESG was chosen as the parameter for judging whether significant damage of the gap surface had any significant effect on the ability of the flame gap to prevent explosion transmission. A significant reduction of MESG compared with that obtained with an undamaged (roughness  $< 6.3 \mu\text{m}$ ) gap surface, would mean that the damage under experiment had destroyed the efficacy of the gap significantly. The guidelines for MESG determination given in (IEC 2002) is followed as accurately as possible, but as described in Chapter 3, the apparatuses used for determining MESG in the present experimental work is not the same as the apparatus shown in figure 2-6. The reason for not using an aperture like the one in figure 2-6, is that the MESG apparatus that were to be used in this experimental work needed to have changeable flanges, to be able to perform experiments with different gap surfaces with different roughness and different damages.

### 2.3.3 Ignition by a jet of hot combustion products

As described in Section 2.2.3, flameproof equipment (Ex "d") ensure that the jet of hot combustion products ejected through the flame gap and into the external surroundings, do not have an energy and temperature large enough to initiate an ignition of the external gas atmosphere. To ignite an explosive atmosphere, the heat generation by the combustion reaction must exceed the heat loss to the surroundings. The "cooling" of the hot jet of

combustion products in Ex "d" equipment is a result from "cooling" of the hot combustion gases in the flame gap, and from entrainment and mixing with "cold" unburned gas in the external atmosphere outside the gap, this is described Section 2.3.4.

The thermal explosion theory by (Frank-Kameneckij 1955) can be used to describe the basic mechanisms for ignition. This theory is based on the ratio between heat-production, due to chemical reaction in an imaginary ignition volume ( $V_C$ ), being heated without expanding, to the loss of heat to the surroundings by conduction. This is described by the temperature-time development from (Beyer 1996) by the equation:

$$\frac{dT}{dt} = \dot{Q}_R - \dot{Q}_L \quad (2.1)$$

Where  $\dot{Q}_R$  and  $\dot{Q}_L$  denote the rate of heat production by chemical reactions and the rate of heat loss by conduction. The rate of heat production  $\dot{Q}_R$  from (Lewis.B. 1987) can be written as:

$$\frac{d\dot{Q}_R}{dt} = V_C \cdot \Delta E \cdot \left( k \cdot \exp\left(-\frac{E_a}{R \cdot T}\right) \right) \quad (2.2)$$

Where  $\Delta E$  is the molar reaction enthalpy,  $k$  is a reaction rate constant which quantifies the speed of the reaction,  $E_a$  is the activation energy for the reaction,  $R$  is the general gas constant. This equation is based on the exponential temperature dependence where the reaction rate increases exponential, this is the Arrhenius law.

The rate of heat loss  $\dot{Q}_L$  from (Lewis.B. 1987) can be given as:

$$\frac{d\dot{Q}_L}{dt} = \beta \cdot A(T - T_0) \quad (2.3)$$

Where  $A$  is the surface area of the volume,  $\beta$  is the heat transfer coefficient and  $T$  and  $T_0$  are the temperature in the ignition volume and in the gas surroundings. The behaviour of the heat production ( $\dot{Q}_R$ ) and the heat loss ( $\dot{Q}_L$ ) with temperature is illustrated in figure 2-7.



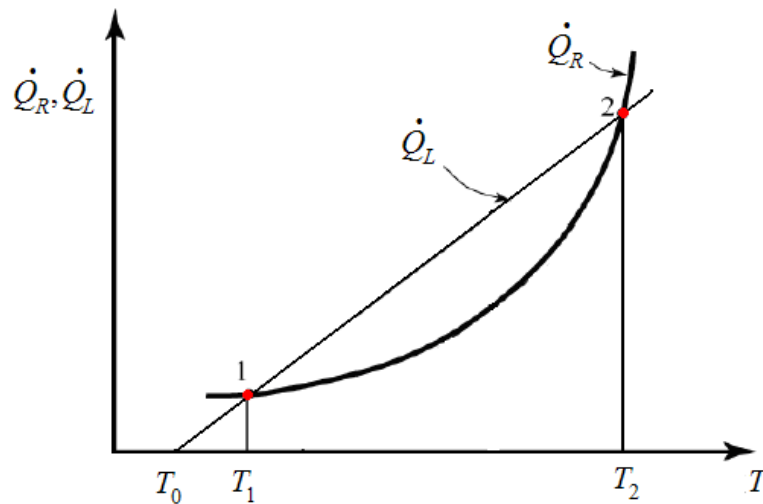


**Figure 2-7** Heat production ( $\dot{Q}_R$ ) and heat loss ( $\dot{Q}_L$ ) as a function of temperature. Based on (Beyer 1996)

If the temperature  $T < T_1$ ,  $\dot{Q}_R > \dot{Q}_L$  this lead to a temperature rise for the reaction. At the point 1 in figure 2-7,  $\dot{Q}_R < \dot{Q}_L$  and the mixture stabilizes at  $T_1$  and hence no ignition is initiated. To get an ignition the temperature must be increased from an external source until the temperature  $T_2$  is exceeded. The temperature will rise further accomplished by the combustion reaction itself, this will lead to an ignition.

This is a basic model for describing ignition, but it does not take in account different important aspects, for instance, the heat loss in this model is only from conduction, the rate of "cooling" by entrainment and mixing with the "cold" surrounding gas is not implemented in this model. The temperature is also assumed to be uniform throughout the ignition volume; this is not the case in real reactions. The ignition volume is also thought to be circular and it does not expand due to heating, in real reactions the shape of the ignition volume can differ a lot from this and it will expand when being heated.

Flammable gases are grouped according to ignition energy and temperature needed to ignite the gas and these values differ somewhat in the litterateur. The energy needed to ignite an explosive gas-air mixture depends on several parameters:

- Air-gas ratio
- Type of gas
- Gas motion, turbulence
- Entrainment and mixing with unburned gas
- Initial pressure and temperature

### 2.3.4 Cooling of the jet of hot combustion products

As mentioned in Section 2.2.3, the "cooling" of the hot jet of combustion products in Ex "d" equipment is a result from "cooling" of the hot combustion gases inside the narrow flame gap,

and from entrainment and mixing with "cold" unburned gas in the external atmosphere outside the gap. This chapter will describe these two parameters.

**2.3.4.1 Heat transfer to gap wall**

When the jet of hot combustion products passes through the narrow gap which has lower temperature, a temperature gradient is established and heat transfer from the hot gas to the colder surface will occur. The faster the gas moves the greater the heat transfer from convection. If there is no motion in the bulk gas, the heat transfer occurs only by conduction. To precisely calculate heat transfer from a flowing jet of hot gas to a surface is almost impossible, because of the change in velocity and temperature throughout the jet. The basic mechanisms for heat transfer from a hot fluid to a colder solid surface are described below.

The following theory is based on (Kanury 1975), (Drysdale 1999) and (McCabe, Harriott et al. 2005): consider a system where a fluid is flowing with a laminar free stream velocity  $u_\infty$ , across a rigid flat plate, the fluid temperature is higher than the surface temperature of the plate (see figure 2-8). The heat transfer process occurs close to the surface in a region called the boundary layer and its structure determines the magnitude of the convective heat transfer coefficient ( $h$ ). Near the wall the fluid velocity is stationary ( $u(0) = 0$ ), the velocity increases when moving away from the wall giving a velocity gradient described by  $u = u(y)$ . The fluid reaches its bulk velocity  $u = u_\infty$ , a given distance away from the wall. This is called the hydrodynamic boundary layer. The fluid temperature is assumed to be equal to the surface temperature of the solid at the surface ( $T(0) = T_s$ ). When moving away from the surface the temperature increases to its bulk temperature a given distance from the wall, this temperature gradient can be described by  $T = T(y)$ . This is called the thermal boundary layer. Figure 2-9 shows a laminar flow  $Re < 2100$  that develops into a turbulent flow  $Re > 4000$  beyond a transition regime.

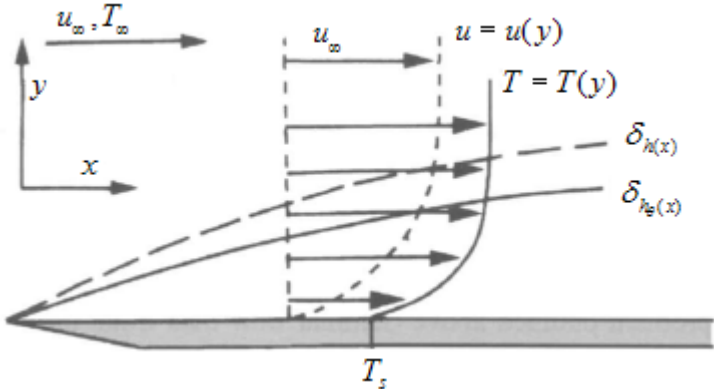


**Figure 2-8** The dashed line shows the hydrodynamic boundary layer, and the solid line shows the thermal boundary layer. From (Kanury 1975)

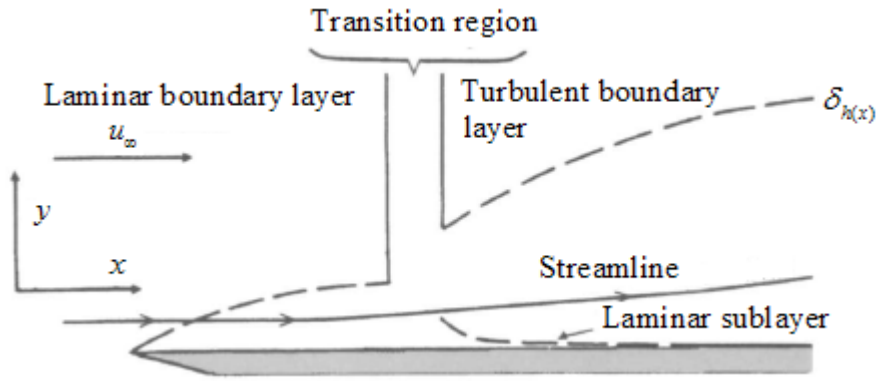


**Figure 2-9** A laminar flow developing into a turbulent flow, note that a laminar sub layer will always exist close to the surface. From (Kanury 1975)

As mentioned above the velocity in most real cases changes throughout the area which is of interest, and as showed in figure 2-9, the flow can be turbulent at one point in the stream and laminar at another point. Due to this, it is difficult to determine the heat transfer from a hot fluid to a wall with absolute confidence. A way to take this into account, is to divide the different regions in the flow and find “local” Reynolds numbers, from (McCabe, Harriott et al. 2005):

$$Re_x = \frac{xu_{\infty}\rho}{\mu} \quad (2.4)$$

$x$  = travel length of fluid

$u_{\infty}$  = fluid velocity

$\rho$  = density of the fluid

$\mu$  = dynamic viscosity of the fluid

Finding the right convective heat transfer coefficient ( $h$ ) for the case of interest is a problem, because  $h$  is found experimentally. But in the literature, recommended convective heat transfer correlations for different cases are given, showed in table 2-4 from (Kanury 1975). The Nusselt number gives the ratio of convective to conductive heat across the boundary layer and is expressed by the equation from (McCabe, Harriott et al. 2005):

$$Nu = \frac{hl}{k} \quad (2.5)$$

Where  $l$  is the characteristic dimension of the surface and  $k$  is the thermal conductivity of the fluid.

As shown in table 2-1, it is possible to find the convective heat transfer coefficient ( $h$ ) by using the recommended convective heat transfer correlations, e.g. for a laminar flow, parallel to a flat plate of length  $l$ , is given by  $Nu = 0,66 Re^{\frac{1}{2}} Pr^{\frac{1}{3}}$  where  $Pr$  is the Prandtl number. This is a dimensionless number that characterizes the regime of convection in the boundary layer. The Prandtl number is often found in property tables and is form (McCabe, Harriott et al. 2005) defined as:

$$\text{Pr} = \frac{\nu}{\alpha} \quad (2.6)$$

$\nu$  = kinematic viscosity

$\alpha$  = thermal diffusivity

If the Prandtl number  $\gg 1$ , the thermal boundary layer lies well within the hydrodynamic boundary layer. If the Prandtl number  $\ll 1$ , the thermal boundary layer is thicker than the hydrodynamic boundary layer. The Prandtl number is almost independent of temperature and only dependent on the fluid and the fluid state.

**Table 2-1** Some recommended convective heat transfer correlations (Kanury 1975)

Nature of the flow and configuration of the surface	$\overline{\text{Nu}} = \frac{hl}{k}$
<b>Forced convection</b>	
Laminar flow, parallel to a flat plate of length $l$ ( $20 < \text{Re} < 3 \cdot 10^5$ )	$0,66 \text{Re}^{\frac{1}{2}} \text{Pr}^{\frac{1}{3}}$
Turbulent flow, parallel to a flat plate of length $l$ ( $\text{Re} > 3 \cdot 10^5$ )	$0,037 \text{Re}^{\frac{4}{5}} \text{Pr}^{\frac{1}{3}}$
Flow round a sphere of diameter $l$ (general equation)	$2 + 0,6 \text{Re}^{\frac{1}{2}} \text{Pr}^{\frac{1}{3}}$

As mentioned in the start of this chapter the heat transfer from a hot fluid to a surface with lower temperature is a combined effect of heat transfer from conduction and convection. The law of heat conduction often referred to as Fourier's law, describe the amount of energy flowing into or out of a body in a given time interval:

$$\frac{dq}{dt} = -kA \frac{dT}{dx} \quad (2.7)$$

$\frac{dq}{dt}$  Is the heat flow through an area ( $A$ ), which is the area heat is being transferred through.

$\frac{dT}{dx}$  Is the temperature gradient over a distance  $dx$ .

$k$  Is a thermal conductivity constant, with units  $\left[ \frac{W}{m \cdot K} \right]$ , the constant  $k$  is available for many materials as a function of  $T$

Heat transfer in gases is due to the collisions by the molecules in the gas, and the thermal conductivity is low compared to solids because gas is a dilute media with small molecules.

The rate of heat transfer by convection is given by Newton's law of cooling:

$$\dot{q}'' = h\Delta T \left[ \frac{W}{m^2} \right] \quad (2.8)$$

Where  $\Delta T = (T_s - T_f)$ ,  $T_s$  is the surface temperature of the solid, and  $T_f$  is bulk fluid temperature away from the surface. This equation assumes that the fluid temperature equals the surface temperature at the surface.

$h$  = the individual convection heat transfer coefficient for each fluid  $\left[ \frac{W}{m^2 \cdot K} \right]$ .

#### **2.3.4.2 The effect of turbulence upon heat transfer to gap walls**

Roughness of the surface in a pipe (or in a flame gap which is the subject of this thesis) can cause fluctuation in the flow and initiate a turbulent flow. In (McCabe, Harriott et al. 2005) it is stated that for equal Reynolds numbers, the heat transfer coefficient in turbulent flow is somewhat greater for a rough tube than a smooth one and that the effect of roughness on heat transfer normally is omitted for practical purposes. (Boust, Sotton et al. 2007) published an experimental study where he examined wall heat losses according to pressure and gas dynamics. The experimental results showed that the velocity was the major contributor with the largest influence on heat loss to the wall, turbulence was found to have only second order effects on heat losses, this supports the practice of omit the effect of turbulence when dealing with heat loss to the gap wall.

#### **2.3.4.3 Cooling from entrainment and mixing with "cold" unburned gas in the external chamber**

When the hot combustion gases are ejected through the flame gap (see figure 2-5, Section 2.2.3) they will be cooled adiabatically as they expand outside the gap exit. From the literature (Redeker 1981), showed that the extent of this cooling is not very large, and not a main contributor for cooling the jet of hot combustion products from a flameproof enclosure.

The cooling from entrainment and mixing with the unburned gases outside the enclosure is of a much higher order. If the gap opening that connects the primary chamber to the external surrounding is large, the velocity ( $u$ ) through the gap will be low, and hence the mixing and turbulence will be small when the gases meet the external mixture. The ratio of cooling form mixing and entrainment will be low and there is high probability for a re-ignition of the external mixture. When the gap opening is decreased, the velocity ( $u$ ) of the gases through the gap is increased (by the pressure rise "pushing" the combustion products through the gap). The turbulence where the jet of hot combustion products meets the external mixture will be large; an illustration of a plane turbulent jet from (Tennekes 1994) is shown in figure 2-10. The ratio of cooling of the hot combustion products by entrainment and mixing with "cold" unburned gas will be high. Near the gap the jet moves with a high velocity and expands so rapidly that the time of contact between hot gas and the unburned "cold" gas is too short and may be insufficient for igniting the external mixture. When the jet moves further away from the gap exit the velocity and the rate of mixing and entrainment decreases. The jet can reach conditions favourable for ignition of the external mixture a given distance away from the gap exit; this is why the ignition in experiments is observed a given distance away from the gap exit. The balance of heat generation and heat loss determines whether the external mixture will be ignited. When the jet has lost its original high velocity it may have been so deformed and lost its energy and temperature, so the entrained mixture will never reach the temperature necessary for ignition.

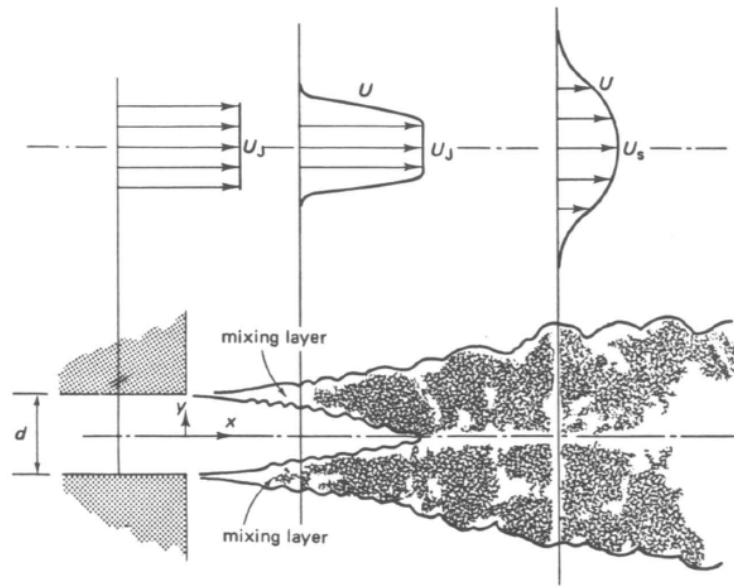


**Figure 2-10** *Illustration of a plane turbulent jet. The jet becomes self-preserving some distances after the two mixing layers near the wall exit have merged. From (Tennekes 1994)*

## 2.4 Literature review of previous work in relation to explosion transmission through narrow gaps and flameproof protection

This chapter introduces relevant literature related to flameproof equipment and explosion transmission through narrow gaps.

### 2.4.1 H. Phillips' work on describing the mechanisms of MESG and flameproof protection

Harry Phillips did extensive work trying to explain the physical mechanisms involved in MESG and flameproof protection.

The aim of Phillips' work was to connect results from the early work of (Beyling 1906), to (Wolfhard and Bruszak 1960)) with his own and to unite it with a set of equations describing all aspects of the mechanisms involved in MESG and flameproof protection. Some of the most important aspects of his work include:

- Describing the ignition process when a transient jet of hot inert gas is ejected through a flange gap
- Describing heat transfer within the flange gap
- Describing the entrainment and mixing into the expelled jet

- Describing the rate of combustion in the expelled jet and the competition with cooling from the entrainment and mixing with “cold” unburned gas
- Influence of the internal explosion pressure and the speed of the hot gas through the gap and into the secondary chamber

### 2.4.1.1 Outline of Phillips’ equations for describing the mechanisms of MESG and flameproof protection

Phillips presented a model of the expelled hot jet (figure 2-11) (H.Phillips 1971). This was based on observations from Schlieren photographs that indicated that a jet of hot gas emerged from the gap, and if an ignition occurs this takes place in a spherical vortex at the head of the jet, some distance away from the gap opening. To assess whether or not the jet would ignite the gas in the secondary chamber, Phillips did an analysis of the temperature of the vortex head. He found that it was at the vortex head the ignition was initiated. He noted that a drop in the temperature at the vortex head due to rapid entrainment and mixing with the “cold” unburned gas would lead to no-ignition, while an increase in temperature to temperatures above the ignition temperature for the gas would lead to ignition. This means that the rate of heat production from combustion must exceed the rate of cooling by mixing with the jet for external ignition to occur.

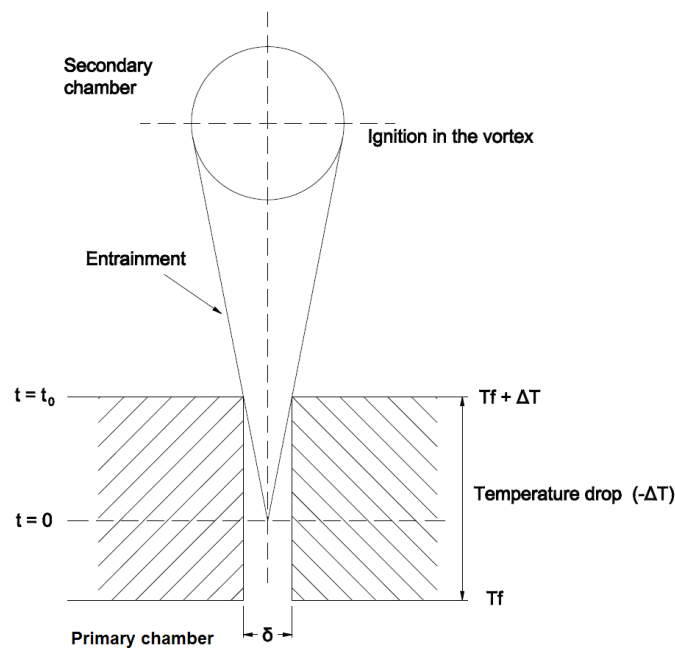


**Figure 2-11** Model of the hot jet, with ignition in the vortex a distance away from the gap opening. From: (H.Phillips 1971)

A summary of the method outline for the ignition model and the procedure describing the mechanisms to calculate the size of the safe gap (MESG) from (H.Phillips 1971 23) is given below. Phillips used analogue computers for solving the equations shown here and to compare them to experimental results.

The first step is to calculate the maximum value of  $\psi$  from the properties of the fuel.  $\psi$  is the rate of combustion derived from an energy balance across an element in the vortex of the hot jet, given as:

$$\psi = \frac{1}{\eta} \cdot \frac{d\eta}{dt} + \frac{1}{m} \cdot \frac{dm}{dt} \quad (2.9)$$

$m$  = mass of gas contained in the vortex

The function:  $\frac{1}{m} \cdot \frac{dm}{dt} = \frac{z}{t}$  is the rate of entrainment into the jet.

The entrainment factor  $z$  has been experimentally determined. Phillips used  $z = \frac{1}{3}$  for a constant velocity jet. Jets with velocities that increase with time have higher values of  $z$ . Phillips assumed that turbulence in the vortex did not affect the volumetric heat release rate. The heat release rate was assumed to be equal to that in the combustion zone of a laminar flame front.

$\eta$  is the combustion efficiency, given as:

$$\eta = \frac{T - T_u}{T_f - T_u} \quad (2.10)$$

$T$  = jet temperature

$T_f$  = the maximum flame temperature

$T_u$  = ambient temperature

If  $(T)$  drops rapidly to ambient temperature (e.g. by cooling from entrainment and mixing of the unburned gas) there will be no ignition and hence no combustion ( $\eta=0$ ). This is illustrated by the bottom line in figure 2-12. The next three lines are also failure to ignite the external mixture, but there will be combustion with a short duration time ( $t_0$ ), followed by a rapid drop of  $(T)$  ambient temperature again. Experiments have shown this as a visible flash of flame that does not lead to a total ignition of the mixture in the secondary chamber.

The three top lines represent ignition; first there is a drop in temperature, but when the rate of combustion heating exceeds the rate of cooling by entrainment, the temperature rises to the maximum flame temperature and ignition will be initiated.



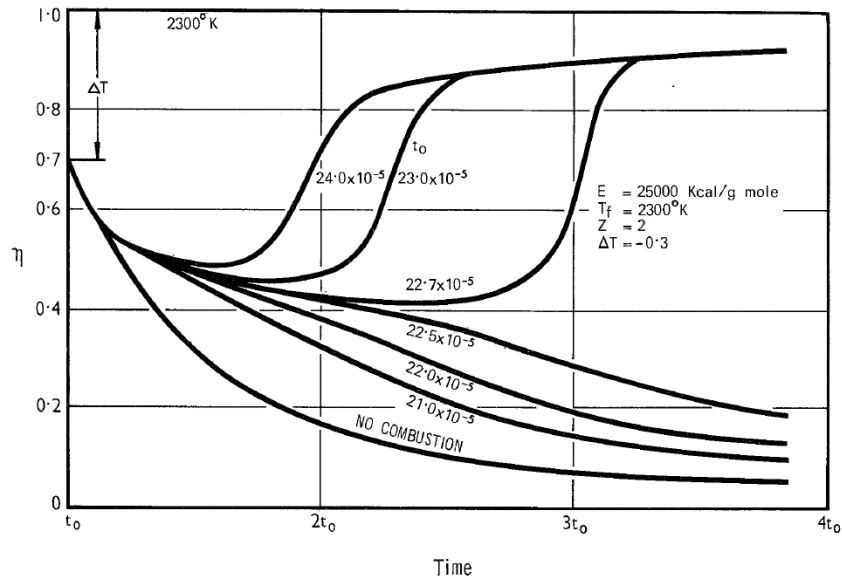


**Figure 2-12** Analog computer curve of vortex temperature.  $\eta$  denotes a non-dimensional temperature  $(T - T_u) / (T_f - T_u)$  and  $t_0$  denotes starting time in seconds from a point source until the vortex fills the orifice. From (H.Phillips 1972)

Phillips further derived the equation expressing that the rate of combustion ( $\psi$ ) in the jet depends on the proportion of entrained gas. The Arrhenius equation is used to describe the overall rate of the reaction:

$$\psi = \frac{B P W}{T R \eta} \frac{\frac{a}{f}}{\left(1 + \frac{a}{f}\right)} \left(1 - \eta + \frac{m_0}{m} \Delta T\right)^2 \exp\left(-\frac{E}{RT}\right) \quad (2.11)$$

B = reaction rate constant

P = pressure

W = mole weight of the actual gas

R = universal gas constant

a/f = air/fuel ratio, by weight

E = activation energy

$\Delta T$  = temperature difference in the gap (dimensionless)

$m_0$  = Initial mass of gas leaving the flange gap

Phillips stated that if the activation energy (E) is not available for the fuel, an approximation for (E) can be taken from (Fenn 1953), in which it is equal to 16 times the flame temperature at the lower limit of downwards flame propagation.

### 2.4.1.2 Effect of pressure and velocity

In (H.Phillips 1987), it is stated that a critical point for external ignition was found from experiments. This critical point, giving the smallest gap opening for no re-ignition, was when the explosion pressure was low so the velocity through the gap was also low. Because of this, he based his equation on heat transfer calculations for laminar flow. He derived a critical jet Mach number, which he found to be a function of the fuel's burning velocity ( $S_u$ ), the volume of the explosion vessel ( $V$ ), and the open area of the flange gap ( $A$ ) together with the acceleration due to gravity. This was called the shape factor which is a dimensionless Mach number:

$$M = \frac{S_u^2 \cdot V}{g \cdot A^2} \quad (2.12)$$

This Mach number was found to be almost equivalent to the critical velocities from experiments giving the lowest gap opening, and is used for calculating the MESG.

Consider figure 2-13, which is a plot from calculations of the safe gap vs. explosion pressure (H.Phillips 1988). With side ignition (close to the gap exit), hot gas is first ejected at a low pressure. As pressure increases, the safe gap falls to a minimum. The minimum occurs at a low explosion pressure. Due to low pressure the heat transfer in the gap is large, relative to the gas flow, and the jet temperature doesn't get sufficient cooling by entrainment and mixing by the unburned gas. Further increase in pressure leads to a rise in the safe gap. This is because the rate of cooling by mixing and entrainment increases and exceeds the rate of heat generation by combustion. At higher pressure, the MESG falls back to its minimum at the break point. This point can not be reached in the 20-ml IEC apparatus (see figure 2-6, Section 2.3.2), nor in the apparatuses used in the experimental work described in this thesis. This because the explosion pressure development by changing the ignition position is not sufficient for reaching this point.

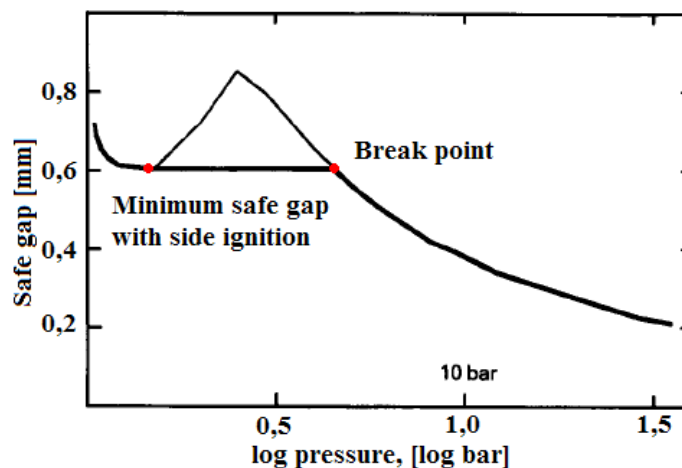


**Figure 2-13** The 's' curve showing a minimum in safe gap at 1,5 bar and a break point at 4,6 bar. From (H.Phillips 1988)

Phillips stated in (H.Phillips 1988) that the break point could not be found in the test apparatuses used to find the MESG (e.g. the 20 ml IEC apparatus), but he expressed a concern that that pressures could become high enough in large enclosures with many internal

components, especially in more reactive fuels like hydrogen. In such cases, external ignition might be possible in small flange gaps, comparable with or smaller than those permitted in the current standards.

In (H.Phillips 1971) he noted that the critical gap size, giving no re-ignition, is related to the starting time ( $t_0$ ). This is the time that elapses during the growth of the imaginary part of the jet within the gap. The gap velocity ( $v$ ), which is the velocity of the gas leaving the gap, was the other variable that was included to determine the critical gap size, giving:

$$\delta = \frac{3}{2} \beta \cdot c \cdot t_0 \cdot v \quad (2.13)$$

Where  $\beta$  and  $c$  are constants found experimentally. These constants are used to take into account the composition of entrainment in the vortex and the jet, and the cone angle of the jet. These are the values used by Phillips:

$$\begin{aligned} \beta &= 0.166 \\ c &= 0.2 \end{aligned}$$

Phillips stated that the main reason for differences in the safe gaps in all experiments were due to heat transfer from the gas to the flange material (H.Phillips 1971). This heat loss,  $\Delta T$ , is included in equation (2.11). Since experimental data on heat transfer to the gap walls was not available, Phillips used a numerical solution by (Norris 1940) which gave a constant Nusselt number of 7.6 for laminar flow. The use of a laminar flow was justified by the assumption that external ignition was most likely to occur early in the explosion development, when the explosion pressure is low - thus so is the velocity of the gases out from the gap. The equation for heat transfer from (H.Phillips 1971):

$$\frac{\Delta T}{\bar{T}} = \frac{7,6 \cdot \lambda}{\rho \cdot C_p \cdot v \cdot \delta^2} \quad (2.14)$$

$C_p$  = specific heat capacity of the gas at the gap exit

$\bar{T}$  = logarithmic mean temperature through the gap

$\lambda$  = thermal conductivity of the gas at the gap exit

$v$  = velocity of the gas at the gap exit

$\delta$  = the gap opening distance

To find the starting time ( $t_0$ ) figure 2-14 can be used when the heat transfer is found from equation (2.14) and the overall rate of the reaction  $\psi$  is found from equation (2.11). Then equation (2.13) can be used to calculate the MESG.

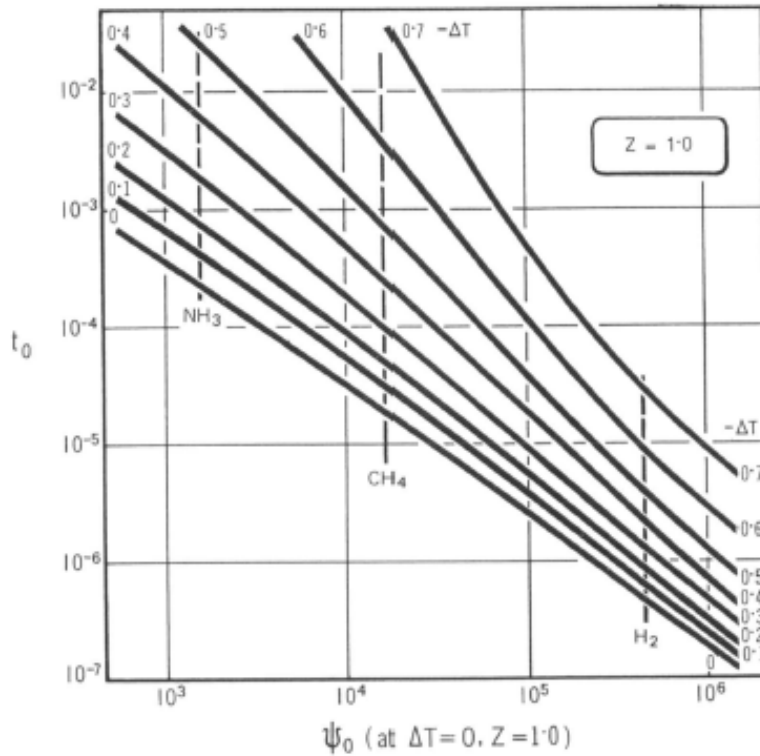


**Figure 2-14.** Starting time,  $t_0$ , as a function of reaction rate  $\psi_0$  and heat transfer  $-\Delta T$ .  
From (H.Phillips 1971)

Phillips found that the calculations gave good agreement with experiments. The calculated data was compared to a range of experimental data, covering the gases: hydrogen, acetylene, carbon disulphide, ethylene, and methane, in vessel volume from about 20 ml to 8000 ml, flange widths from 3 mm to 75 mm, initial temperatures from 27 to 250°C, and initial pressures from 0.5 to 3 atmospheres.

### 2.4.1.3 Limitations to Phillips's calculations

Phillips only performed calculations that assumed that the flow in the gap was laminar. He did no calculations on turbulent flow through the gap, nor the effect turbulence will have on the limiting gap opening. Phillips assumed that turbulence in the vortex did not affect the volumetric heat release rate. There is no parameter included in the equations that is taking into account the properties of the wall with respect to heat transfer, e.g. effect of change in the surface roughness. (Beyer 1996) pointed out that Phillips' theory was somewhat insufficient related to the exit temperature in the jet. This temperature was assumed to be a factor of 0.75 of the flame temperature and assumed no heat loss. In addition, Phillips did not account for the inhomogeneous nature of the jet, and jet velocity was also omitted. The jet velocity is coupled to the explosion pressure; hence variations in the explosion pressure lead to variations in the jet velocity.

## 2.4.2 Ballal and Lefebvre's work on examining the influence of different flow parameters on flowing combustible mixtures

*The influence of flow parameters on minimum ignition energy and quenching distance (Ballal and Lefebvre 1975)*

*Flame quenching in turbulent flowing gaseous mixtures (Ballal and Lefebvre 1977)*

The experimental work described in these articles examines the influence of various flow parameters as: pressure, velocity, fuel/air ratio, turbulence intensity and turbulence scale, on quenching distance and the minimum ignition energy of flowing combustible mixtures.

Ballal and Lefebvre found that the turbulence affects the ignition process. Turbulence gives rise to the burning velocity and propagation by wrinkling and lacerating of the flame front, thereby effectively increasing its surface area. Moreover, within the flame zone itself the transport of radicals and other active species are accelerated. These effects should reduce the quenching distance. However, at the same time they pointed out that turbulence increases the heat loss to the electrodes, and increases the mixing of fresh mixture surrounding the spark kernel and loss of heat by diffusion to the surrounding unburned gas. This effect should increase the quenching distance. They found that the latter effect is strongest and it was found that both quenching distance and minimum ignition energy increases with an increase in turbulence intensity, as shown in figure 2-15. Other parameters that gave an increase in the quenching distance were found to be:

- reduction in pressure
- departures from stoichiometric fuel/air ratio
- increase in gas velocity

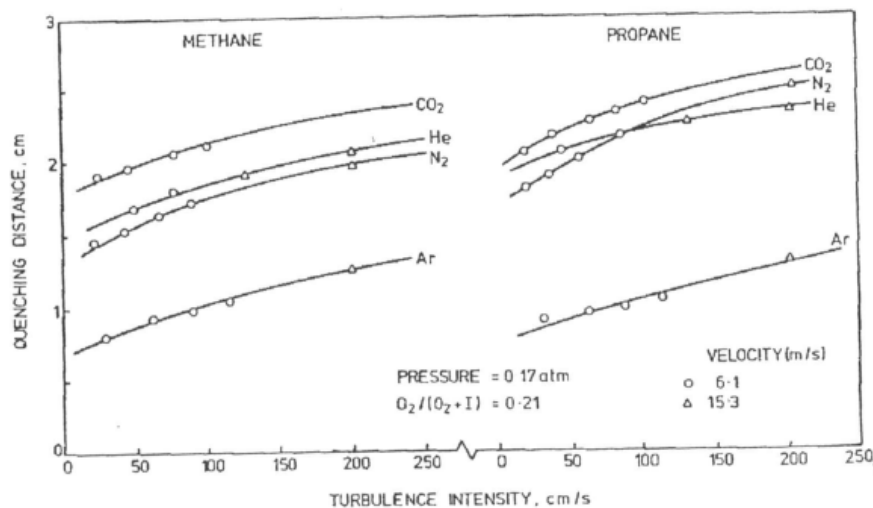


**Figure 2-15** Effect of turbulence intensity on quenching distances for different inert gases.  $\phi = 1$ . From: (Ballal and Lefebvre 1977)

In Ballal and Lefebvre's work the process of spark ignition in a flowing combustible mixture was described as follows: initial passage of the spark creates a cylindrical volume of hot gas between the electrodes. If the heat generation by chemical reaction at the kernel surface

exceeds the rate of heat loss by turbulent diffusion, the spark kernel will continue to expand and a successful ignition is initiated. However if the rate of heat generation at the kernel surface is less than the rate of heat loss, the temperature within the kernel will continue to fall until the reactions cease altogether. This conclusion is in agreement with the ignition model described in Section 2.3.3.

The work from Ballal and Lefebvre are focused on the influences different flow parameters will have upon the quenching distance, and minimum ignition energy. It is believed that the parameters that influences on the quenching distance and minimum ignition energy, will have similar influences upon the flow of hot combustion products and re-ignition in MESG experiments and flameproof enclosures.

### **2.4.3 Classification of flammable gases and vapours by the flameproof safe gap and the incendivity of electrical sparks. (Redeker 1981)**

The aim of Redeker's work was to get a better understanding of how different parameters influenced MESG and the safety of flame proof equipment. Parameters studied in this report include:

- deviation in MESG values obtained from two different apparatuses used for determining the MESG value
- influence of the inner volume of enclosure
- influence of the location of the ignition source
- influence of the gap length
- influence of the shape of the gap edge
- influence of change in the air to fuel ratio mixture
- influence of change in the initial pressure
- initial temperature of the mixture
- relationship between flame propagating capability and incendivity of electrical sparks

All of the experimental results are not referred here, but the results that are found to be most relevant for the present thesis is discussed below.

#### **2.4.3.1 Influence of the inner volume of the enclosure**

Redeker used two different apparatuses in the experimental work. Both had a spherical inner volume. The first apparatus could vary the inner volume from 1-8 litres, and the second apparatus could vary the inner volume from 0.5-20 cm<sup>3</sup>. The effect from change in inner volume upon the safe gap distance, both with a closed outer volume (no pressure relive), and with pressure relive of the outer volume was examined.

From the experiments with closed outer volume, he found that if the inner volume was increased, the safe gap distance decreased for volume up to 20 ml. For inner volumes above 20 ml, the safe gap distance was near constant until the inner volume was increased to above 1 litres.

From experiments with a pressure-relieving flexible outer enclosure, he found that there were no effect on the safe gap distance for inner volumes from 20 ml up to 8 litres (see figure 2-16)

Both of the experimental apparatuses used in the present work consist of a primary chamber with volume  $\approx 1$  litre, with an external chamber with pressure relive.

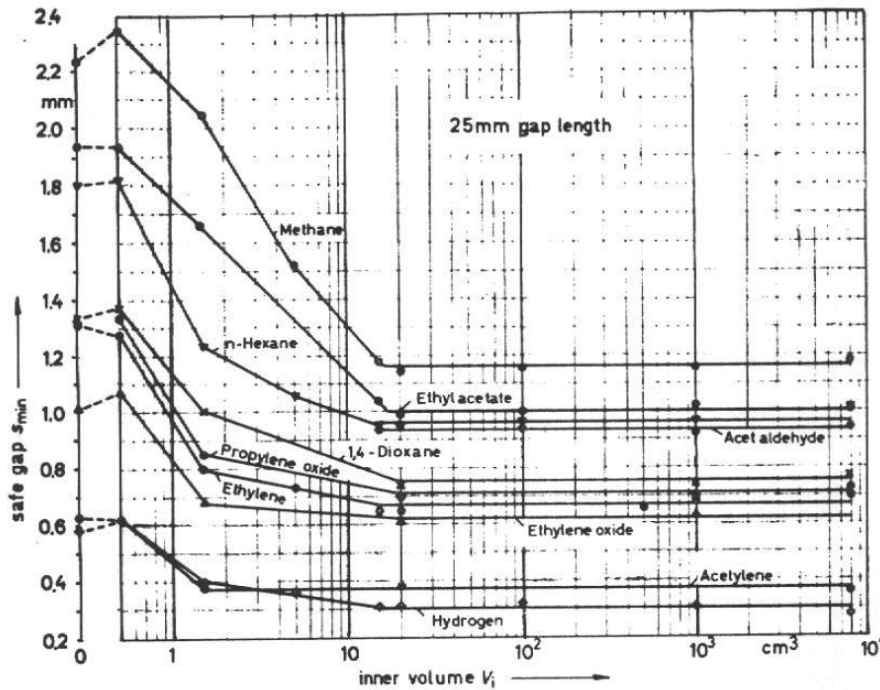


**Figure 2-16** Safe gap  $s_{min}$  for the most incendive mixtures as a function of the inner volume of the PTB test apparatus. In the test apparatus with larger volume ( $> 1$  litre) the inner volume was surrounded by a pressure relieving flexible outer enclosure. From (Redeker 1981)).

#### 2.4.3.2 Influence of the location of the ignition source

The development of the explosion in the inner chamber and the resulting gas flow in, and behind the gap at the moment of flame propagation is influenced by the location of the ignition source in dependence upon the size of the inner volume. Redeker found that for large inner volumes  $> 20 cm^3$ , the influence of the position of the ignition source location were much bigger than with a small inner volume (see figure 2-17 and 2-18).

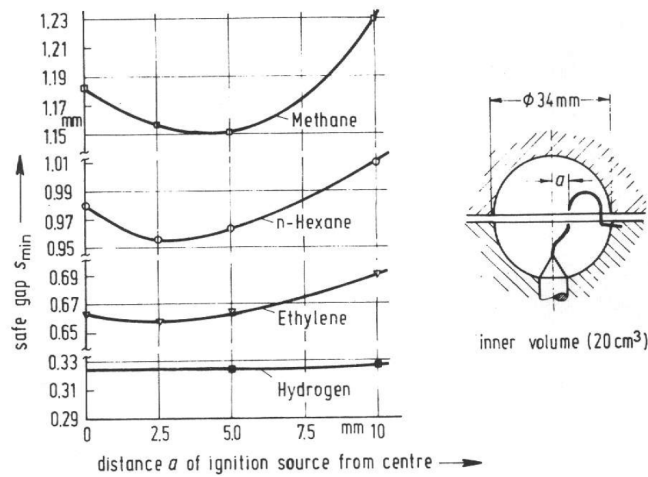


**Figure 2-17** Safe gap  $s_{min}$  for the most incendive gas/air and vapour air mixture as a function of location of ignition source, determined in the test apparatus of  $20 \text{ cm}^3$  and a gap length of 25 mm. From (Redeker 1981)

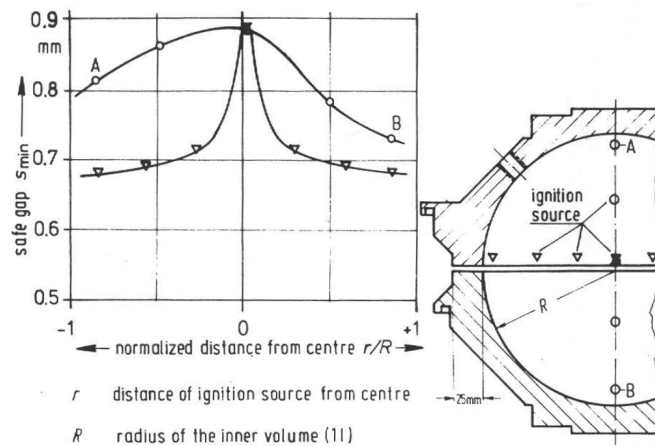


**Figure 2-18** Safe gap  $s_{min}$  for the most incendive ethylene/air mixture as a function of the location of the ignition source, determined in a test apparatus with an inner volume of 1 litre and a gap length of 25 mm. From (Redeker 1981)

Redeker described the effect from changing the ignition location in the gap plane from the gap edge towards the middle in the 1-l inner volume, as the effect of going from laminar to turbulent flow through the gap.

The effect of changing the ignition position is also examined in the present work.

### 2.4.3.3 Influence of the gap length

Redeker did experiments with different gap lengths in the  $20 \text{ cm}^3$  apparatus and found that when the gap length was decreased, so was the safe gap opening, but it did never decreased to zero. When the gap was increased the safe gap distance increased up to a length of around 25mm, further increase in gap length had small influence on the safe gap distance (see figure



2-19). This is the standard gap length used for determining MESG values from the IEC test method. This is also the gap length used in the present experimental work.

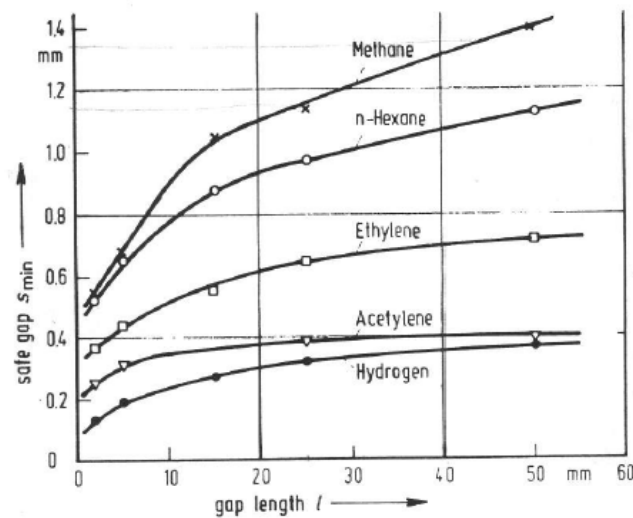


**Figure 2-19** Safe gap  $s_{min}$  for the most incendive gas/air and vapour air mixture as a function of location of gap length  $l$ , determined in the test apparatus of  $20 \text{ cm}^3$ . From (Redeker 1981)

#### 2.4.3.4 Influence of change in the initial pressure

Redeker's experiments showed that a higher initial pressure of the mixture resulted in a reduction of the safe gap distance (see figure 2-20)

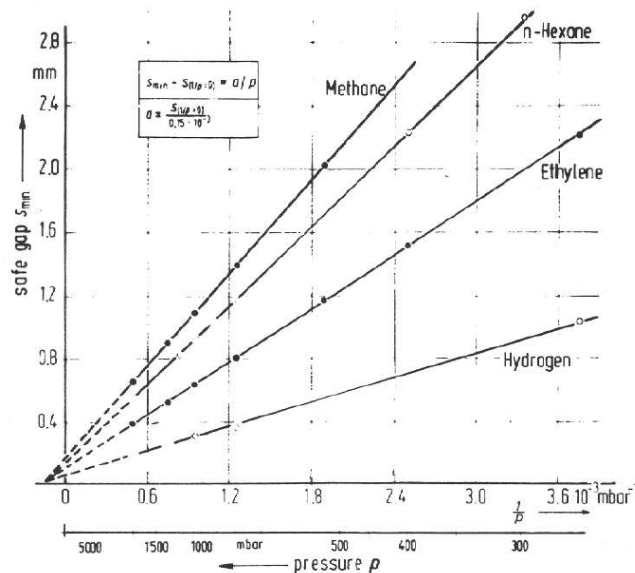


**Figure 2-20** Safe gap  $s_{min}$  as a function of the pressure  $p$  for the most incendive gas/air and vapour air mixture prior to ignition, determined in the  $20 \text{ cm}^3$  standard safe gap test apparatus. From (Redeker 1981)

#### **2.4.4 Transmission of an explosion through an orifice (Thibault, Liu et al. 1982)**

This paper investigates the quenching of flames as they propagate from one chamber to another through an orifice; the main parameter examined being the influence of the resulting explosion pressure in the primary vessel and how a higher initial pressure in the secondary vessel influences the quenching diameter. They stated that the latter effect for flame quenching for very low flame velocities (and reasonably deep orifices), the quenching phenomenon is essentially determined by the rate of loss of heat and free radicals to the orifice wall, the quenching occurs at orifice diameters, smaller than the so-called quenching diameter. But transmission of explosion can also occur for diameters smaller than the quenching diameter, this is accomplished by increasing the flow velocity, so as to decrease the time of the gas near the tube wall. They also pointed out the fact that higher gas velocity also results in a higher rate of cold gas entrainment into the hot combustion products downstream of the tube, this leads to a minimum value for quenching which is the MESG value (described in Section 2.3.2).

Experiments were performed that showed that the resulting explosion pressure in the primary vessel gave values for what they called quenching overpressures, which would choke the flow at the orifice. When the explosion pressure was increased (by change in the ignition position) the quenching diameter also increased. At the value for the so-called quenching overpressure no ignition in the secondary connected vessel was possible.

Experiments where the overpressure in the secondary vessel was varied were also performed and these showed that the quenching diameter increased, when the overpressure was increased up to a value where the quenching diameter started to decrease again. This is in agreement with the Phillips theory figure 2-13. The experiments from this work showed that re-ignition outside a narrow opening is pressure dependent.

#### **2.4.5 A Study of Critical Dimensions of Holes for Transmission of Gas Explosions and development & Testing of a Schlieren System for studying Jets of Hot Combustion Products (Larsen 1998)**

Larsen studied explosion transmission from a 1 litre cylindrical primary chamber through holes with different diameters, to an external chamber. He did experiments with different air-propane ratios.

He found that there exists a limiting hole-diameter for transmission of explosion in the same way as for gap openings (MESG). He called this the Maximum Experimental Safe Diameter (MESD). He also did experiments on the effect of change in the ignition position in the primary chamber and found that the most "dangerous" ignition position (giving the lowest MESD), (see figure 2-21), was closely coupled to the volume of the primary chamber. This he explained to be an effect of the different pressure rise for different volumes. He explained that when the ignition position was moved away from the gap opening and further into the primary chamber, the pressure rise (see figure 2-22) increase the flow velocity through the hole. The cooling of the combustion products inside the hole before the combustion products is ejected to the external chamber is decreased. This is because the increase in gas velocity through the hole decreases the resident time of the gas inside the hole. This promotes the flame transmission up to the most "dangerous" position of the internal ignition position, and

decreases the MESD. When the ignition position is moved further into the primary chamber, the gas velocity in the hole reaches a level where the cooling from entrainment and mixing with unburned gas outside the hole exceeds the heat generation from the reaction and there is no ignition, and the MESD value increases (shown in figure 2-21).

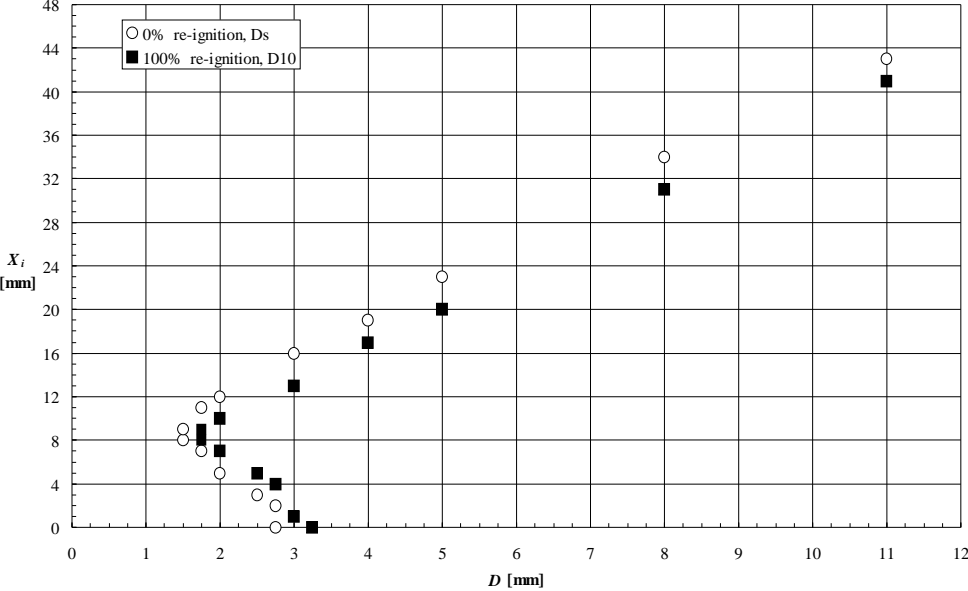


**Figure 2-21** Safe diameter  $D_s$  and  $D_{10}$  for various ignition-distances  $X_i$ . Primary volume  $V = 1\text{ l}$  and 4.2 vol. % propane-air. From (Larsen 1998)

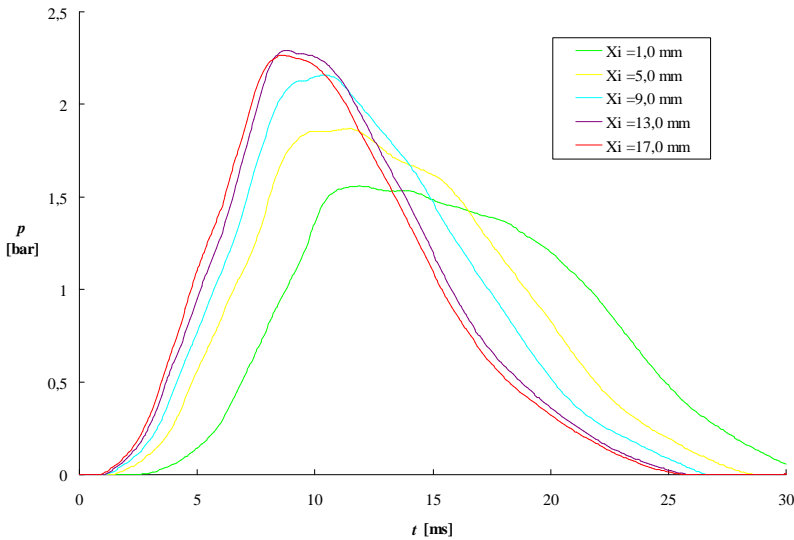


**Figure 2-22** Explosion pressure as a function of time for various ignition distances. Hole diameter  $D = 2.0\text{ mm}$ , primary volume  $V = 21\text{ ml}$  and 4.2 vol. % propane-air concentrations.  $X_i = 1.0\text{ mm}$  is in the gap opening and the ignition point is moved further into the primary chamber giving higher explosion pressures. From (Larsen 1998).

Larsen used existing literature to try to describe the different velocities through and from the cylindrical opening obtained from different explosion pressures. The flow of unburned gas

and later combustion products is compressible. He stated that for compressible fluids simplifications have to be done because the variations in both density and temperature are significant throughout the flow. From (Fox and McDonald 1994) it is said that compressible flow through a hole with constant cross-section cannot exceed the velocity of sound for the specific fluid. The flow regime can then be sub-sonic or sonic. The flow through an orifice becomes sonic when the pressure in the primary chamber reaches a value known as the critical pressure. Larsen calculated this pressure by the following equation:

$$P_{crit} = P_0 \left( 1 + \frac{\gamma - 1}{2} \right)^{\frac{\gamma}{\gamma - 1}} \quad (2.15)$$

Where  $P_0$  is the initial pressure and  $\gamma$  is the specific heat ratio for the gas.

Larsen pointed out the fact that the specific heat ratio decreases when the temperature increases. From (Çengel and Boles 2007) it is said that for common ideal gasses at 300K the specific heat ratio varies from 1.044 to 1.677, which then gives a critical pressure range from about 1.676 bar to 2.059 bar. Further pressure rise do not increase the flow speed in the fluid if the temperature is constant, and the flow speed is almost constant above critical pressure. This is shown by the temperature dependence equation of the speed of sound in an ideal gas from (McCabe, Harriott et al. 2005):

$$a = \sqrt{\frac{\gamma TR}{M}} \quad (2.16)$$

M= molecular weight of gas [g/mol]

$\gamma$ = specific heat of gas [J/K]

R= molar gas constant, 8.314 [J / Kg · mol]

T= Temperature of gas [K]

#### **2.4.6 Experimental determination of holes and slits in flameproof enclosures, for preventing transmission to external explosive gas clouds. (Einarsen 2001)**

Einarsen continued the work done by (Larsen 1998), and further investigated the MESD phenomenon. He used a slightly modified version of the apparatus used by Larsen; the test gas was 4.2 vol. % Propane. He performed experiments with different length of the cylindrical holes shown in figure 2-23, and he examined the effect of threaded holes upon the obtained MESD value.



**Figure 2-23** Various length of nozzles tested. From left; 100 mm, 50 mm, 25 mm, 12.5 mm all smooth nozzles, outermost right is threaded nozzles. From (Einarsen 2001).

Larsen found that the MESD value increased with increase in the length of the cylindrical holes. The experiments on threaded nozzles did not give any noticeable effect on MESD.

Einarsen started investigating the effect of damage of plane flame gap surfaces, he tested the effect of different lengthwise grooves with different width and depth. Unfortunately it was discovered that the adjustment of the gap openings in Einarsen`s work were inaccurate. He used distance pieces that were made with equipment with low accuracy, therefore the actual value of the distance pieces varied a lot. When the gap opening was to be fastened, the gap was only tightened in the upper part of the gap, and there is no information on the value of torque used when assembling the gap. This led to a gap opening that was not uniform over the whole gap opening, the opening was smaller in the upper part where screws were used to fasten the gap, and the gap opening was larger in the start of the gap opening. In Einarsen`s experiments with damage on the flame gap, he used slits with gap width of 12.5 mm (shown in figure 2-24).

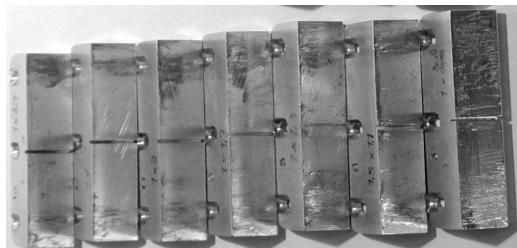


**Figure 2-24** The exchangeable parts in the slit for test with damages. The damages are in an extent that makes it easy to observe visually. The width of the slits depicted is 12.5 mm. From (Einarsen 2001)

Due to the inaccuracy and insufficient descriptions of his experimental procedures, Einarsen`s work cannot be used to provide quantitative conclusions. Even so, his results indicated that the damage in form of lengthwise grooves had to be large to affect the efficiency of the flame gap. This was the foundation and gave the motivation to continue the work of investigating the effect and influence of damage of flame gap surfaces, which is studied in the present thesis.

## 2.4.7 Investigation of ignition by hot gas jets (Sadanandan, et. al)

*Detailed investigation of ignition by hot gas jets. (Sadanandan, Markus et al. 2007)*

*Observation of the transmission of gas explosions through narrow gaps using time-resolved laser/Schlieren techniques. (Sadanandan, Markus et al. 2009)*

This is an investigation of ignition by a hot exhaust gas jet, ejected into a quiescent unburned hydrogen/air mixture, through a nozzle. They studied the phenomenon both with experimental and numerical investigations.

The experimental setup is shown in figure 2-25. It consists of two vessels connected by a nozzle. The first vessel has a volume of 12 litres and a movable electrical spark ( $X_i$ ) that can ignite the gas mixture. The secondary vessel has a volume of 0.226 litres and is connected to the first vessel by a nozzle; the opening distance of this nozzle can be varied. The test gas used is 28 vol. % hydrogen air/mixture which is filled in both the vessels before igniting the mixture.

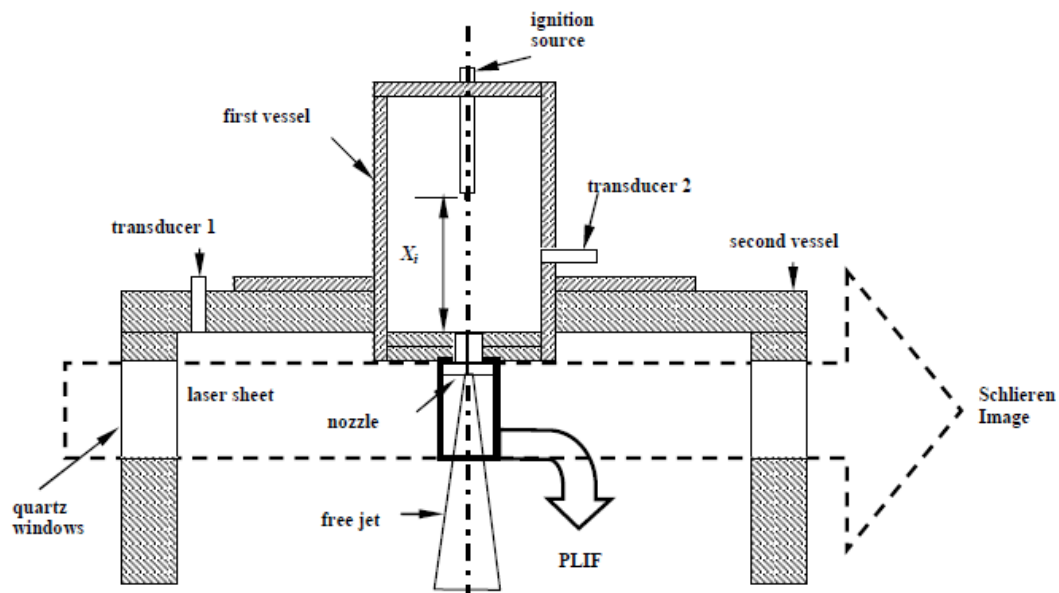


**Figure 2-25** Schematic drawing of the Explosion Vessel. From: (Sadanandan, Markus et al. 2009)

The hot jet is ejected from the first vessel through the nozzle and into the secondary vessel.

To gain information of the ignition process and get experimental observation in the second vessel they used combined Schlieren and high speed laser-induced fluorescence (LIF) images of the hydroxyl-radical (OH). OH is used to identify where the reaction zone is, due to its nature as an intermediate species formed during the combustion process

Experiments were performed with different pressure ratios over the nozzle, and different nozzle diameters, to study the influence of different jet velocities on the gas expansion and ignition processes.

In figure 2-26, the simultaneous Schlieren and OH-PLIF images obtained from experiment with ignition distance  $X_i = 32$  mm, and diameter of nozzle  $d = 0.8$  mm is shown. The structure visible from the Schlieren images is not associated with ignition and combustion, but simply with the mixing of the hot jet with the unburned mixture. From the OH-PLIF images, it can be seen that some OH radicals are visible, but the absence of a significant amount of OH radicals at the nozzle exit indicates quenching caused by cooling in the nozzle before the gas is ejected into the second vessel. In this experiment no ignition in the second vessel was initiated. This indicates that the weak OH radical formation from chemical reaction is not large enough and is going much to slow compared to the rate of cooling by entrainment and mixing with the unburned gases, therefore no ignition occurs.

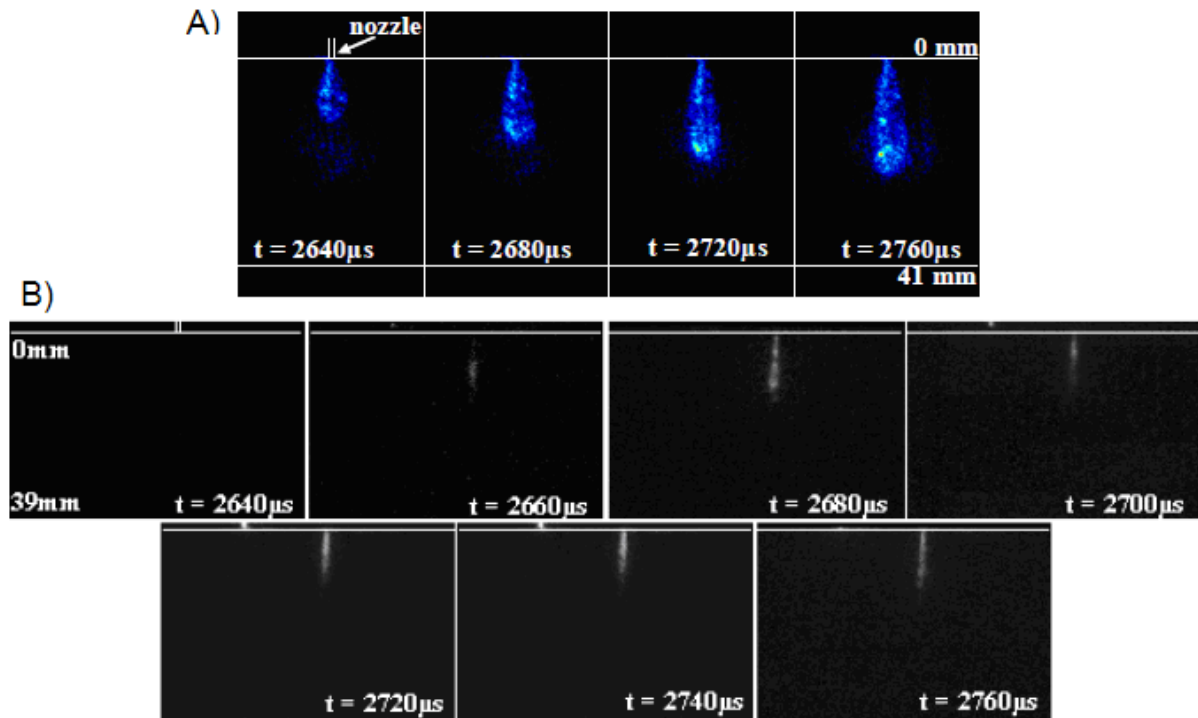


**Figure 2-26** Ignition distance  $X_i = 32$  mm, diameter of nozzle  $d = 0.8$  mm. A) Show the sequential laser Schlieren images from the experiment, B) Show the simultaneous time-resolved OH-PLIF images from the experiment. From (Sadanandan, Markus et al. 2009)

In figure 2-27, the simultaneous Schlieren and OH-PLIF images obtained from experiment with ignition distance  $X_i = 56$  mm and diameter of nozzle  $d = 1.1$  mm is shown. These images show a successful ignition of the hydrogen gas in the second vessel. The region where ignition and subsequent combustion occurs can be clearly recognized by the sudden increase in OH radicals at  $t = 3492 \mu s$ . The chemical rate of combustion exceeds the rate of cooling by entrainment and mixing with the unburned gas, and ignition is initiated. It can be seen that the first ignition occurs well within the zone reached by the jet, rather than at the jet border.

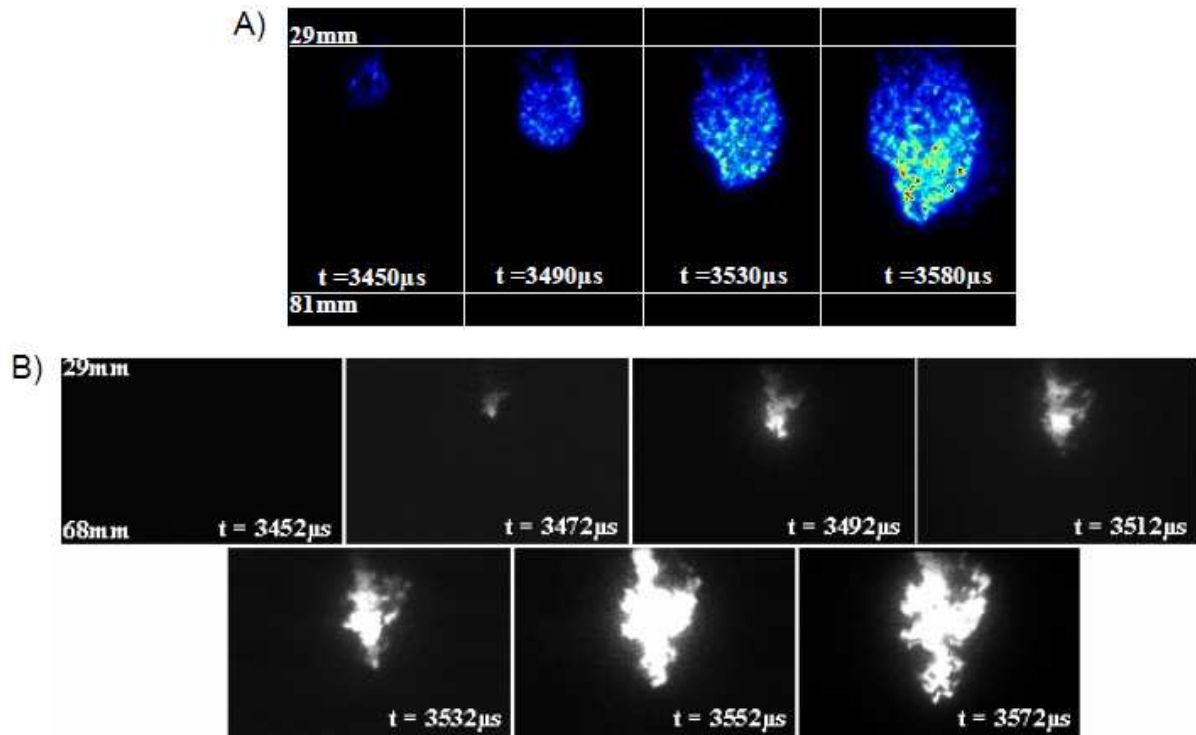


**Figure 2-27** Ignition distance  $X_i = 56\text{mm}$ , diameter of nozzle  $d = 1.1\text{mm}$ . A) Show the sequential laser Schlieren images from experiment, B) Show the simultaneous time-resolved OH-PLIF images from experiment. From (Sadanandan, Markus et al. 2009)

They pointed out that the ignition occurs at a distance of 29 mm from the nozzle exit, indicating that near the gap exit, the velocity and hence the mixing and cooling is at a higher order than the heat generation from the chemical combustion reaction. With increasing distance from the nozzle exit, velocity and mixing decreases and finally the chemical reaction rate exceeds the mixing rate leading to the ignition of the system.

In this experimental work they have successfully visualized the processes of ignition or no ignition by a hot jet of combustion products, showing the competition of the rate of cooling by mixing with unburned gas, and rate of heat production by chemical reaction. They have also verified results from other literature where it was stated that the pressure and velocity through the gap and into the second vessel is of great importance when it comes to re-ignition in the secondary vessel. They found that when the nozzle diameter is reduced, the velocity increases, increasing the rate of mixing and entrainment with cold unburned gas into the hot jet of combustion products. At the same time the time the gas is inside the nozzle and hence the time to get cooled down by the nozzle decreases, but it is believed that this is more than compensated by the increase in mixing outside the nozzle. They found that when the pressure was increased by changing the ignition position, the nozzle diameter needed for 100% re-ignition increased. This gives further evidence that the mixing rate is increased when the velocity in and out from the nozzle is increased.



#### **2.4.8 Experimental investigation of the influence of mechanical and corrosion damage of gap surfaces on the efficiency of flame gaps in flameproof apparatus (Opsvik 2010)**

The experimental research in the present work is a continuation of the work done by (Opsvik 2010). Opsvik designed and built an experimental apparatus which made it possible to inflict various damages of flame gap surfaces. This experimental apparatus is used in the work in this present thesis, and the experimental setup is described in chapter 3.4.

Opsvik, together with Grov (Opsvik et.al 2010), tested the effect of sandblasting of the flame gap surface, to create a roughness well above the permitted value of  $6.3 \mu m$ . Furthermore, a rusted surface was tested to see the effect this had upon the efficiency of the gap. Quite surprisingly, the rusted surface showed a better ability to prevent explosion transmission than an undamaged gap surface. The sandblasted gap surface gave only slightly lower MESG values compared to an undamaged gap surface. New experiments with sandblasted and rusted gap surfaces is performed in the present thesis, in another apparatus (described in chapter 3.5), and the results found by (Opsvik 2010) is compared with the new results, and discussed in chapter 4.



## **3 Experimental apparatuses and procedures**

### **3.1 Overall experimental approach**

Two different apparatuses were used in the experiments in the present work for determining MESH (detailed descriptions of the apparatuses are given in section 3.4 and 3.5). The Plane Circular Flange Apparatus, (referred to as PCFA further in this thesis), is identical with the apparatus designed and used by (Opsvik 2010) (see figure 3-5, section 3.5 for a cross section of the apparatus). This apparatus is designed to fulfil the standard MESH test requirements of the IEC standards as regards to overall geometry, gap widths etc. Some of the experiments in the PCFA are performed by Opsvik and some in cooperation with Grov, and the results are also discussed in (Opsvik 2010) and (Opsvik et.al 2010).

Performing experiments in the PCFA turned out to be quite time consuming, it was therefore decided to construct and do experiments with a simpler one-dimensional apparatus called the Plane Rectangular Slit Apparatus (referred to as PRSA further in this thesis) (see figure 3.16, section 3.5 for a cross section of the apparatus). This apparatus is smaller than the PCFA and the experiments are far less time consuming. This is mainly because gas filling went faster due to the smaller secondary chamber of only 3 litres as opposed to the 13 litres in the PCFA. The original idea was to carry out only some preliminary experiments in the PRSA with various kinds of damage of the gap surfaces. Then if the experiments gave interesting results, similar gap surfaces were to be tested in the more time-consuming PCFA. However it turned out that the experiments in the two different apparatuses with similar gap surface structures gave very good correlations, despite the large differences in the two apparatuses (this is discussed in Chapter 4). Due to this not all of the gap surface configurations are tested in both of the apparatuses. In both apparatuses the slits are changeable; this is because experiments on many different gap surface configurations with different damage should be performed. The PCFA was also slightly modified of reasons described in section 3.4.6. Experiments performed in the slightly modified PCFA are referred to as tests in the Modified Plane Circular Flange Apparatus (MPCFA) further in this thesis.

In the present work the test gas was 4.2 vol. % propane in air throughout. MESH (see section 2.3.1) was chosen as the parameter for judging whether damage of the gap surface had any significant effect on the ability of the flame gap to prevent flame transmission. A significant reduction of MESH compared with that obtained with undamaged (roughness  $< 6.3 \mu\text{m}$ ) gap surfaces (see Sections 3.4.4.1 and 3.5.4.2), would mean that the damage under experiment had destroyed the efficacy of the gap significantly.

The experimental procedures for the two apparatuses are enclosed in Appendix A.

### **3.2 Different flame gap surfaces examined in experiments in the present work**

In the experimental work performed in the present work, flame gap surfaces with different roughness and damage are examined; this include experiments of gaps with different grooves and direction of the grooves on the gap surface, gap surfaces with different fabrication and hence different roughness, rusted gap surfaces and gap surfaces with materials other than

steel. The aim of the experimental work is to examine how different damage and configurations of the flame gap surfaces will affect the Maximum Experimental Safe Gap (MESG), and to investigate the degree of damage a flame gap in Ex "d" equipment can suffer before it doesn't function satisfactorily anymore.

In table 3-1 and 3-2, all the different gap configurations, which apparatus they have been tested in and the name they have been given is listed. A more detailed description of each slit is given in this chapter. This chapter is also provided to clarify the term used for distinguish between direction of grooves on the gap surfaces, which in this work is referred to as crosswise or lengthwise grooves (see Section 3.3). The undamaged, sandblasted and rusted gap surfaces tested in the PCFA are the experiments performed by and reported by Opsvik in (Opsvik 2010), some of the experiments are done in corporation with the author of the present work, and results are also presented in (Opsvik et.al 2010).

**Table 3-1** *Overview of experiments with different gap surfaces configurations investigated in the present work*

Apparatus	Gap surface configuration	Explanation
PCFA	Undamaged	Gap surface with roughness <6.3 μm
PCFA	Sandblasted circular	Sandblasted gap surface
PCFA	Rusted circular	Rusted gap surface
PCFA	Plexiglas circular	Flange made of Plexiglas
PCFA	CH-8.2.3	8 crosswise grooves with width 2mm and depth 3mm
MPCFA	Undamaged	Gap surface with roughness <6.3 μm
MPCFA	CV-20.1.4	20 lengthwise grooves with width 1mm and depth 4mm
PRSA	Undamaged	Gap surface with roughness <6.3 μm
PRSA	Sandblasted	Sandblasted gap surface
PRSA	PH-7.2.3	7 crosswise grooves with width 2mm and depth 3mm
PRSA	PV-10.1.4	10 lengthwise grooves with width 1mm and depth 4mm
PRSA	Plexiglas plane Slit	Slit made of Plexiglas
PRSA	Rusted rectangular slit 1	Rusted gap surface
PRSA	Rusted rectangular slit 2	Rusted gap surface

**Table 3-2** Overview of experiments of gap surfaces with single lengthwise grooves through the direction of flow with different depth and width of grooves, tested in the PRSA in the present work

Apparatus	Name	Depth of groove	Width of groove
PRSA	1.4	4	1
PRSA	2.01	0.1	2
PRSA	2.02	0.2	2
PRSA	2.05	0.5	2
PRSA	2.1	1	2
PRSA	3.01	0.1	3
PRSA	3.02	0.2	3
PRSA	3.05	0.5	3
PRSA	3.1	1	3
PRSA	4.01	0.1	4
PRSA	4.05	0.5	4

### 3.3 Crosswise or lengthwise grooves

For gap surfaces with grooves it is distinguished between grooves that goes in the same direction as the flow/reaction through the flame gap, and grooves that goes in the opposite direction in relation to the direction of flow.

Figure 3-1 shows a gap with one groove in the Plane Circular Flange Apparatus, and figure 3-2 shows a gap with one groove in the Plane Rectangular Slit Apparatus. These grooves perforate the whole slit width in the same direction as the hot combustion products are being "pushed" out from the primary chamber through the flame gap and into the external chamber. These grooves are referred to as lengthwise grooves in this thesis.

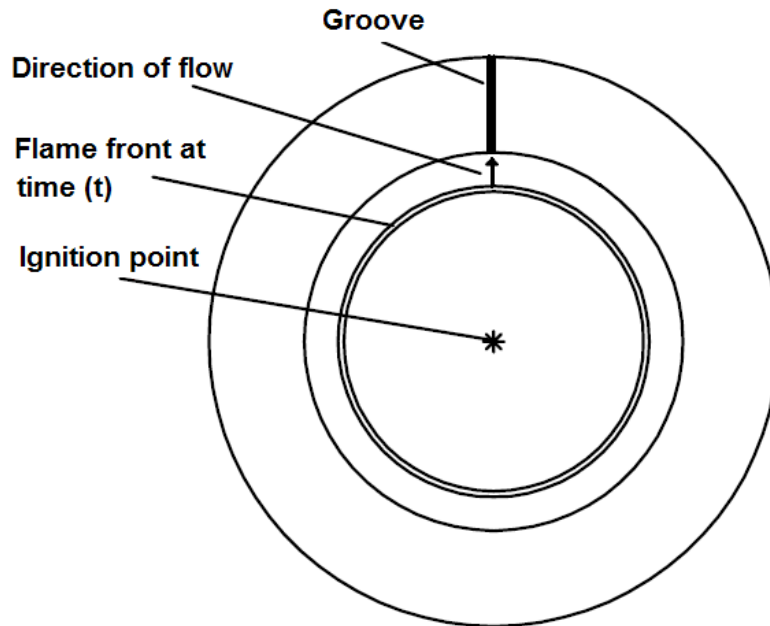


**Figure 3-1** A sketch of a gap surface with a lengthwise groove in the plane circular flange apparatus, the groove perforates through the whole slit width making a "channel" from the primary chamber to the external chamber. The ignition point in this sketch is in the centre of the primary chamber, in the experiments the ignition position was 14 mm from the gap entrance

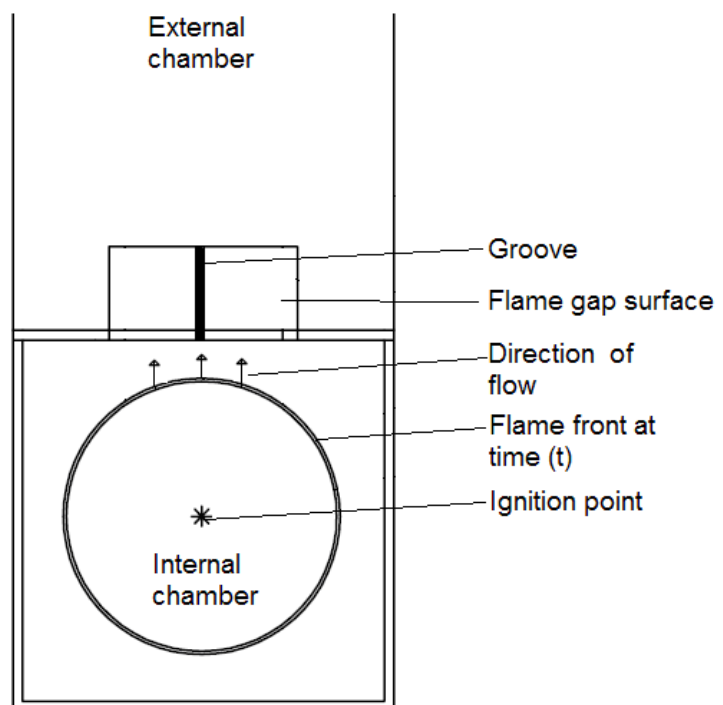


**Figure 3-2** A cross section of the cylindrical primary chamber, with a gap surface with a lengthwise groove in the plane rectangular slit apparatus, the groove perforates through the whole slit length making a "channel" from the primary chamber to the external chamber. The ignition position in this sketch is in the centre of the primary chamber, in the experiments the ignition position was 14 mm from the gap entrance

The other direction of grooves, are grooves that don't perforate the slit, and goes in the opposite direction in relation to the flow/reaction in the flame gap. These grooves are referred to as crosswise grooves in this thesis. This is illustrated in figure 3-3 and 3-4. Figure 3-3 shows the primary chamber of the Plane Rectangular Slit Apparatus, with the slit mounted on the top, the gap surface has multiple crosswise grooves. Figure 3-4 shows a gap surface with one crosswise groove in the Plane Circular Flange Apparatus.

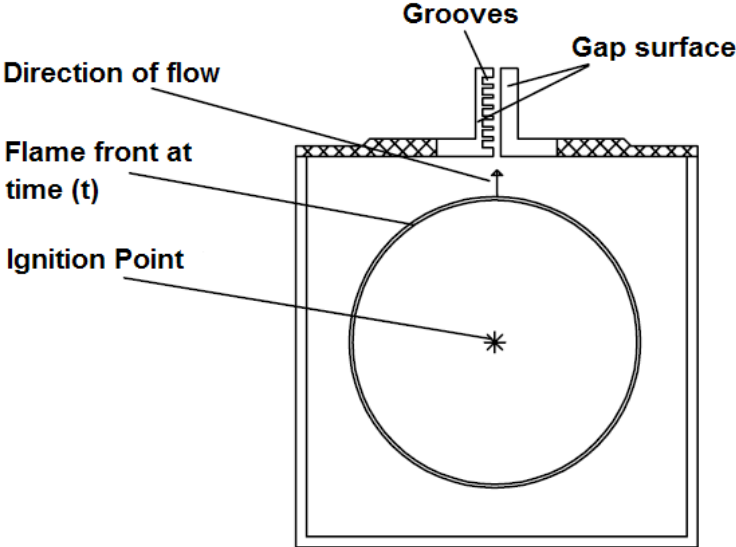


**Figure 3-3** A cross section of the cylindrical primary chamber, with a gap surface with multiple crosswise grooves in the Plane Rectangular Slit Apparatus. The ignition position in this sketch is in the centre of the primary chamber, in the experiments the ignition position was 14 mm from the gap entrance

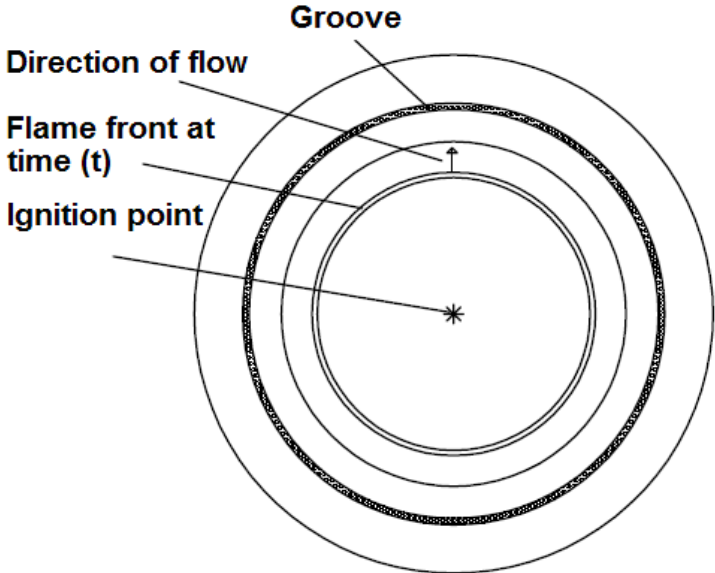


**Figure 3-4** A sketch of a slit with a single crosswise groove in the Plane Circular Flange Apparatus. The ignition position in this sketch is in the centre of the primary chamber, in the experiments the ignition position was 14 mm from the gap entrance

### 3.4 The Plane Circular Flange Apparatus (PCFA)

The Plane Circular Flange Apparatus (PCFA), was constructed and used by Opsvik in experiments in the work with (Opsvik 2010), Opsvik did some of the experiments in cooperation with Grov, and the experimental results are also presented in (Opsvik et.al 2010). A cross section of the apparatus is given in figure 3-5. In the present work additional gap surfaces were prepared and tested. The apparatus is constructed to comply with the requirements in the IEC standard. It was also desirable to make the apparatus as realistic as possible in relation to commercial Ex "d" equipment. The apparatus was built with exchangeable flanges, to permit investigation of the influence various kinds of damage of the flame gap surfaces would give. Complete construction drawings of the PCFA can be found in (Opsvik 2010)

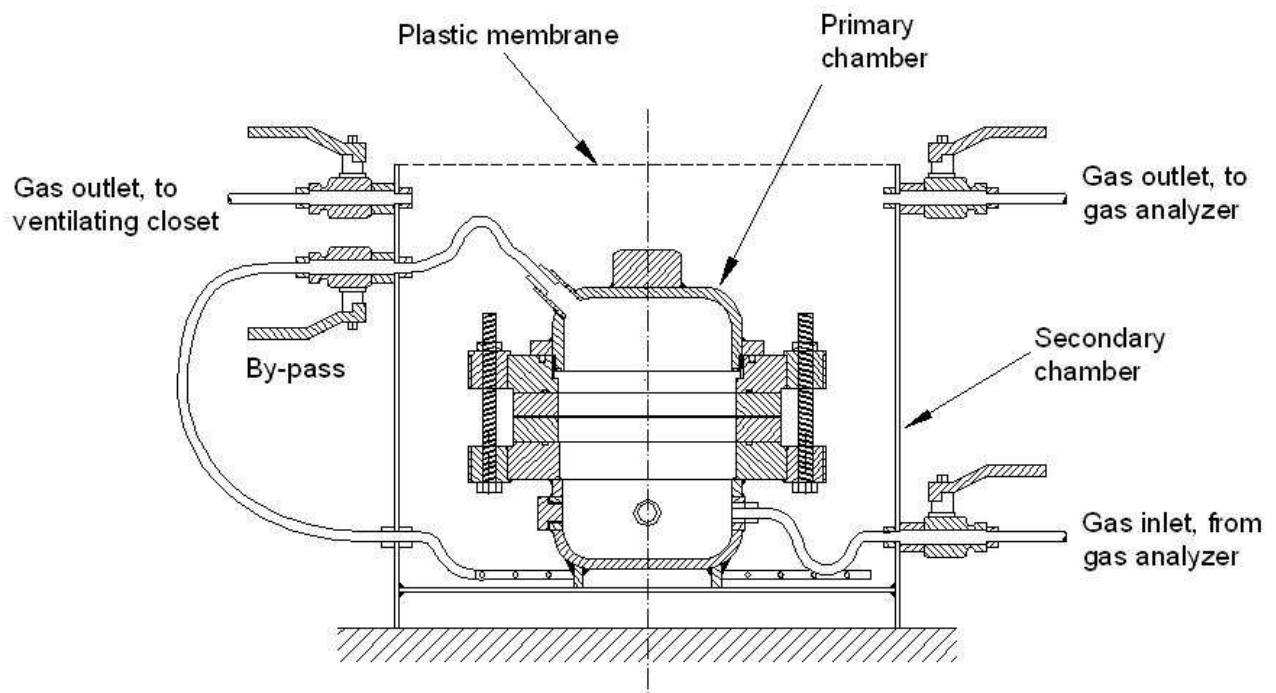


**Figure 3-5** Cross section of the Plane Circular Flange Apparatus used for determining MESG for propane/air. From (Opsvik 2010)

In (Opsvik 2010) the flange width of the different flange configurations are said to be 1 inch or 25 mm, this is a length used for research and determination of the maximum experimental safe gap (MESG) in several experimental studies e.g. (H.Phillips 1987) and this is from (IEC 2007a) given as the minimum allowed width when the volume of the enclosure is between  $500 < V < 2000$  (see Figure 2-4 in Section 2.2.2). When the length of the flange was control measured it was found to be 27 and not 25 mm as was the reported length, but this minor difference has no significant influence on the results.

#### 3.4.1 Specifications of the Plane Circular Flange Apparatus (PCFA)

The apparatus consists of two cylindrical chambers, a primary chamber with volume,  $V_p = 1150 \text{ cm}^3$ , where a spark can ignite the explosive gas mixture (the spark ignition system is



described in Appendix B), and an external chamber with volume,  $V_E = 13000 \text{ cm}^3$ , both of the chambers are made of stainless steel. A 4.2 vol. % propane/air mixture is flushed through the apparatus (see Section 3.6) a cross section of the apparatus is shown in figure 3-5.

The primary chamber is connected by a flame gap with changeable flanges with width of 27 mm to the external chamber. The flame gap opening was adjusted by placing distance "shims" between the interchangeable flanges. The distance "shims" are of standard industrial quality used in industry to set distances in motors, the distance "shims" used, made it possible to adjust the gap in steps of 0.01 mm. To get a uniform opening over the whole gap opening 4 distance "shims" were placed before assembling the flanges and tightening of bolts with a torque of 10 Nm, placing of the shims is shown in figure 3-6 and 3-7 (a more thorough description of the adjusting procedure is enclosed in Appendix A-2.1).

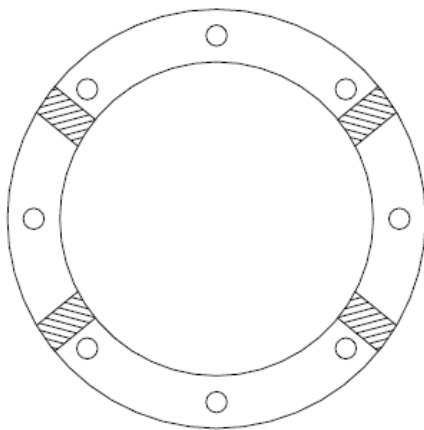


**Figure 3-6** Drawing of apparatus flange, (flame gap) with the distance shims in correct position. From (Opsvik 2010)



**Figure 3-7** Photograph of apparatus flange, (flame gap) with the calibration shims in correct position. From (Opsvik 2010)

### 3.4.2 Adjustment of ignition position in the Plane Circular Flange Apparatus (PCFA)

The ignition position in the primary chamber is adjustable in the X-direction, making it possible to vary the ignition position from being at the entrance of the gap, to the centre of the cylindrical primary chamber, shown in figure 3.8. Experimental procedures are given in Appendix A.

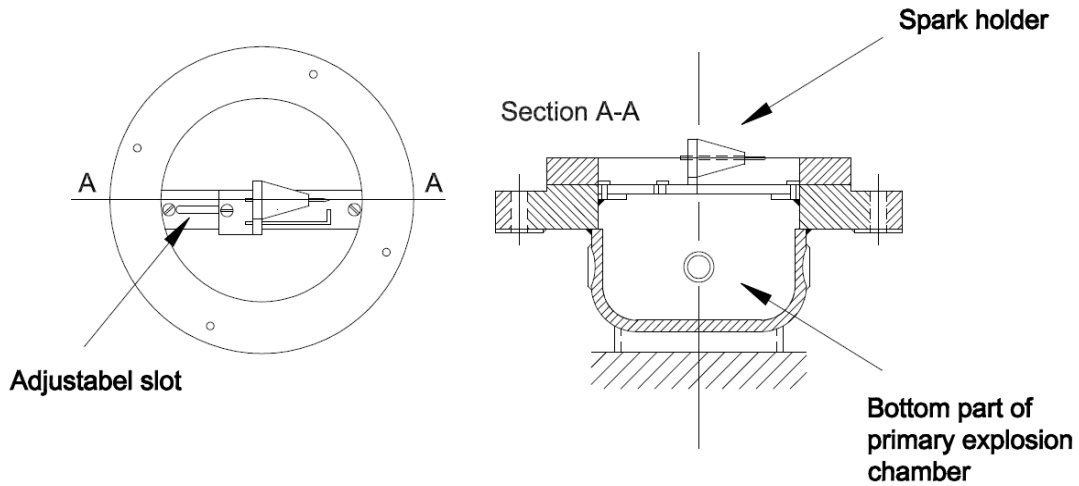


**Figure 3-8** Illustration of the adjustable spark gap. From: (Opsvik 2010)

### 3.4.3 Flow from primary chamber in the Plane Circular Flange Apparatus (PCFA)

If the ignition is centric in the primary chamber, the flame front will propagate like a spherical flame towards the gap opening, the flame is "quenched" in the gap opening. Hot combustion gases will be "pushed" out by the pressure rise in the primary chamber and be ejected from the primary chamber into the external chamber. The hot combustion gases will be vented through the circular flange and flow out in all direction as indicated in figure 3-9.

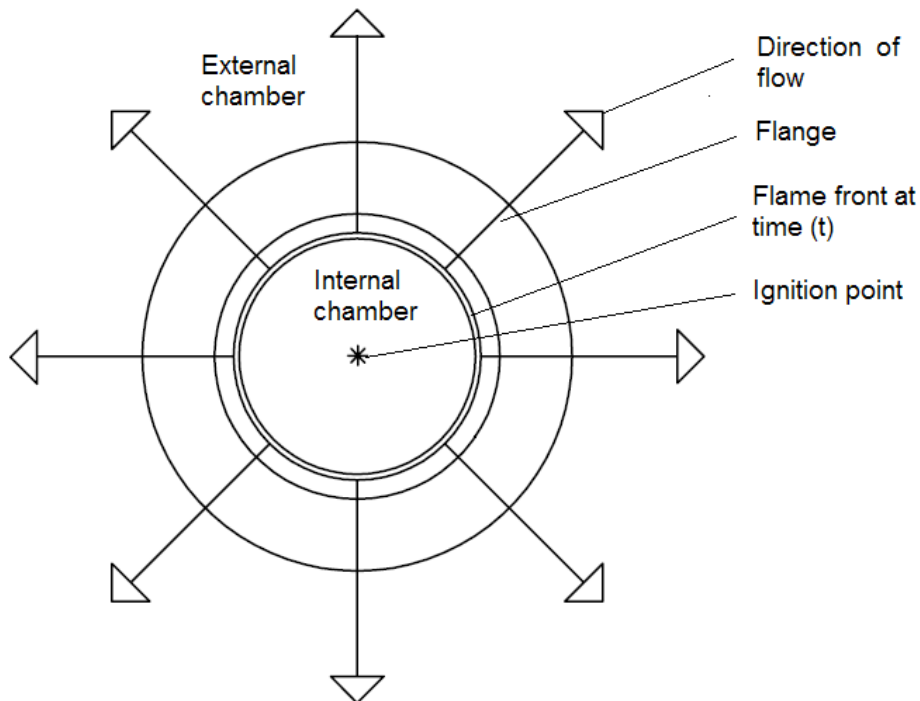


**Figure 3-9** Illustration of how the combustion products will be "ejected" out from the circular flange opening in the PCFA. The ignition position in this illustration is in the centre of the primary chamber, in the experiments the ignition position was 14 mm from the gap entrance

### 3.4.4 Flame gap surfaces tested in the Plane Circular Flange Apparatus (PCFA)

In the PCFA five different flame gap surface configurations were tested. A description of the different gap surfaces, data and motivation for testing these different slit configurations are given in this chapter. The undamaged, sand blasted and rusted gap surfaces have been tested by Opsvik and some experiments is done in company with Grov, and more data and information of these slits are available in (Opsvik 2010) and (Opsvik et.al 2010).

#### 3.4.4.1 Flame gap surfaces with different materials and roughness tested in the Plane Circular Flange Apparatus (PCFA)

**Table 3-3** Specifications of the undamaged flame gap surface examined in the PCFA

Specifications	Undamaged gap surface
Material	Carbon steel
Ra [ $\mu\text{m}$ ]	0.2
Rz [ $\mu\text{m}$ ]	2.0
Heat capacity [ $\text{J/g}\cdot\text{C}^\circ$ ]	0.452
Thermal conductivity [ $\text{W/mK}$ ]	45
Length of slit [cm]	2.7
Inner diameter [cm]	10.7
Thickness of slit [cm]	1.4



**Figure 3-10** Photograph of the undamaged flame gap surface examined in the PCFA

All gap surfaces are manufactured at the mechanical workshop at the University of Bergen; the undamaged gap surface is made of standard carbon steel. The undamaged flame gap surface are made to be within the requirement in the (IEC 2002) which states that: “*The surfaces of joints shall be such that their average roughness Ra (derived from ISO 468) does not exceed 6.3  $\mu\text{m}$* ”. The undamaged flame gap surface has an average roughness (Ra) of 0.2  $\mu\text{m}$  and an Rz of 2.0  $\mu\text{m}$ , which is well inside the requirements. Figure 3-10 shows a photograph of the undamaged flame gap surface used in the experiments. Figure 3-11 shows a sketch of the flange with dimensions, all flanges tested in the PCFA had the same dimensions.

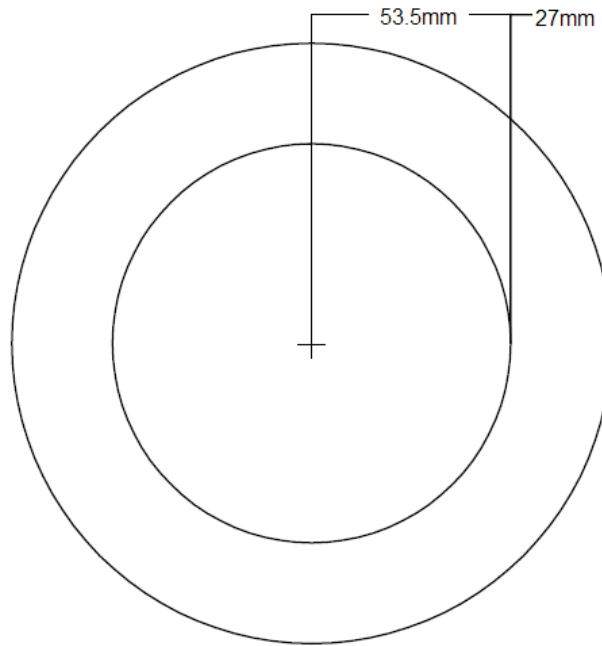


**Figure 3-11** *The dimensions of the flanges in the PCFA*

**Motivation**

Experiments with the undamaged flame gap surface were performed to have a reference value, which could be compared with gap surfaces with damage. Experiments were carried out to find the MESG value for the undamaged gap surface; it was also tested with two different ignition distance at  $\approx 0$  mm and 14 mm from the start of the gap.

**Table 3-4** *Specifications of the sandblasted flame gap surface examined in the PCFA*

Specifications	Sandblasted gap surface
Material	Carbon steel
Ra [ $\mu\text{m}$ ]	12 *
Rz [ $\mu\text{m}$ ]	65 *
Heat capacity [J/g-C°]	0.452
Thermal conductivity [W/mK]	45
Length of slit [cm]	2.7
Inner diameter [cm]	10.7
Thickness of slit [cm]	1.4

\* The values of roughness for the sandblasted surfaces are very uncertain; this is because the roughness varies over the gap surface. To get a value as accurate as possible the roughness is measured in every 36° of the circular flange, and the mean average of these 10 measurements is the value reported in the specification for each flame gap surface. Detailed description of roughness measurements and more on how the surface roughness measurements are carried out is described in Appendix D.

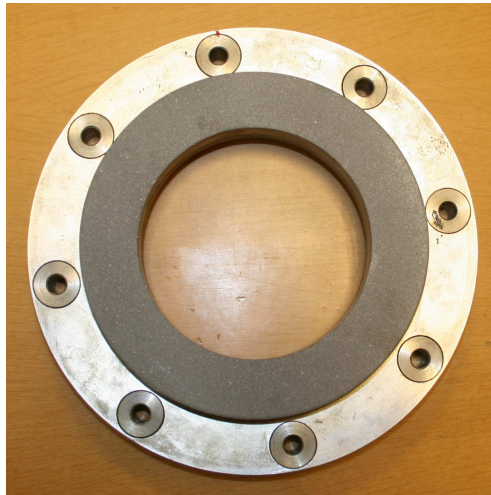


**Figure 3-12** Photograph of the sandblasted flame gap surface examined in the PCFA. From (Opsvik 2010).

### Motivation

A gap surface which in basis had similar specifications as the undamaged flame gap surface were sandblasted to create a considerable damage (see figure 3-12), with a roughness that was far above the allowed maximum value of roughness given in (IEC 2002). This was done to see how a much rougher surface will influence on the MESG and the efficiency of the gap.

**Table 3-5** Specifications of the rusted flame gap surface examined in the PCFA

Specifications	Rusted circular gap surface
Material	Carbon steel
Ra [ $\mu\text{m}$ ]	6,1*
Rz [ $\mu\text{m}$ ]	28*
Heat capacity [J/g-C°]	1.47*
Thermal conductivity [W/mK]	45*
Length of slit [cm]	2.5
Width of slit [cm]	5.63
Thickness of slit [cm]	0.5

\* The value of roughness for the rusted flame gap surface is very uncertain; this is because the degree of rust and pitting varies a lot over the whole gap surface. The heat capacity and thermal conductivity may also change due to the formation of iron oxides from the rust on the slit steel surface.



**Figure 3-13** Photograph of the sandblasted flame gap surface examined in the PCFA. From (Opsvik 2010).

A gap surface which in basis had the same specifications like the undamaged flame gap surface was exposed to a corrosive environment to get rust formation on the surface. Figure 3-13 shows a photograph of the rusted flame gap surface used in the experiments. The rusted steel surface was prepared by hanging the flanges outdoors at the sea side, midway between high and low tide, for about two months.

### Motivation

Rust formation is one of the most common damages that can occur on equipment that operates in an outdoor environment. Equipment that is used in offshore operations for example Ex "d" equipment, operates in a highly corrosive environment (because the presence of sea water). Therefore it is a high probability for rust formation on this type of equipment, if the material used is not stainless steel or other non-corrosive materials.

The aim for testing a gap surface with rust damage is to examine how the rust formation in the flame gap will influence the MESG value and the efficiency of the gap.

**Table 3-6** Specifications of the Plexiglas flame gap surface examined in the PCFA

Specifications	Plexiglas gap surface
Material	Plexiglas
Ra [ $\mu\text{m}$ ]	2.9
Rz [ $\mu\text{m}$ ]	15
Heat capacity [ $\text{J/g}\cdot\text{C}^\circ$ ]	1.47
Thermal conductivity [ $\text{W/mK}$ ]	0.2
Length of slit [cm]	2.7
Inner diameter [cm]	10.7
Thickness of slit [cm]	1.4



**Figure 3-14** *Photograph of Plexiglas flame gap surface examined in experiments in the PCFA*

A slit made of Plexiglas or Poly(methyl methacrylate) (PMMA), were made at the mechanical workshop at the University of Bergen and tested in the PCFA, shown in figure 3-14.

**Motivation:**

The gap surface made of Plexiglas was made to examine the effect a different material of the flame gap will have upon the MESG value and the efficiency of the gap.

### **3.4.5 Flame gap surfaces with grooves tested in the Plane Circular Flange Apparatus (PCFA)**

Gap surfaces with different grooves are tested in the PCFA, this chapter describes the naming of the gap surfaces with grooves, the specifications and motivation for testing the different gap surfaces with grooves are also given.

#### **3.4.5.1 Naming of gap surfaces with grooves**

The name given to slits with grooves refers to the configuration of the gap surface. The first letter in the name tells us whether the slit is used in the Plane Circular Flange Apparatus (PCFA) or the Plane Rectangular Slit Apparatus (PRSA). The second letter in the name stands for Horizontal (Crosswise) or Vertical (Lengthwise) which is the direction of the grooves on the gap surface as described in Section 3.3. The first number in the name refers to the number of grooves on the current gap surface, the second number refers to the width of the groove, and the third number refers to the depth of the groove.

Example: A slit with name: **CV-20.1.4**: the C, tells us that it is a slit used for experiments in the Plane Circular Flange Apparatus (PCFA), the V, tells us that the grooves are Vertical (lengthwise). The numbers 20, 1 and 4 refers to respectively number of grooves, width of grooves and depth of grooves on the gap surface.

**Table 3-7** Specifications of the CH-8.2.3 flame gap surface examined in the PCFA

Specifications	Gap surface CH-8.2.3
Material	Carbon steel
Ra [ $\mu\text{m}$ ]	0.2
Rz [ $\mu\text{m}$ ]	2.0
Heat capacity [ $\text{J/g}\cdot\text{C}^\circ$ ]	0.452
Thermal conductivity [ $\text{W/mK}$ ]	45
Length of slit [cm]	2.7
Inner diameter [cm]	10.7
Thickness of slit [cm]	1.4
Number of grooves	8
Width of grooves [mm]	2.0
Depth of grooves [mm]	3.0



**Figure 3-15** Photograph of flame gap surface CH-8.2.3, with eight crosswise grooves with width:2.0 mm and depth: 3.0 mm, investigated in experiments in the PCFA

Eight Grooves 2.0 mm wide and 3.0 mm deep, were milled into a flange which in basis had the same specifications as the undamaged flame gap surface. The grooves follow the circular flange around the gap surface, these grooves are referred to as crosswise grooves (see Section 3.3). Figure 3-15 shows a photograph of the gap surface, and figure 3-16 shows a figure with the dimensions of the gap surface and the grooves on the gap surface. A similar gap surface is tested in the PRSA, gap surface PH-7.2.3 (see Section 3.5.4.4, figure 3-32 and 3-33).



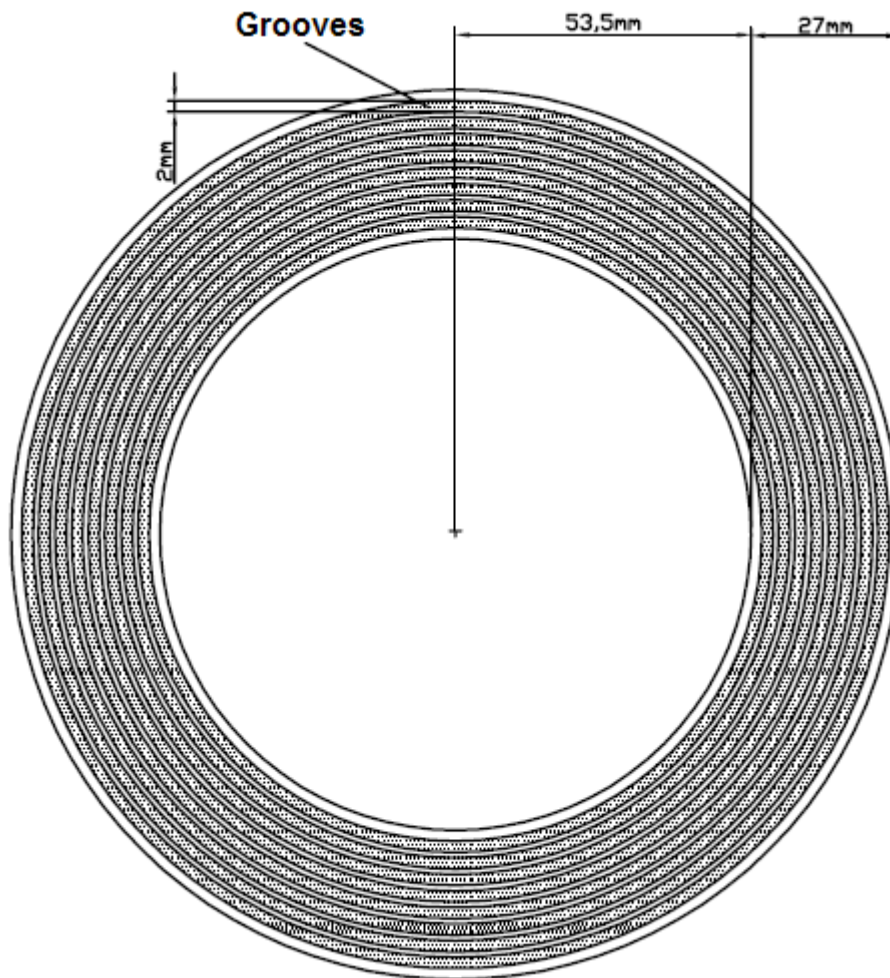


**Figure 3-16** Dimensions of the gap surface CH-8.2.3 with eight crosswise grooves with width: 2.0 mm and depth: 3.0 mm, examined in the PCFA

**Motivation:**

This flame gap surface was made to examine how large crosswise grooves on the gap surface would affect the MESG and the efficiency of the gap. When damage occurs on a flame gap for example from dismounting of the enclosure under inspection of a flame gap, the operator may scratch the surface of the gap with a screwdriver. The direction of this scratch/groove can go through the width of the gap in the direction of flow<sup>1</sup>, or just be a groove for example in the middle of the flame gap. The aim with the experiments with this gap surface was to get an understanding of how different damage influences the efficiency of the gap, and the MESG due to the direction of the damage on the flame gap surface.

Another interesting aspect of these grooves is that they most likely create more initial turbulence in the external chamber and turbulence in the gap, when the pressure rise in the primary chamber "pushes" the hot combustion products through the gap. It was than possible to examine whether the turbulence generation in the gap increases or decreases the probability of re-ignition in the secondary chamber.

---

<sup>1</sup> Direction of flow refers to the direction that the combustion zone will have in relation to the direction of the grooves on the gap surface.

### 3.4.6 Slightly modified Plane circular Flange Apparatus (MPCFA)

When experiments with the gap surface of Plexiglas were to be tested in the PCFA, it was revealed that the PCFA used by (Opsvik 2010) had some limitations when it came to ensuring that the gap opening was uniform over the whole opening. Plexiglas which is a less rigid material than steel was bent when the gap was fastened with torque. This made the gap opening larger near the distance "shims" and smaller between the distance "shims". This is shown in figure 3-17. This was because when the flanges in the primary chamber was assembled, the upper and the lower flange was fastened by applying a torque of 10 Nm on the screws over the distance "shims", but also over parts of the flange where no distance "shims" were placed.

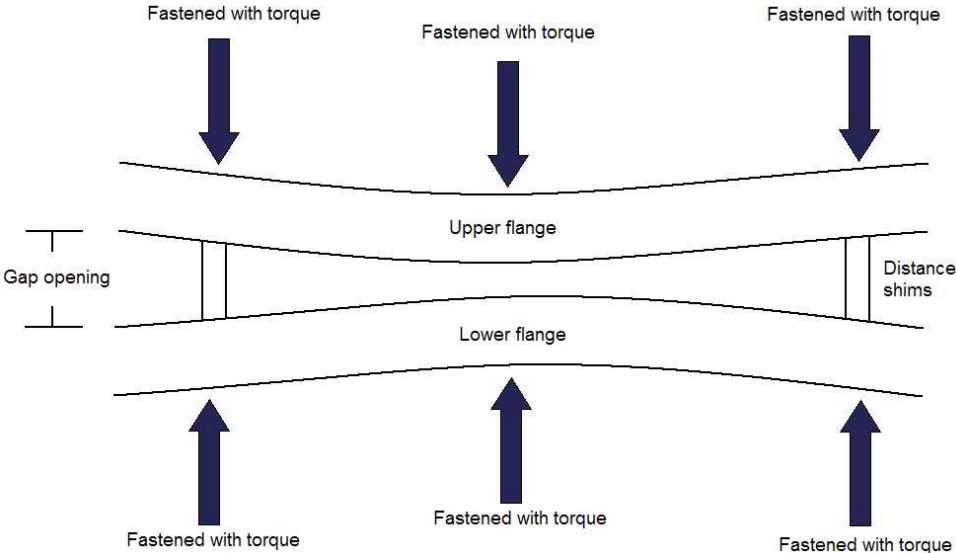


**Figure 3-17** The photograph in the top shows how the gap is pinched more together where the screws are tightened and no distance shims is placed. It is illustrated in the bottom figure to get a better understanding of the effect. The illustration is somewhat exaggerated

Due to this, the gap opening became smaller on the part of the flanges where the flanges was fastened with torque and no distance "shims" was placed, as shown in figure 3-17. This effect was discovered on the Plexiglas gap surface, but the same will also to some extent occur with

other slits of more rigid metal as steel, but it will not give such a dramatic error in the uniformity of the gap opening. Nevertheless this showed that efforts had to be made to ensure that the gap opening was uniform over the whole flange opening. It was also discovered that the lower flange was fastened with only three screws, because of an error made when designing the apparatus. This made the part of the lower slit which was not fastened to be higher than the rest of the slit giving further error in the gap opening distance.

Because of these uncertainties for assuring that the gap opening was uniform, the PCFA was slightly modified. The PCFA was modified so that the lower slit could be fastened with 4 screws to assure that the flange was at the same level over the whole length. It was also decided to only apply torque on the screws that were placed over the 4 distance shims to counter the effect discussed above. Reference experiments were performed to compare the MESH values found by (Opsvik 2010) and values obtained after the apparatus was modified. Flanges with new gap surface configurations were tested in this slightly modified apparatus. From control measurements of the gap opening, it showed that by applying these minor modifications there was a large improvement when it came to ensuring that the gap opening was uniform over the whole flange opening. The results from the slightly modified PCFA are referred to as the Modified Plane Circular Flange Apparatus (MPCFA).

### 3.4.7 Flame gap surfaces tested in the Modified Plane Circular Flange Apparatus (MPCFA)

**Table 3-8** Specifications of the undamaged flame gap surface examined in the MPCFA

Specifications	Undamaged gap surface
Material	Carbon steel
Ra [ $\mu\text{m}$ ]	0.2
Rz [ $\mu\text{m}$ ]	2.0
Heat capacity [ $\text{J/g}\cdot\text{C}^\circ$ ]	0.452
Thermal conductivity [ $\text{W/mK}$ ]	45
Length of slit [cm]	2.7
Inner diameter [cm]	10.7
Thickness of slit [cm]	1.4



**Figure 3-18** Photograph of the undamaged slit used in the experiments in the PCFA

This flange has the same specifications as the undamaged flame gap surface, tested in the original Plane Circular Flange Apparatus (PCFA).

**Motivation:**

The undamaged flange was tested in the slightly Modified Plane Circular Flange Apparatus (MPCFA), this was done to see how the changes in the apparatus affected the value of the MESG.

**Table 3-9** Specifications of the CV-20.1.4 flame gap surface examined in the MPCFA

Specifications	CV-20.1.4 gap surface
Material	Carbon steel
Ra [ $\mu\text{m}$ ]	0.2
Rz [ $\mu\text{m}$ ]	2.0
Heat capacity [ $\text{J/g}\cdot\text{C}^\circ$ ]	0.452
Thermal conductivity [ $\text{W/mK}$ ]	45
Length of slit [cm]	2.7
Inner diameter [cm]	10.7
Thickness of slit [cm]	1.4
Number of grooves	20
Width of grooves [mm]	1.0
Depth of grooves [mm]	4.0
Area of Groves [ $\text{mm}^2$ ]	80



**Figure 3-19** Photograph of the CV-20.1.4 flame gap surface, with twenty lengthwise grooves with width: 1.0 mm and depth: 4.0 mm, investigated in experiments in the MPCFA

Twenty grooves of 1.0 mm width and depth 3.0 mm were milled into a flange which in basis had the same specifications as the undamaged flame gap surface. The grooves on this flange goes through the whole flange-width and makes "channels" in the same direction as the direction of flow/reaction. The direction of these grooves is referred to as lengthwise grooves in this thesis (see Section 3.3). Figure 3-19 shows a photograph of the flange, and figure 3-20 shows the dimensions of the flange and the grooves on the gap surface.

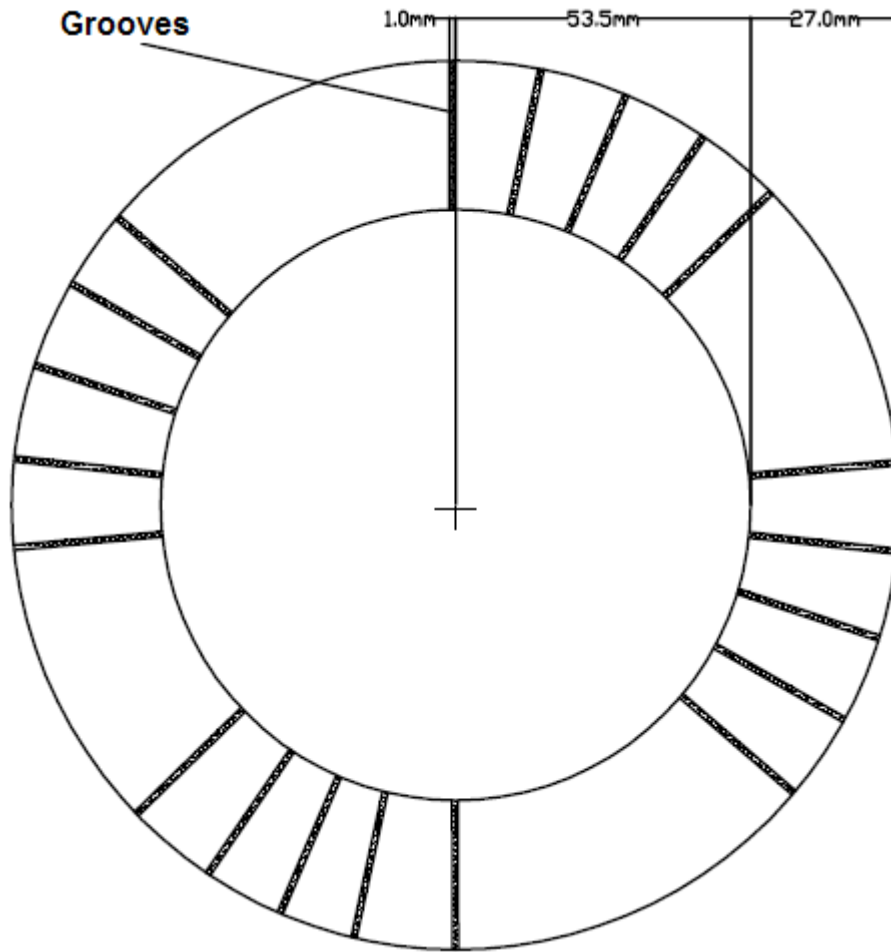


**Figure 3-20** *The circular flange CV-20.1.4 with dimensions*

**Motivation:**

This slit was made to examine the effect of lengthwise grooves that perforates through the whole slit width. This is to further examine how the direction of damage influences on the efficiency of the gap, compared to the crosswise grooves on the gap surface CH-8.2.3 (see Section 3.4.5 figure 3-15 and 3-16). And to compare with the similar gap surface with lengthwise grooves tested in the PRSA (see Section 3.5.4.4, figure 3-33 and 3-34)

It was from preliminary tests in PRSA found that lengthwise grooves of 1 mm width and depth 4 mm, did not affect the MESG value, and hence not the efficiency of the gap. It was therefore resolved to make 20 grooves of 1 mm width and depth 4 mm, to examine whether the MESG then was affected by the grooves. Another motive for making this slit was to see whether multiple grooves with a width that did not support explosion transmission, could create a turbulent regime that made probability of re-ignition in the secondary chamber higher or lower.

### 3.5 The Plane Rectangular Slit Apparatus (PRSA)

As mentioned in section 3.1, the Plane Rectangular Slit Apparatus (PRSA), is a smaller and simpler apparatus than the PCFA, giving a much shorter time between each experiment compared to the PCFA. A cross section of the apparatus is shown in figure 3-21.

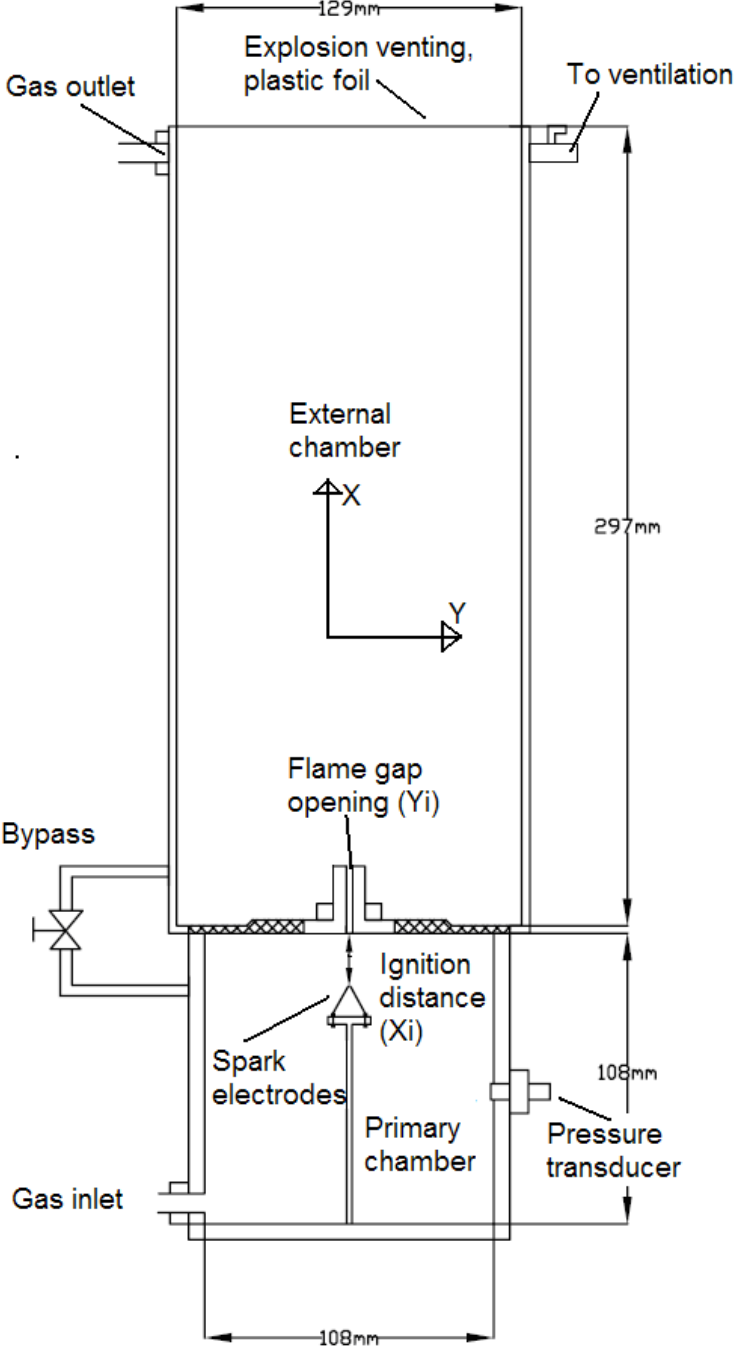


**Figure 3-21** A Cross section of the cylindrical PRSA, with a  $1000\text{ cm}^3$  primary chamber, and a plane flame gap with 25mm width, used for determining MESG for different gap surfaces in propane/air

The original idea was to carry out only some preliminary experiments in the PRSA with various kinds of damage of the gap surfaces, and to verify the results found in the PCFA. Then if the experiments gave interesting results, similar gap surfaces were to be tested in the more time-consuming PCFA. However it turned out that experiment in the two different apparatuses with similar gap surface structures gave very good correlations despite the large differences in the two apparatuses (this is discussed in Chapter 4). Because of this not all of the gap surface configurations are tested in both of the apparatuses

The PRSA is a modified version of the apparatus designed by Prof. R K. Eckhoff, and used by (Larsen 1998) and (Einarsen 2001). Einarsen started the work of investigating the effect of damage of flame gap surfaces (discussed in Section 2.4.6); the need for modification of the apparatus used by Einarsen was to make experiments more reproducible. It was discovered that the adjustment of the gap openings in Einarsen`s work were inaccurate. He used distance pieces that were made with equipment which had low accuracy, so the actual value of the distance pieces varied a lot. When the gap opening was to be fastened the gap was only tightened in the upper part of the gap, and there is no information on the value of torque used when assembling the gap. This led to a gap opening which was not uniform over the whole gap opening. The opening was smaller in the upper part where screws were used to fasten the gap, and the gap opening was larger in the start of the gap opening.

Due to the inaccuracy and insufficient descriptions of the experimental procedures in (Einarsen 2001), the apparatus was modified. It was determined to use commercial produced distance "shims", used in the industry for setting distances in motors. These distance "shims" made it possible to vary the gap opening in steps of 0.01 mm. The apparatus were further improved by using a low torque of 20 cNm, and the gap was fastened both in the upper part and in the start of the gap in the lower part. This was done to get a uniform gap opening over the whole gap opening, this is shown in figure 3-22 and 3-23. Figure 3-22 is a photograph of the upper part of the gap with the distance "shims" placed in the gap, the screws which were tightened with torque can be seen. Figure 3-23 is a photograph of the underside of the gap, the numbers 1-4 is the screws fastened with torque, to get a uniform gap opening over the whole gap opening, the distance shims can be seen on the sides of the gap.

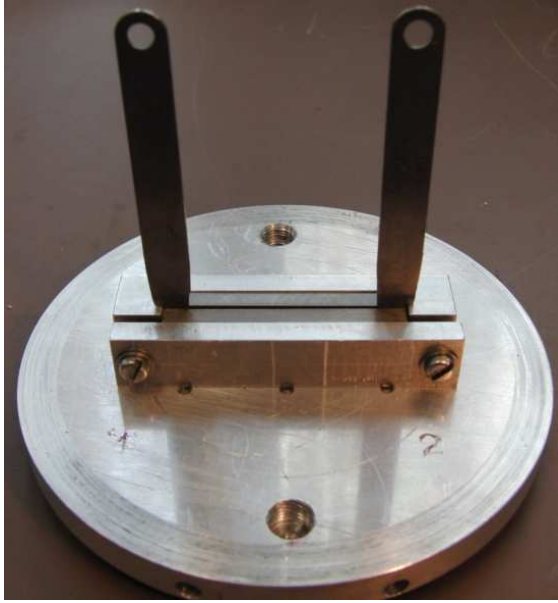


**Figure 3-22** Photograph of the upper part of the flame gap in the PRSA, with distance "shims" placed, the gap is fastened with a low torque applied on the screws, seen in the photograph

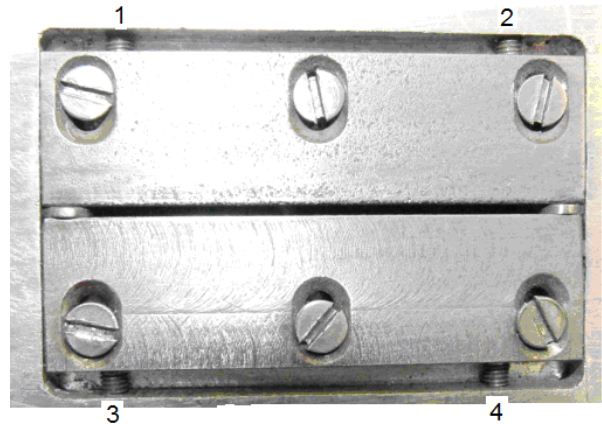


**Figure 3-23** Photograph of the lower part of the flame gap in the PRSA, this is the part which is inside the primary chamber. The numbers 1-4 on the photograph is the screws which are tightened with the same torque as the screws in the upper part of the flame gap, ensuring a uniform gap opening over the whole width of the gap. On the sides of the flame gap the distance "shims" can be seen

Another reason for using a low torque when setting the gap opening distance, was to counter the effect which were found in (Opsvik 2010). In the experiments with rusted gap surfaces the distance "shims" were compressed into the porous rusted surface, making the actual gap opening smaller than the actual value of the shims used for setting the gap opening. Another inaccuracy when dealing with uniformity over the gap opening in the PCFA is that torque was applied on screws over the gap where no distance "shims" were placed, and this made the actual gap opening smaller some places around the flange opening, and hence the gap opening were not uniform over the whole flange opening (this is discussed in Section 3.4.6).

### 3.5.1 Specifications of the Plane Rectangular Slit Apparatus (PRSA)

The apparatus consists of two cylindrical chambers, a primary chamber with volume,  $V_p \approx 1000 \text{ cm}^3$ , where a spark can ignite the explosive gas mixture (the spark generator system is described in Appendix B), and a external chamber with volume,  $V_E \approx 3000 \text{ cm}^3$ . The primary chamber is made of steel and the external chamber made of Perspex. A propane/air mixture is flushed through the apparatus (see Section 3.6) a cross section of the apparatus is shown in figure 3-21.

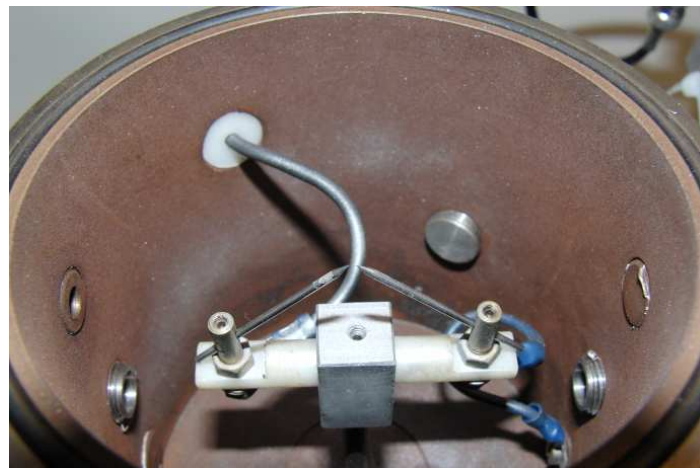
The primary chamber is connected by a flame gap with changeable rectangular slits with width of 25 mm to the external chamber; the length of the slits is 56 mm. The flame gap opening was adjusted by placing distance "shims" between the interchangeable slits (see



figure 3-22 and 3-23), the shims are of standard industrial quality used in industry to set distances in motors, the distance "shims" made it possible to adjust the gap in steps of 0.01 mm. To get uniform opening over the whole gap opening, 2 shims were placed before assembling the flanges, and tightening the screws with a torque of 20 cNm. To further insure a uniform gap opening over the whole slit width, the gap was fastened both in the upper and lower part of the gap as shown in figure 3-22 and 3-23 (a more thorough description of the adjusting procedure is enclosed in Appendix A-2.4).

### **3.5.2 Adjustment of ignition position in the Plane Rectangular Slit Apparatus (PRSA)**

The ignition position in the primary chamber is adjustable, making it possible to vary the ignition position from being in the start of the gap, to be almost in the bottom of the primary chamber. The spark electrodes are shown in the photograph of the primary chamber in figure 3-24. When experiments to find the MESG for different gap surfaces was performed the ignition distance was 14 mm from the entrance of the gap. Experimental procedures are given in Appendix A.



**Figure 3-24** *Photograph of the spark electrodes in the primary chamber in the PRSA, the ignition position could be varied up towards the gap opening and, down away from the gap opening*

### **3.5.3 Flow from primary chamber in the Plane Rectangular Slit Apparatus (PRSA)**

If the ignition is centric, the flame front will spread like a spherical flame and be quenched in the gap opening. Hot combustion products will be "pushed" out by the pressure rise in the primary chamber and be "ejected" from the primary chamber into the external chamber (see figure 3-25). Compared to the PCFA, the venting area is smaller and the resulting explosion pressure will be of a higher order in this apparatus than in the PCFA (see Section 3.4.3, figure 3-9).

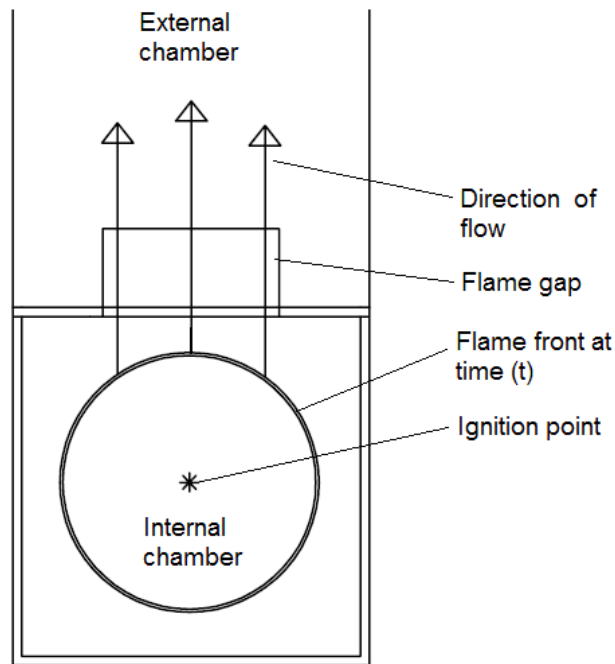


**Figure 3-25** Illustration of how the combustion products will be vented out from the rectangular gap opening in the PRSA. The ignition position in this illustration is in the centre of the primary chamber, in the experiments the ignition position was 14 mm from the gap entrance

### 3.5.4 Flame gap surfaces tested in the Plane Rectangular Slit Apparatus (PRSA)

In the PRSA eighteen different flame gap surface configurations were tested, some of the gap surfaces tested had the same specifications except from change in width and depth of grooves on the gap surfaces. Some of the gap surfaces tested had approximately similar gap surface structure as gap surfaces tested in the PCFA, the results obtained from the similar gap surfaces in the different apparatuses is discussed in Chapter 4. A description of the different gap surfaces, data and motivation for testing these different slit configurations are given in this chapter. Experiments to find the ignition point most favourable for re-ignition in the external chamber is also performed and described here.

#### 3.5.4.1 Experiments to find the ignition point most favourable for re-ignition in the secondary chamber

Experiments were performed with the undamaged flame gap surface to find the ignition point in the primary chamber, which was the point that gave the lowest gap opening in respect to re-ignition in the secondary chamber.

#### **Motivation:**

When dealing with Ex "d" equipment an ignition can occur anywhere inside the enclosure, it was therefore necessary to find the most "dangerous" ignition position. This is the ignition position which gives the lowest gap opening in respect to re-ignition in the secondary

chamber. This ignition position was than the position that all the slits with different gap surface configurations were to be tested with.

**3.5.4.2 Flame gap surfaces with different materials and roughness tested in the (PRSA)**

**Table 3-10** *Specifications of the undamaged flame gap surface examined in the PRSA*

Specifications	Undamaged gap surface
Material	Carbon steel
Ra [ $\mu\text{m}$ ]	0.2
Rz [ $\mu\text{m}$ ]	2.0
Heat capacity [ $\text{J/g}\cdot\text{C}^\circ$ ]	0.452
Thermal conductivity [ $\text{W/mK}$ ]	45
Length of slit [cm]	2.5
Width of slit [cm]	5.63
Thickness of slit [cm]	0.5

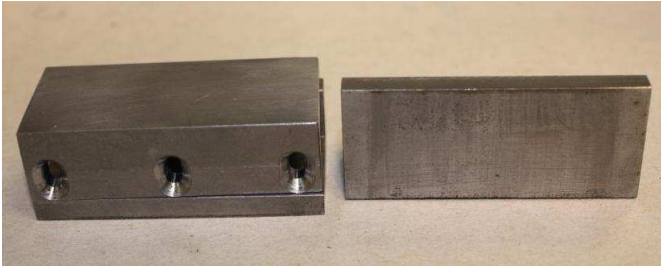


**Figure 3-26** *Photograph of the undamaged flame gap surfaces examined in the PRSA*

The undamaged flame gap surface is made of carbon steel and made to be within the requirement in the (IEC 2002), with respect to surface roughness less than  $6.3 \mu\text{m}$ . This gap surface is similar to the flange with undamaged gap surface tested in the PCFA. Figure 3-26 shows a photograph of the slit, figure 3-27 shows the slit with dimensions. The dimensions of the slit are the same in all experiments with different flame gap surface configurations examined in the PRSA.

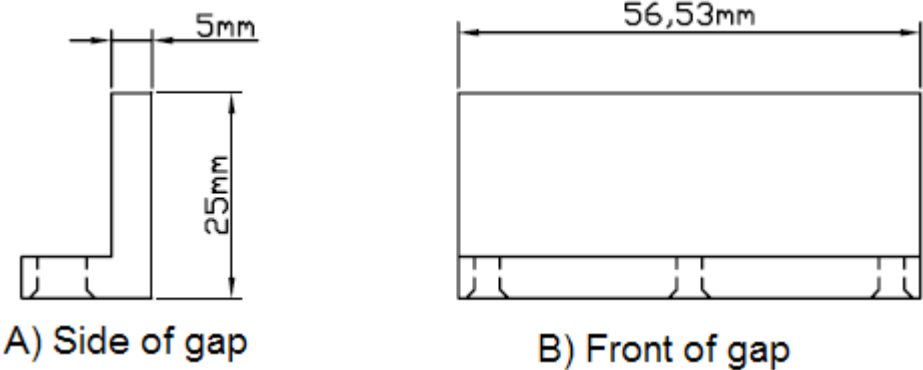


**Figure 3-27** *The undamaged flame gap surface examined in the PRSA with dimensions.*

**Motivation:**

The undamaged flame gap surfaces were made to have a MESG reference which could be compared with the undamaged slit in the PCFA, and to compare with other flame gap surfaces with damage examined in the PRSA.

**Table 3-11** Specifications of the sandblasted flame gap surface examined in the PRSA

Specifications	Sandblasted gap surface
Material	Carbon steel
Ra [ $\mu\text{m}$ ]	12 *
Rz [ $\mu\text{m}$ ]	65 *
Heat capacity [J/g-C°]	0.452
Thermal conductivity [W/mK]	45
Length of slit [cm]	2.7
Inner diameter [cm]	10.7
Thickness of slit [cm]	0.5

\* The value of roughness of the sandblasted surfaces is very uncertain; this is because the roughness varies over the slit-surface. To get a value as accurate as possible, roughness is measured in 3 positions on the slit, and the mean average of the 3 measurements is the value reported in the specification for each gap surface, a detailed description of roughness measurements and more on how the surface roughness measurements are carried out is described in Appendix C.

**Motivation:**

A gap surface which in basis had a roughness equal to the undamaged flame gap surface were sandblasted to make a considerable damage, with a roughness that was far above the allowed maximum value of roughness given in (IEC 2002). This was done to see how a much rougher surface will influence on the MESG and the efficiency of the gap. Sandblasted slits were tested in both apparatuses to compare the results.

**Table 3-12** Specifications of the Plexiglas flame gap surface examined in the PRSA

Specifications	Plexiglas gap surface
Material	Carbon steel
Ra [ $\mu\text{m}$ ]	2.9
Rz [ $\mu\text{m}$ ]	14.6
Heat capacity [J/g-C°]	1.47
Thermal conductivity [W/mK]	0.2
Length of slit [cm]	2.5
Width of slit [cm]	5.63
Thickness of slit [cm]	0.5

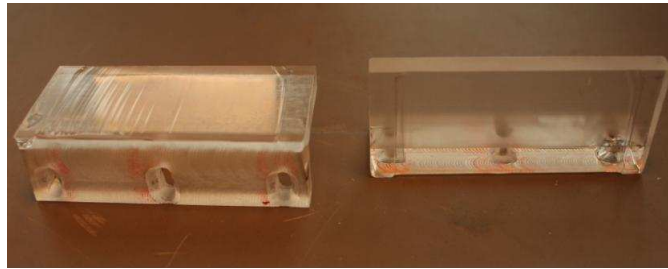


**Figure 3-28** Photograph of the Plexiglas gap surfaces examined in the PRSA.

A slit made of Plexiglas or Poly(methyl methacrylate) (PMMA), were made at the mechanical workshop at University of Bergen and tested in the PRSA.

**Motivation:**

The Plexiglas slit was made to examine the effect a different material of the flame gap will have upon the MESG value and the efficiency of the gap.

**3.5.4.3 Rusted flame gap surfaces examined in the Plane Rectangular Slit Apparatus (PRSA)**

Experiments with two set of slits with rusted gap surfaces have been tested in the PRSA. The rusted steel surface was prepared by hanging the flanges outdoors at the sea side, midway between high and low tide, for about two months. One of the slits was sandblasted before exposure to saltwater; the other was of standard machined carbon steel with the same specifications as the undamaged gap surface before exposure to saltwater.

**Table 3-13** Specifications of the rusted flame gap surface 1, examined in the PRSA

Specifications	Rusted gap surface 1
Material	Carbon steel
Ra [ $\mu\text{m}$ ]	5.3*
Rz [ $\mu\text{m}$ ]	30.5*
Heat capacity [ $\text{J/g}\cdot\text{C}^\circ$ ]	1.47*
Thermal conductivity [ $\text{W/mK}$ ]	45*
Length of slit [cm]	2.5
Width of slit [cm]	5.63
Thickness of slit [cm]	0.5

\* The value of roughness of the corroded surfaces is very uncertain; this is because the degree of rust and pitting vary a lot over the gap surface. The heat capacity and thermal conductivity may also change due to the formation of iron oxides from the rust on the gap steel surface. To get a value as accurate as possible, roughness is measured in 3 positions on the slit, and the mean average of the 3 measurements is the value reported in the specification for each slit, detailed description of roughness measurements and more on how the surface roughness measurements are carried out is described in Appendix C.

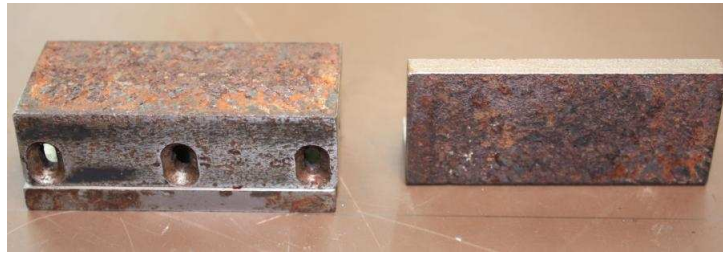


**Figure 3-29** Photograph of rusted gap surface 1 examined in the PRSA

A gap surface which in basis had a roughness equal to the undamaged flame gap surface was exposed to a corrosive environment to get rust formation on the surface. The rusted steel surface was prepared by hanging the slits outdoors at the sea side, midway between high and low tide, for about two months.

**Motivation:**

Rust formation is one of the most common damages that can occur on equipment that operates in an outdoor environment. Equipment that is used in offshore operations for example Ex "d" equipment, operates in a highly corrosive environment (because of the presence of sea water). Therefore it is a high probability for rust formation on this type of equipment, if the material used is not stainless steel or other non-corrosive materials.

The motivation for testing gap surfaces with rust damage is to see how rust formation in the flame gap influences on the MESH value and the efficiency of the gap. Experiments with rusted surfaces was first performed in the PCFA by (Opsvik 2010), the reason for testing rusted slit surfaces also in the PRSA is to validate the results found in the PCFA, and to see if the results were equal in a another apparatus.

**Table 3-14** Specifications of the rusted flame gap surface 2, examined in the PRSA

Specifications	Rusted gap surface 2
Material	Carbon steel
Ra [ $\mu\text{m}$ ]	11.2*
Rz [ $\mu\text{m}$ ]	58*
Heat capacity [ $\text{J/g}\cdot\text{C}^\circ$ ]	1.47*
Thermal conductivity [ $\text{W/mK}$ ]	45*
Length of slit [cm]	2.5
Width of slit [cm]	5.63
Thickness of slit [cm]	0.5

\* The value of roughness of the corroded surfaces is very uncertain; this is because the degree of rust and pitting vary a lot over the gap surface. The heat capacity and thermal conductivity may also change due to the formation of iron oxides from the rust on the gap steel surface. To get a value as accurate as possible, roughness is measured in 3 positions on the slit, and the mean average of the 3 measurements is the value reported in the specification for each slit, detailed description of roughness measurements and more on how the surface roughness measurements are carried out is described in Appendix C.



**Figure 3-30** *Photograph of rusted gap surface 2, examined in the PRSA*

A slit which in basis had the same specifications like the sandblasted surface was exposed to a corrosive environment to get rust formation on the surface. The rusted steel surface was prepared by hanging the flanges outdoors at the sea side, midway between high and low tide, for about two months.

**Motivation:**

This gap surface was sandblasted before placing it in the sea water, the aim for testing this slit was to see if there were some differences on the MESH and efficiency of the gap, compared to the rusted surfaces that had a roughness that were inside the requirements in the (IEC 2002) before being placed in the sea water. Note that the final roughness is slightly larger for this slit than for the slit that was undamaged before rusting.

**3.5.4.4 Flame gap surfaces with multiple grooves tested in the Plane Rectangular Slit Apparatus (PRSA)**

In the PRSA slits with similar multiple crosswise and lengthwise grooves (see Section 3.3) on the gap surfaces, like the gap surfaces tested in the PCFA was tested, this was done to compare the results from the two different apparatuses and see if the same kinds of results would be found in both apparatuses. Slits with single lengthwise grooves with different width and depth of grooves that perforates the slit in relation to the flow direction is also tested in the PRSA (see Section 3.5.4.5). This chapter describes the specifications and motivation for testing the different gap surfaces with grooves in the PRSA.

**Table 3-15** Specifications of the PH-7.2.3 flame gap surface examined in the PRSA

Specifications	PH-7.2.3 gap surface
Material	Carbon steel
Ra [ $\mu\text{m}$ ]	0.2
Rz [ $\mu\text{m}$ ]	2.0
Heat capacity [J/g-C°]	0.452
Thermal conductivity [W/mK]	45
Length of slit [cm]	2.5
Width of slit [cm]	5.63
Thickness of slit [cm]	0.5
Number of grooves	7
Width of grooves [mm]	2.0
Depth of grooves [mm]	3.0
Area of Groves [ $\text{mm}^2$ ]	126

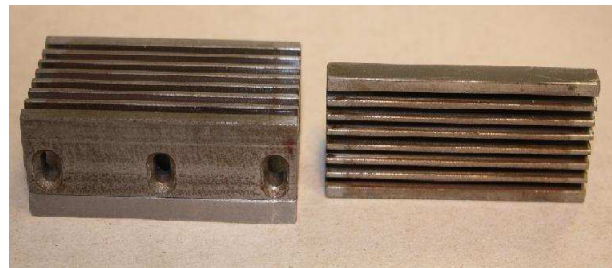


**Figure 3-31** Photograph of PH-7.2.3 flame gap surface examined in the PRSA

Seven grooves of 2.0 mm width and depth 3.0 mm were milled into a gap surface which in basis had the same specifications as the undamaged flame gap surface. The grooves are crosswise over the whole length of the slit, but do not perforate the slit in the flow/reaction direction (see Section 3.3). Figure 3-31 shows a photograph of the slit, and figure 3-32 shows the slit with dimensions of the grooves.

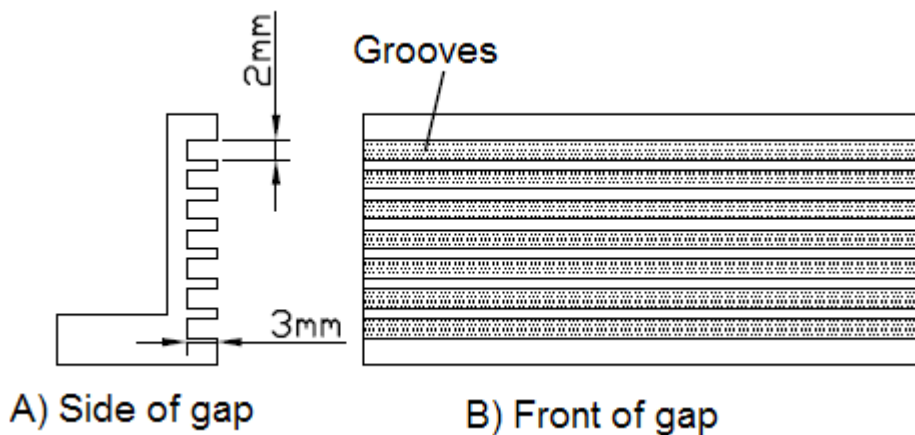


**Figure 3-32** The PH-7.2.3 flame gap surface examined in the PRSA with dimensions.



## **Motivation**

This gap surface is similar to the flange CH-8.2.3 tested in the PCFA described in Section 3.4.5. This gap surface configuration was first tested in the PRSA, and the motivation is the same as described under motivation of the CH-8.2.3, repeated here:

This flame gap surface was made to examine how large crosswise grooves on the gap surface would affect the MESG and the efficiency of the gap. When damage occurs on a flame gap, for example from dismounting of the enclosure under inspection of a flame gap, the operator may scratch the surface of the gap with a screwdriver. The direction of this scratch/groove can go through the width of the gap in the direction of flow<sup>2</sup>, or just be a groove for example in the middle of the flame gap. The aim with the experiments with this gap surface was to get an understanding of how different damage influences the efficiency of the gap, and the MESG due to the direction of the damage on the flame gap surface.

Another interesting aspect of these grooves is that they most likely create more initial turbulence in the external chamber and turbulence in the gap when the pressure rise in the primary chamber "pushes" the hot combustion products through the gap. It was than possible to examine whether the turbulence in the gap increases or decreases the probability of re-ignition in the secondary chamber. A comparison of this slit and the CH-8.2.3 is given in Section 4.2.

---

<sup>2</sup> Direction of flow refers to the direction that the combustion zone will have in respect to the direction of the grooves on the gap surface.

**Table 3-16** Specifications of the PV-10.1.4 flame gap surface examined in the PRSA

Specifications	Gap surface PV-10.1.4
Material	Carbon steel
Ra [ $\mu\text{m}$ ]	0.2
Rz [ $\mu\text{m}$ ]	2.0
Heat capacity [ $\text{J/g}\cdot\text{C}^\circ$ ]	0.452
Thermal conductivity [ $\text{W/mK}$ ]	45
Length of slit [cm]	2.5
Width of slit [cm]	5.63
Thickness of slit [cm]	0.5
Number of grooves	10
Width of grooves [mm]	1.0
Depth of grooves [mm]	4.0
Area of Groves [ $\text{mm}^2$ ]	40

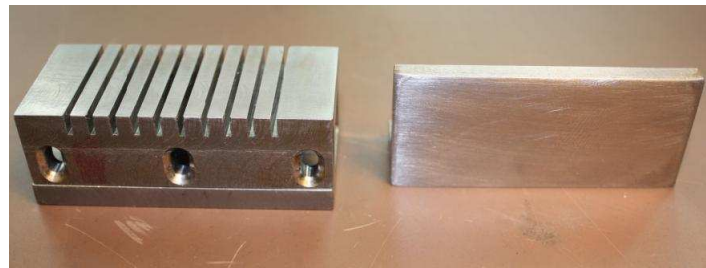


**Figure 3-33** Photograph of PV-10.1.4 flame gap surface examined in the PRSA, when the gap is assembled one part of the slit has a gap surface like the undamaged gap surface and the other is the one with lengthwise grooves shown to the left in the photograph

Ten grooves 1mm wide and 4mm deep were milled into a flame gap surface which in basis had the same specifications like the undamaged gap surface. The grooves are lengthwise (see Section 3.3). Figure 3-33 shows a photograph of the gap surface, and figure 3-34 shows the slit with the dimensions of the grooves on the gap surface.

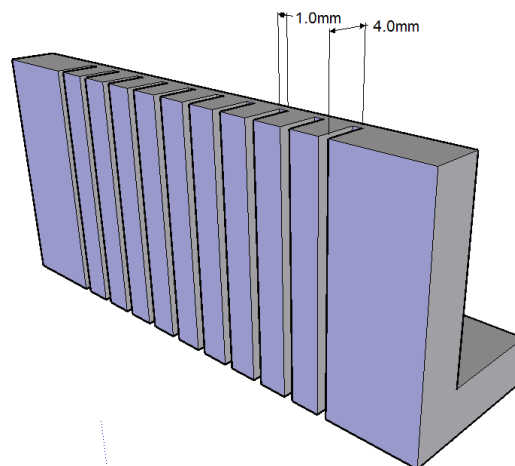


**Figure 3-34** The PV-10.1.4 slit examined in the PRSA with dimensions of the grooves on the surface

**Motivation:**

This gap surface configuration was tested to examine the effect of lengthwise grooves that perforates through the whole slit length. It was from preliminary tests in the plane rectangular slit apparatus with only one groove in the flow/reaction direction found that grooves with width less than 1mm did not affect the MESH value, and hence not the efficiency of the gap. It was therefore resolved to make 10 grooves to see if the MESH then was affected by the grooves. Another motive for making this slit was to see whether grooves which had a width that did not support explosion transmission, could create a turbulent regime that made probability of re-ignition in the secondary chamber higher or lower. This slit was the basis for making the CV-20.1.4 flange tested in the slightly modified PCFA (see Section 3.4.7), and the results from these gap surface configurations are compared and discussed in Section 4.2.

### 3.5.4.5 Experiments with single lengthwise grooves through the direction of flow, with known depth and width of grooves tested in the (PRSA)

A total of eleven different slits with single grooves on the gap surface, with different width and depth that perforates the slit lengthwise (see Section 3.3) in relation to the flow direction is examined. The slits had in basis the same specifications as the undamaged gap surface before applying the grooves.



**Figure 3-35** Photograph of five slits with different width and depth of the grooves on the gap surface that perforates the slit in the flow direction (lengthwise). Width and depth of grooves on slits, from left to right: Slit 1: width: 1 mm, depth: 4 mm. Slit 2: width 2 mm, depth: 1 mm. Slit 3: width: 3 mm, depth: 1 mm. Slit 4: width 4 mm, depth: 0,5 mm.

**Table 3-17** Specifications of the slits with single lengthwise grooves examined in the PRSA

Specifications	Slits with single lengthwise groove
Material	Carbon steel
Ra [ $\mu\text{m}$ ]	0.2
Rz [ $\mu\text{m}$ ]	2.0
Heat capacity [ $\text{J/g}\cdot\text{C}^\circ$ ]	0.452
Thermal conductivity [ $\text{W/mK}$ ]	45
Length of slit [cm]	2.5
Width of slit [cm]	5.63
Thickness of slit [cm]	0.5

In figure 3-35 four slits with different width and depth of grooves are shown, figure 3-36 shows how the grooves are orientated on the slit; all the single grooves are made in the midpoint of the slit and perforate through the whole slit width.

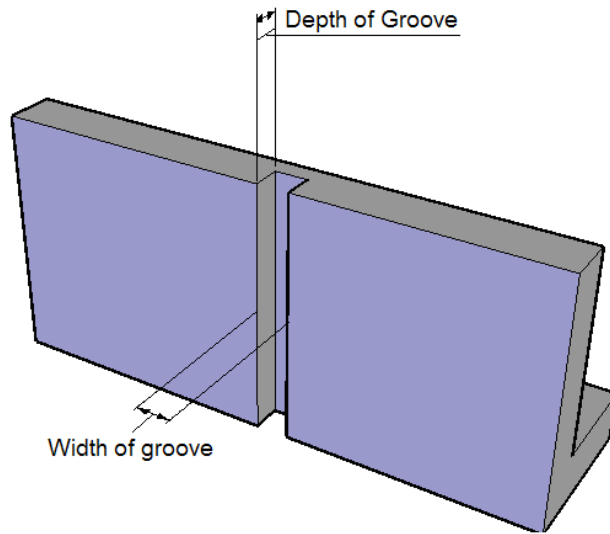


**Figure 3-36** Sketch of a lengthwise groove in the middle of the slit, to clarify what is depth and width of the groove in the slit.

### **Motivation**

Under inspection of Ex "d" equipment grooves from tools used for dismounting and mounting of the enclosure can cause damage of the flame gap. Lengthwise grooves are thought to be the damage most critical for the flame gap efficiency. The tested slits have grooves with different widths and depths. The motivation for testing these slits are to examine whether there is a limiting width and depth value which the grooves can have before the grooves affect the MESH value and efficiency of the gap in a negative way. If such a value is found, it could maybe in the future be used to distinguish between grooves and damage that is critical for the efficiency of a flame gap in Ex "d" equipment and damage that are not.

### **Naming of slits with single grooves in flow direction**

In table 3-18 an overview of the different slits with single grooves are given. The name of the slits with single lengthwise grooves that perforates the slit in the flow direction refers to the width and the depth of the groove in the current slit.

Example: A slit with name: **1.4**. The first number refers to the width of the groove, in this case 1 mm. The second number refers to the depth of the groove, in this case 4 mm.

**Table 3-18** Overview of experiments on slit surfaces with single lengthwise grooves through the whole slit width, with known depth and width of grooves investigated in the PRSA

Apparatus	Name	Depth	Width
PRSA	1.4	4	1
PRSA	2.01	0.1	2
PRSA	2.02	0.2	2
PRSA	2.05	0.5	2
PRSA	2.1	1	2
PRSA	3.01	0.1	3
PRSA	3.02	0.2	3
PRSA	3.05	0.5	3
PRSA	3.1	1	3
PRSA	4.01	0.1	4
PRSA	4.05	0.5	4

### 3.6 Gas mixture preparation, analysis and filling

*The method for gas mixture preparation, analysis and filling is the same as used in (Opsvik 2010), and this chapter is similar to chapter 3.4 in (Opsvik 2010)*

The same system for gas mixture preparation, analysis and filling was used for both the PCFA and the PRSA. Figure 3.37 gives an overview of the total system. To ensure that the entire volume of the experimental apparatus was filled with the desired mixture of propane and air, the gas filling system consisted of various vents, valves, tubes, flow meters and a gas analyzer. First propane from a storage tank was mixed with air supplied from the pressurized air system of the laboratory. The propane concentration was measured by an infrared gas analyzer (Servomex 1991).

The premixed gas was introduced into the primary chamber close to the bottom. The subsequent flow into the secondary chamber occurred through the gap between the two chambers. In addition it was possible to use a bypass to direct gas mixture from the primary to the secondary chamber. In this way the gas filling time could be reduced in the case of narrow flame gaps. The gas mixture used in the present work was 4.2 vol. % propane in air.

(IEC 2002) does not require a purity of the test gas (propane) better than 95%. However, in the present investigation both the calibration and test gas were of considerably better quality, with a purity of 99.95%. This was done to minimize any uncertainty due to uncertain chemical composition of the gas. The detailed procedures for calibration and use of the infrared gas analyzer are given in Appendix A-2.6 and gas quality certificate is enclosed in Appendix E.

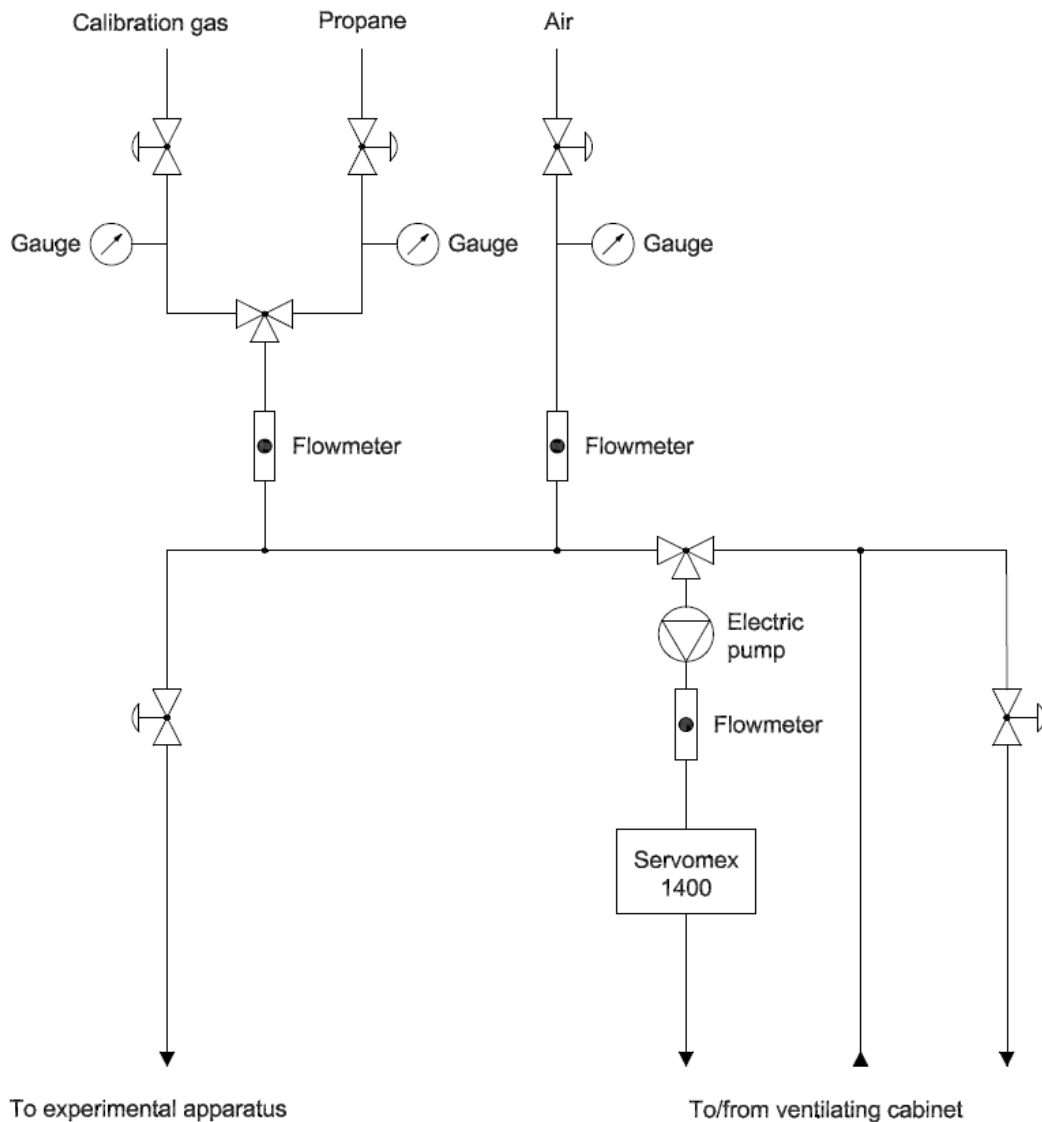


**Figure 3-37** The gas filling system with the Servomex 1400 B4 SPX infrared gas analyzer. The different valves, pressure gauges, supply pump and flow meters as important parts. From (Opsvik 2010)

### 3.7 Measurement and data logging system

The method for measurement and data logging system is the same as used in (Opsvik 2010), and this chapter is similar to chapter 3.6 in (Opsvik 2010)

#### 3.7.1 Data acquisition system

When the homogenous propane-air mixture was contained within the explosion apparatus a spark was generated in the primary chamber and the explosion pressure build up in the

primary chamber was measured. Measurements data were stored after each experiment in a computer in such a way that it could be analyzed at a later date.

A NI USB 6009 card, connected to a computer, performed both controlling and logging of the experiment. The card controlled the timing of ignition. This NI-CAD card is programmed by Labview software, which is documented in Appendix A-2.7. The software enables the user to change all setup parameters, within the limitations of the card and the hardware.

### 3.7.2 Control system

A tailor made data acquisition and control system was made to control the experiments. A NI USB 6009 card sends signals to trig the ignition. Digital ports are used for remote triggering of the experiment and to reset and activate the pressure measurement system. Figure 3.38 shows the control and measurement system.

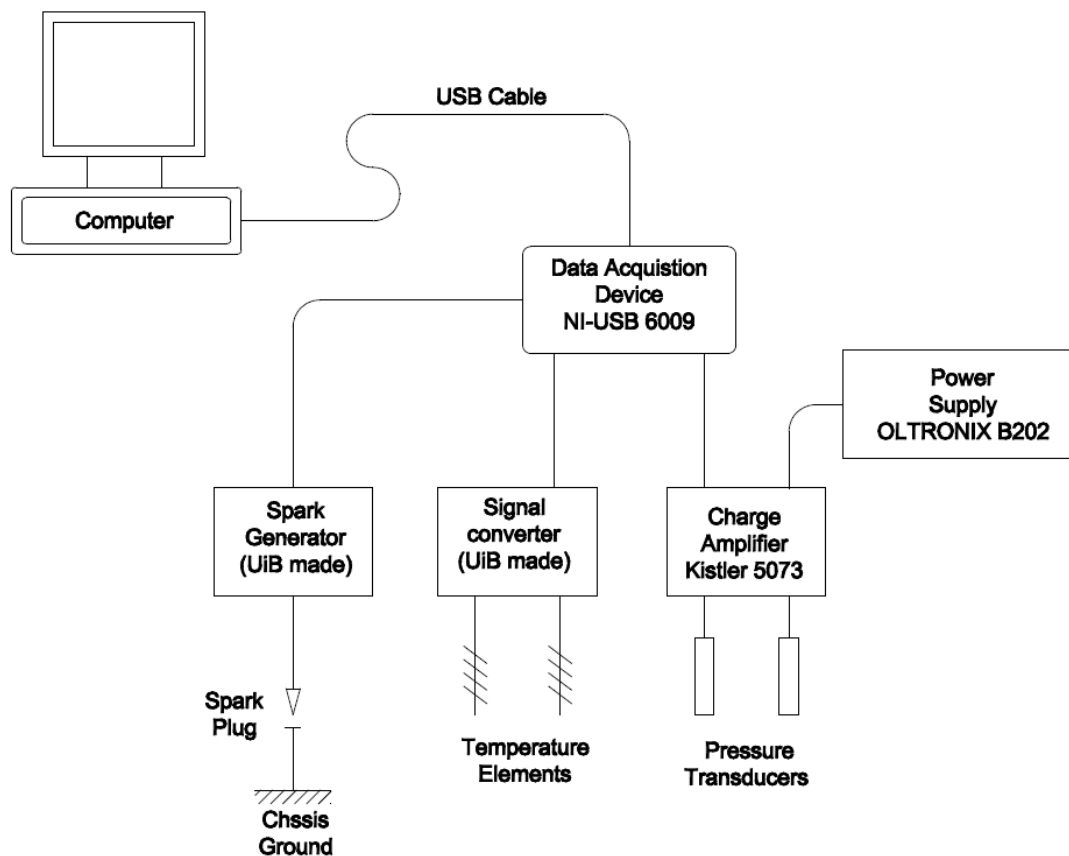


Figure 3-38 Data acquisition and control system. From (Opsvik 2010)

### 3.7.3 Pressure measurements

In order to measure the explosion pressure in the primary chamber as a function of time  $p_i(t)$ , a set of piezo electric transducers with a charge amplifier was mounted in the cylinder wall in both apparatuses. In connection with each experiment a zero-calibration of the pressure

transducers were conducted just prior to the release of the igniting spark in the primary chamber. Additional information and calibration certificates are enclosed in Appendix E.

### **3.8 Sources of error**

*This chapter is similar to chapter 3.8 in (Opsvik 2010)*

#### **3.8.1 Data Acquisition System**

The experience from the work performed in this thesis shows that amplification of measured signal is important. One A/D converter reads all the channels and has switches inside the card which chooses which channel to read. If one channel is not satisfactorily amplified, then the signal from one channel would influence the signal from the next reading.

#### **3.8.2 Gas concentration measurements**

Calibration of the gas analyzer was done with a certified span gas containing 5.00 % propane in nitrogen. The measurements close to these values would have the highest accuracy and as the gas mixture departs from these values then the accuracy would be somewhat lower. For mixtures far from the reference point, the accuracy depends on the linearity between the two points or the extrapolation towards a richer mixture. The alternative is how well the analyser calibrates for nonlinearity.

During experiments the gas concentration has to be 4.2 vol.% +/- 0.1 % as stated in (IEC 2007a) Insufficient calibration could result in uncertainties with respect to concentration measurements. To ensure that there is performed an adequate amount of calibration a calibration log has been established. All calibration of the gas analyzer has been executed in accordance with the calibration procedure enclosed in Appendix A-2.6.

Changes in flow rate affect accuracy and a change from 0 to 200 ml will introduce an error <0.1 % (Servomex 1991). Adjustment of flow was done with a flow meter that actually measures the momentum of the moving gas particles rather than volume flow, so the flow could also change as a result of variation in specific gravity between air and propane. In general the flow was not changed for every interval and was on some occasions not changed at all so it is assumed that variation of flow is not likely to affect the accuracy of the gas concentration measurement.

Another parameter which can have an influence on the actual gas concentration both in the primary and secondary chamber is that the mixture in the chambers may not always be homogenous.

#### **3.8.3 Atmospheric pressure and temperature**

The normal mode of operation of the gas analyser is to discharge the gas sample from the measuring cell at atmospheric pressure, the sensitivity of the cell will be proportional to the atmospheric pressure. The effect is that of a span change, so the error introduced is zero at



zero concentration and maximum error at full scale. This leads to a change of 1 % in the atmospheric pressure thus will cause a change of typical 1 % of reading.

The manufacturer has stated that the effect of temperature change is less than (0.2 % of full scale display + 0.4 of reading) per degree Celsius.

### **3.8.4 Air humidity**

The propane used in the experiments is mixed with pressurized air supplied from local distribution network. No measurements of humidity are done, but the air is filtrated and dried in a unit downstream the air compressor. In any case the quality of the air is not documented and pollution in form of oil, dust particles or water may exist in the supplied air. This may have effects on the results.

### **3.8.5 Pressure**

There is uncertainty in the pressure readings due to the resolution of the pressure transducer. Kistler, the manufacturer of the piezoelectric transducer, states that the accuracy of the transducer is  $\leq \pm 0.08\%$  of Full Scale Output when the calibration range is in the area of 0 to 25 bar. This gives an accuracy of  $\pm 0.02$  bar at the used measuring range, which is well within acceptable limits.

The pressure transducer is mounted a fixed distance at the vertical chamber wall of the primary chamber. The transducer may not detect local pressure gradients in the chamber.

### **3.8.6 Condensed water**

After a few explosions water will typically condense on the inside of the walls of the primary chamber and may represent a significant source of error. Water may evaporate from the warm vessel walls during gas filling and the subsequent period of turbulence settling, altering the gas composition. Water in the gas mixture may affect reaction mechanisms and heat capacity, whereas a small portion of the water at the vessel walls may evaporate during the explosion. It is generally assumed that the explosions will be too rapid for significant amounts of water to evaporate.

### **3.8.7 Experiments**

There are uncertainties due to construction tolerances in size of volumes, ignition positions and flange diameters and distances. In addition there is accuracy related to the experimental work, although good experimental procedures would counteract this, with reference to Appendix A.

The dimension of the distance "shims" is observed to have a variation of approximately  $\pm 1$  hundredths of a millimetre.



## 4 Experimental results and discussion

In this chapter the results gained from experiments with the different flame gap surfaces in the two apparatuses used in this work is given and discussed. The main parameter examined and reported is the change in MESG and efficiency of the gap compared to the MESG (see section 2.3.2) value found from experiments of the undamaged flame gap surfaces (see section 3.4.4.1 and 3.5.4.2 for specifications of the undamaged gap surfaces in the different apparatuses). This aim is to get an understanding of how different roughness and damage of surfaces of flame gaps in Ex "d" equipment influence on the integrity of this type of equipment. The degree of damage and direction of damage in relation to the direction of the flow/reaction zone (see section 3.3) is investigated. The degree of damage and the position of damage a flame gap in Ex "d" equipment can suffer, before it doesn't function satisfactorily anymore is also investigated.

A comparison of the results with the gap surfaces which has approximately similar configuration in the different apparatuses is given in this chapter.

Table 4-1 shows an overview of all the MESG experiments and values found from experiments of the different flame gap surface configurations in the different apparatuses. A detailed description and discussion of the results is given in this chapter. In Appendix C measurement data for the MESG experiments is enclosed.

**Table 4-1** *Overview of experiments and MESG from different flame gap surface configurations*

Apparatus	Gap surface Configurations	MESG 14 mm	MESG 0 mm	Mean pressure at MESG [barg]
PCFA	Undamaged	0.95	0.95	0.128
PCFA	Sand blasted	0.91	0.91	0.144
PCFA	Rusted/Corroded	1.07	1.0	0.100 (14mm)
PCFA	Plexi	N/A	N/A	N/A
PCFA	CH-8,2,3	1.14	N/A	0.286
MPCFA	Undamaged	0.91	N/A	0.195
MPCFA	CV-20,1,4	0.93	N/A	0.118
PRSA	Undamaged	0.98	N/A	3.157
PRSA	PH-7,2,3	1.10	N/A	4.209
PRSA	PV-10,1,4	1.12	N/A	1.783
PRSA	Plexi Plane Slit	0.98	N/A	3.147
PRSA	Corroded 1	0.83	N/A	3.137
PRSA	Corroded 2	0.82	N/A	3.217
PRSA	Sand blasted	0.93	N/A	3.815

### 4.1 Results and discussion from experiments for finding the ignition point most favourable for re-ignition in the secondary chamber in the PRSA

Experiments to find the ignition position most favourable for re-ignition in the secondary chamber was performed in the PRSA. Motivation for these experiments is given in Section 3.5.4.1.

#### 4.1.1 Results

In figure 4-1, the results from experiments for finding the ignition position most favourable for re-ignition are presented.

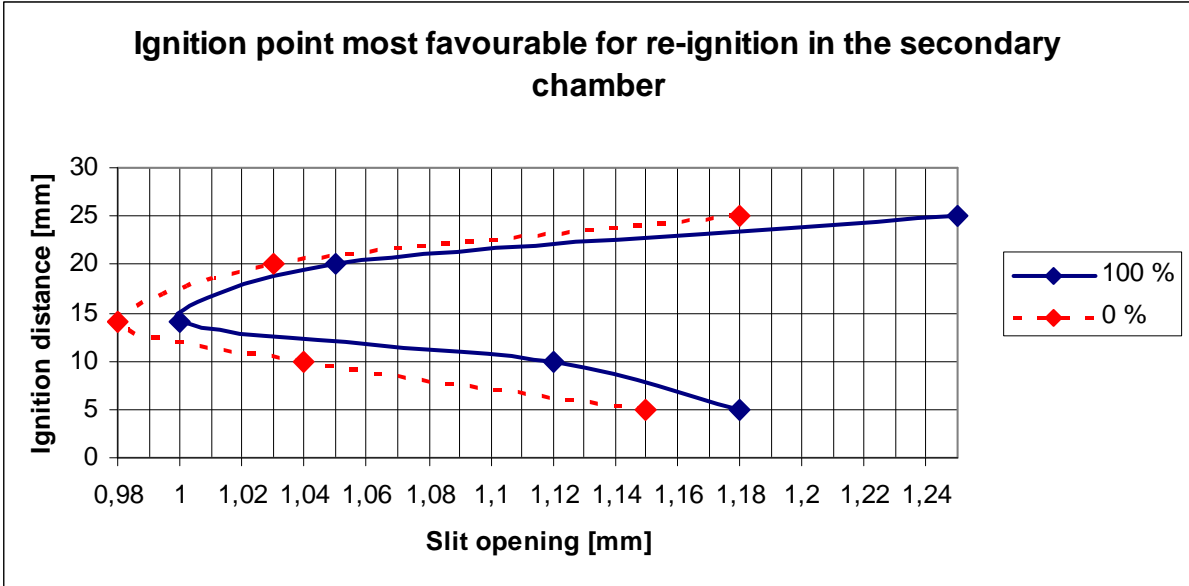


**Figure 4-1** Determination of the ignition position most favourable for re-ignition in the secondary chamber in the Plane Rectangular Slit Apparatus with 4.2 vol. % propane in air. The solid line is the gap opening giving re-ignition for ten experiments for the given ignition position, the dotted line is the gap opening giving no re-ignition for ten experiments for the given ignition position

As shown in figure 4-1, the ignition point that gave the lowest slit opening in respect to re-ignition in the secondary chamber was 14mm from the gap opening. It was therefore decided to use 14mm as the ignition position when experiments on the damaged gap surfaces were to be carried out. It should be mentioned that the ignition position examined was only the following ignition positions: 5mm, 10 mm, 14 mm, 20 mm, 25 mm (distance from the gap entrance).

#### 4.1.2 Discussion

All of the literature reviewed in Chapter 2, agrees upon the fact that the pressure inside the primary chamber, and hence the velocity of the combustion gases through the flame gap, is of great importance when considering whether a re-ignition in the secondary chamber can occur.

From figure 2-22 in chapter 2 from (Larsen 1998), the change in explosion pressure is shown when the ignition position is moved into the primary chamber. The pressure increases when the ignition position is moved towards the centre of the primary chamber. The velocity of the combustion gases through the flame gap, and into the external chamber will increase when the pressure is increased. Change in ignition position will also affect the flame which will reach the walls of the primary chamber at different times due to the changed position. This can influence on the pressure increase and temperatures of the combustion gases, because the combustion products can be cooled before combustion is completed.

In the experiments performed in the present work, the ignition position being most favourable for re-ignition in the secondary chamber was found to be 14 mm from the start of the gap. From the review of the Phillips theory (see Section 2.4.1), he introduced the term critical velocity, which was the velocity that gave the smallest safe gap opening. Phillips stated that this critical velocity was found when the explosion pressure was low; because of this he based his calculations of heat transfer for laminar flow. This does to some extent support the results found in the present work. When the ignition position is moved away from the start of the gap, the gap opening giving no re-ignition (safe gap distance) is decreased up to a point  $Z_i = 14$  mm (from experiments in the present work). When the ignition position is moved further into the primary chamber the safe gap distance is increased. This demonstrates that there is a critical pressure and velocity of the burnt gases through the flame gap, which gives a higher probability for re-ignition in the secondary chamber. This can be explained by the fact that increased velocity (from change in ignition position and hence increased pressure), reduce the cooling of the gases in the gap. Because the time the hot combustion gases can be cooled in the gap is reduced, when the gases flow with a higher velocity through the gap. When the velocity is further increased the increased rate of cooling by entrainment of cold unburned gases more than compensates for the reduced cooling in the gap, and the safe gap distance increases again. This is in agreement with the theory in Chapter 2, except for the theory of increased initial pressure by Redeker. Redekers' experiments showed that a higher initial pressure reduced the safe gap distance, but this can not be directly correlated to the change in resulting explosion pressure as a result of change in the ignition position. Redeker also examined the effect of changing the ignition position, and came to the same conclusion that when the ignition position is moved away from the centre, the safe gaps distance decreases (see Section 2.4.3.2, figure 2-18).

From the review of the Phillips theory in Section 2.4.1.2, figure 2-13, he pointed out that if the pressure was raised further, a new minimum point called the break point, where the safe gap distance once again reached the lowest safe gap distance (found with a lower pressure) could be reached. If the pressure is raised further, a safe gap distance which is smaller than the first safe gap distance can be found. This point can not be found in the IEC apparatus for testing of MESH, or in the apparatuses used in the experiments in the present work. The reason for this is because the maximum explosion pressures developed in these apparatuses are not sufficient for reaching this point. But Phillips expressed a concern that this could occur in large enclosures with many internal components, giving rise to a high explosion pressure, especially in the more reactive fuels like hydrogen. External ignition might than be possible for small gap openings, comparable with or smaller than those permitted in the current standards.

## 4.2 Results and discussion from experiments with similar gap surface configurations in the PCFA and PRSA

In this chapter the results gained from approximately similar gap surfaces in the PCFA and the PRSA are given and discussed.

### 4.2.1 Results and discussion from experiments with reference flame gap surface, undamaged gap surface

To get reference values to compare the results gained from the gap surfaces with damage and different roughness, it was tested with gap surfaces which fulfilled the requirements in the (IEC 2002). Gap surfaces with this type of specifications were tested in both apparatuses and also in the slightly modified PCFA (MPCFA). The results from the MESG experiments with undamaged gap surfaces in the different apparatuses are shown in table 4-2. The specifications of the undamaged gap surfaces can be found in section 3.4.4.1 and 3.5.4.2.

#### 4.2.1.1 Results

**Table 4-2** MESG values from experiments on undamaged gap surfaces in the different apparatuses

Apparatus	Gap surface Configurations	Ignition distance [mm]	MESG [mm]	Mean pressure [bar(g)]
PRSA	Undamaged	14	0.98	3.157
PCFA	Undamaged	14	0.95	0.128
PCFA	Undamaged	0	0.95	0.128
MPCFA	Undamaged	14	0.91	0.195

Note that there is no change in the MESG value as a result of change in the ignition position from 0 mm to 14 mm from the entrance of the gap opening in the PCFA. From table 4-2 it is shown that there are only small differences in the MESG value obtained from the different apparatuses. The largest difference is from the PRSA to the slightly modified MPCFA, the change in MESG is from (0.98-0.91) mm, the difference in percentage is 7.14%, but this is only 0.07 mm so the difference is not significant. The difference from the PRSA to the PCFA is only 3.06 %. These differences indicate that the MESG value is somewhat apparatus dependent. Because of these differences it was determined to perform some of the tests with damaged gap surfaces in both apparatuses, this was done to make sure that the results found came from change in the gap surface configurations, and not from how the apparatus was constructed. The gap surface configurations tested in all apparatuses were those found to be most interesting after testing in the less advanced PRSA that had a much shorter gas filling time, which made it possible to perform a larger number of experiments each day.

From table 4-2 it can be seen that the maximum pressure build up in the PRSA is much higher than in the PCFA when the MESG value is reached. This is because the gap opening area where the combustion gases is vented is smaller in this apparatus. The maximum pressure at the opening of MESG in the PCFA is 0.126 bar(g), in the PRSA the maximum pressure is 3.15 bar(g) at the opening of MESG for the apparatus (see figure 4-2 and 4-3). In the MPCFA

the maximum explosion pressure at the opening of MESG for the apparatus is 0.264 bar(g). Despite these large differences in the resulting explosion pressure, the MESG value is almost equal in the different apparatuses.

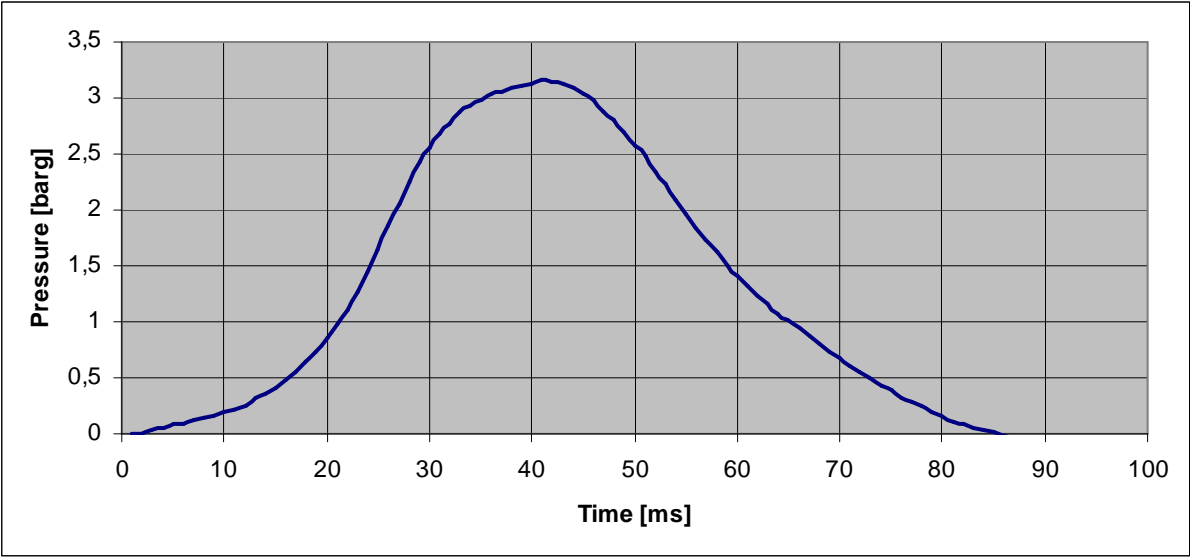


**Figure 4-2** Pressure rise in the primary chamber of the PRSA at MESG for this apparatus with undamaged gap surface, gap opening of 0.98 mm. Mixture concentration 4.2 vol. % propane in air, ignition distance  $X_i$  :14 mm. The maximum pressure is reached after about 40 ms, the pressure is than approximately 3.15 bar(g)

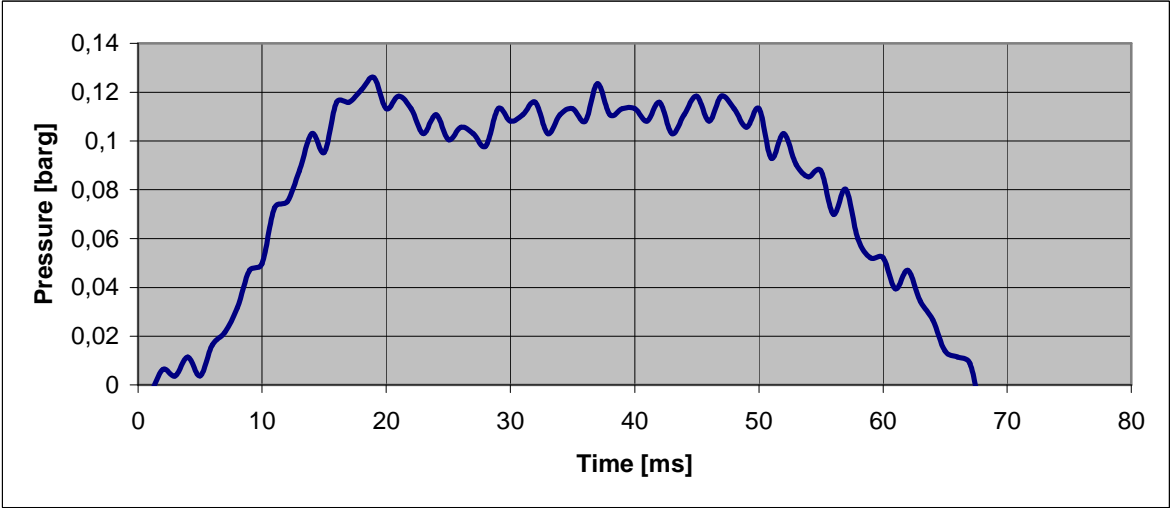


**Figure 4-3** Pressure rise in the primary chamber of the PCFA at MESG for this apparatus with undamaged gap surface, gap opening of 0.95 mm. Mixture concentration 4.2 vol. % propane in air, ignition distance  $X_i$  :14mm. The maximum pressure is reached after about 20 ms, the pressure is than approximately 0.126 bar(g).

#### 4.2.1.2 Discussion

The experimental results from the undamaged gap surfaces in the different apparatuses gave almost equal MESG values. This is quite surprisingly when considering the large difference in the apparatuses, and the differences in the resulting maximum explosion pressure. The maximum explosion pressure in the PCFA at MESG opening of 0.95 mm was 0.128 bar(g), in the PRSA the maximum explosion pressure was 3.157 bar(g) at its MESG opening of 0.98 mm. As discussed in the literature review of Larsen's work (see section 2.4.5), this indicates that the flow is sub sonic in the PCFA, because the pressure is under the critical pressure that was given to be in the range of 1.7 - 2.0 bar, to achieve sonic flow. In the PRSA the flow will therefore be sonic when maximum pressure is reached and the combustion gases flow out through the gap opening. But the case is not that straightforward. The pressure and hence the velocity of the gases will vary throughout the time that the explosion develops inside the primary chamber. When the gas is ignited in the primary chamber, the explosion will start to propagate with a spherical shape out towards the walls and the gap entrance in the primary chamber. The pressure rise created will at first "push" unburned gas towards and through the gap opening. Finally, when the first flame front reaches the gap opening, the flame gets "quenched" in the gap, and the first jet of hot combustion products will be "pushed" out from the flame gap and ejected into the unburned gas in the secondary chamber. The first jet will be "pushed" out with a low pressure build up behind the gases; hence the velocity is also low. The explosion will continue to propagate and grow in the primary chamber, "pushing" new jets of combustion products out through the gap, with gradually higher pressures and velocities until the maximum explosion pressure of the given gap opening is reached.

When considering that the MESG values in the different apparatuses were almost equal, it can be assumed that it is the first jet of hot combustion products which is the one most favourable for re-ignition in the external chamber. As illustrated in figure 4-4, the ignition position in the different apparatuses is at the same point, 14 mm from the gap entrance. The primary chambers have almost equal volumes approximately 1 litres. The width of the flame gap is approximately the same, 25 mm in the PRSA, and 27 mm in the PCFA. Because of this it is assumed that this first jet that is ejected through the flame gap has almost the same conditions when it comes to velocity, turbulence and temperature of the combustion products in the different apparatuses. This can explain why the MESG values were almost equal in the different apparatuses.



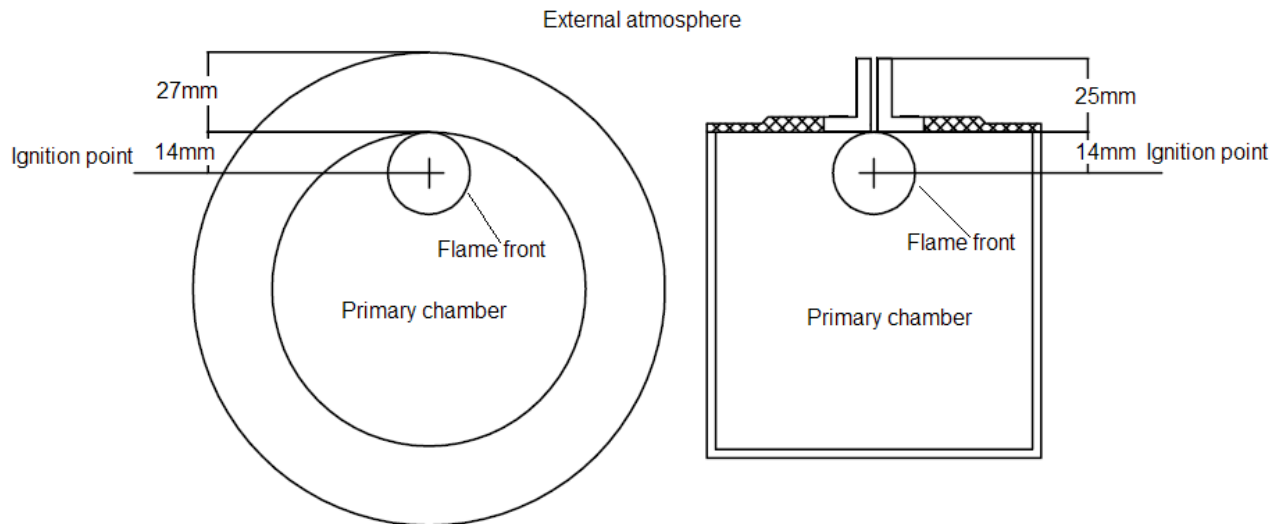


**Figure 4-4** *Illustration of the first flame front which reaches the start of the gap at the same point in the two apparatuses, giving approximately the same conditions of the first jet of hot combustion products into the external atmosphere. The illustration to the left is the inner chamber of the PCFA with ignition distance 14 mm from the start of the gap, the illustration to the right is a cross section of the cylindrical primary chamber in the PRSA with ignition distance 14 mm from the start of the gap.*

The assumption that this first jet is the one most favourable for re-ignition in the external chamber is in agreement with the literature reviewed in chapter 2. This first jet will have a velocity that is low; this will give a low rate of "cooling" by mixing and entrainment with the "cold" unburned gas in the external chamber. This jet will give the highest probability of re-ignition because the rate of heat generation from the chemical reaction will exceed the rate of cooling by entrainment and mixing. New jets of combustion gases will be ejected with higher velocities. Hence the rate of cooling by mixing with the unburned gases will increase and the jet is less favourable for re-ignition in the external chamber.

When the PCFA was slightly modified to ensure that the gap opening was uniform over the whole gap length (described in section 3.4.6), the change in MESG was from 0.95 mm to 0.91 mm compared to the original PCFA. This value is closer to the reported value of MESG for propane in the (IEC 1996) which is 0.92 mm. This indicates that the original PCFA did not have a uniform gap opening, and that the opening was larger on some of the positions around the gap opening.

The difference in the MESG value found in the difference apparatuses can come from the difference in the area of ventilation opening. Even though the gap opening is the same, the gap is wider and the velocities out from the gap will differ somewhat despite the ignition position and the assumed equal conditions of the first jet. The gap in the PCFA and the MPCFA is 27 mm, compared to 25 mm in the PRSA. This can decrease the temperature of the combustion gases somewhat more when they pass through the gap opening in the PCFA, and the MPCFA, than in the PRSA, because the time the gases are inside the gap is somewhat shorter in the PRSA.

## 4.2.2 Results and discussion from experiments on sandblasted flame gap surfaces

Experiments with sandblasted flame gap surfaces were performed in the PRSA and the PCFA. The experiments with sandblasted gap surface performed in the PCFA are the results reported by (Opsvik 2010). The results from the MESH tests in the different apparatuses are shown in table 4-3 and 4-4. The specifications of the sandblasted gap surfaces can be found in section 3.4.4.1 table 3-4 and section 3.5.4.2 table 3-11.

### 4.2.2.1 Results

**Table 4-3** MESH values from experiments on sandblasted gap surfaces in the different apparatuses

Apparatus	Gap surface Configurations	Ignition distance [mm]	MESH [mm]	MESH undamaged gap surface [mm]
PRSA	Sandblasted	14	0.93	0.98
PCFA	Sandblasted	14	0.91	0.95
PCFA	Sandblasted	0	0.91	0.95

**Table 4-4** Mean pressures obtained at MESH for sandblasted gap surfaces, pressure from sandblasted gap surface at the same opening as MESH opening for undamaged gap surface

Apparatus	Gap surface Configurations	Mean pressure MESH [barg]	Pressure at MESH for undamaged surface[barg]	Pressure MESH undamaged [barg]
PRSA	Sandblasted	3.815	3.153(0.97 mm)	3.157
PCFA	Sandblasted	0.144	0.138	0.128

Note that there is no change in the MESH value as a result of change in the ignition position from 0 mm to 14 mm in the PCFA; this was also the case for the undamaged gap surface.

From table 4-3 it is shown that it is only a marginal difference of 0.02 mm or 2.15 % in the MESH value from experiments performed in the two different apparatuses on sandblasted flame gap surfaces. Compared to the undamaged gap surfaces, the MESH value found for the sandblasted slits are slightly lower. In the PRSA the change is from 0.98 mm to 0.93 mm, which is a decrease of 5.1 %. In the PCFA the change in MESH is from 0.95 mm to 0.91 mm, which is a decrease of 4.2%.

From table 4-4 it can be seen that the pressure when the sandblasted gap surface reaches its MESH is slightly higher than the pressure from the MESH of undamaged gap surface. When the sandblasted gap surface had the same opening as the MESH opening of the undamaged gap surface, the pressure build up is slightly higher in the PCFA. It was not done experiments with the MESH opening for undamaged gap surfaces on the sandblasted gap surface in the PRSA, the value in table 4-4 is with a gap opening of 0.97 mm which is 0.01 mm less than the MESH opening of 0.98 mm from the undamaged gap surface, the pressure value is almost

equal to the pressure obtained from the MESG opening with undamaged gap surface at MESG in the PRSA.

#### 4.2.2.2 Discussion

The results gained from experiments of the sandblasted gap surface in the PRSA support the results found by (Opsvik 2010) on sandblasted gaps in the PCFA. There was a small decrease in the MESG value compared to the MESG value of the undamaged gap surface from 0.98 mm to 0.93 mm in the PRSA, and from 0.95 mm to 0.91 mm in the PCFA. The decrease is not considered to be significant enough to be considered "dangerous" when considering the efficiency of a flame gap in Ex "d" equipment. The maximum allowed gap opening for Ex "d" equipment is also provided with a safety factor, which for the actual gap width of 25 mm and inner volume of 1 litres gives a maximum allowed gap opening of only 0.40 mm. From these results it is therefore assumed that a flame gap can have a considerably higher roughness than the allowed maximum average roughness (Ra) of  $6.3 \mu\text{m}$ , before the flame gap doesn't function satisfactorily anymore and can constitute a danger for re-igniting an explosive atmosphere outside the Ex "d" enclosure. The average roughness Ra of the sandblasted gap surfaces in the experiments was about  $12 \mu\text{m}$ , which is almost twice the allowed value given in (IEC 2007a). The results found cannot support the requirement for only allowing a surface roughness of  $6.3 \mu\text{m}$ .

It should be pointed out that there are some elements of uncertainty when considering the experiments with sandblasted gap surfaces. The sandblasting of the gap surface produces a random roughness which may vary a lot over the whole gap-surface. This can give completely different value of roughness on different position of the gap surface. To ensure that the roughness value obtained from roughness measurements were as correct as possible; measurements were performed on several position of the gap surface (described in Appendix C). But as pointed out by Opsvik in (Opsvik 2010), the decrease in MESG found in experiments with sandblasted gap surfaces, can be a result of increased gap opening, rather than a effect of change in the flow regime through the gap. This is because the distance "shims" used for setting the gap opening can be placed on peak of the roughness giving a larger gap opening. But they can also be placed were the roughness is low therefore the uniformity of the gap opening is uncertain. The maximum pressure is slightly higher when the gap opening with sandblasted gap surfaces is set to be the same as the MESG for the undamaged opening. This can be a result of the mentioned uneven roughness of the gap surfaces, or it can be a result from the fact that a rougher surface can make more resistance of the flow of gas through the gap. The pressure build up must be higher before the combustion products can successfully flow through the gap and enter the external chamber. This can therefore mean that the velocity and fluctuation of the flow is of a higher order when the gases are ejected into the external atmosphere. Slightly higher velocity reduces the time the hot combustion products are inside the gap and hence the time to be cooled down by the gap walls decreases. Therefore the hot combustion gases can have a higher temperature when they are ejected into the primary chamber, leading to re-ignition at a lower gap opening compared to the MESG for undamaged surface. It is difficult to give an absolute conclusion of the effect a sandblasted gap surface will have upon the efficiency of the flame gap, due to the random roughness on the gap surface.

### 4.2.3 Results and discussion from experiments on rusted flame gap surfaces

Experiments with three gap surfaces that had different degree of rust were performed. Two of the gap surfaces were tested in the PRSA, and one in the PCFA. The experiments with rusted gap surface performed in the PCFA, are the results reported by (Opsvik 2010). The results from these experiments are summarized in table 4-5 and 4-6. The specifications for the rusted gap surfaces can be found in Section 3.4.4.1 table 3-5 and Section 3.5.4.3 table 3-13 and 3.14.

#### 4.2.3.1 Results

**Table 4-5** *MESG values from experiments on rusted flame gap surfaces in the different apparatuses*

Apparatus	Gap surface Configurations	Ignition distance [mm]	MESG [mm]	MESG Undamaged gap surface [mm]
PRSA	Rusted surface 1	14	0.83	0.98
PRSA	Rusted surface 2	14	0.82	0.98
PCFA	Rusted Circular	14	1.07	0.95
PCFA	Rusted Circular	0	1.00	0.95

**Table 4-6** *Mean pressures obtained at MESG for rusted gap surfaces, pressure from rusted gap surface at the same opening as MESG opening for undamaged gap surface.*

Apparatus	Gap surface Configurations	Mean pressure MESG [barg]	Pressure at MESG for undamaged surface [barg]	Pressure MESG undamaged [barg]
PRSA	Rusted surface 1	3.137	N/A	3.157
PRSA	Rusted surface 2	3.217	N/A	3.157
PCFA	Rusted circular	0.100	0.142	0.128

The results from the experiment with rusted surface in the plane circular flange apparatus found by Opsvik in (Opsvik 2010) are quite surprising, as shown in table 4-5, there was an improvement of the gap efficiency with 12.6 % and 5.3 % for 14 mm and 0 mm ignition distance, compared to the undamaged gap surface. Note that this was the only flange tested in the PCFA that gave different MESG values as a result of change in the ignition position from 14 mm to 0 mm from the entrance of the gap. These surprising results was the reason for testing two other rusted gap surfaces in the PRSA, this was done to see if the MESG value increased in the same way in this apparatus when it was tested with a rusted flame gap surface. From table 4-5 it is shown that this was not the case in the PRSA. The two rusted gap surfaces gave a reduction of the MESG value with 15.3 % and 16.3 %. One of the gap surfaces was sandblasted before it were put in saltwater and rusted, this gave the smallest MESG value.

When tests with the two rusted slits were performed in the PRSA, it was observed that the first test with a gap opening of 0.98 mm, which is the MESG value for the undamaged gap surface, did not give re-ignition in the secondary chamber for both of the rusted gap surfaces. But after the first test it was observed that some of the porous rust formation on the slit

surface was blown of the slit surface. This came from the pressure which "pushes" the hot combustion gases through the gap and tears/blow the rust from the surface. This led to re-ignition with the same opening as the first test, and hence the MESG decreased. Because of the rust that were blown of the gap surface it was from control measurement of the gap found that the actual gap opening were larger than the shims used for setting the gap after the first experiment with these slits.

From table 4-6 it can be seen that the pressures when the rusted surfaces tested in the PRSA reaches its MESG value are approximately the same as the maximum pressure at MESG value for the undamaged surface in the PRSA. The pressure for the same opening as the undamaged MESG opening is not available for the rusted surfaces in the PRSA; this is because the surface was enlarged after the first explosion experiment, as described above.

The pressures obtained from the experiments on rusted gap surfaces in the PCFA show that the pressure is 0.100 bar(g) when the MESG value is reached for this gap configuration, the pressure at MESG for undamaged gap surface was 0.128 bar(g). When the gap opening with rusted gap surface was set to be the same as the MESG opening for the undamaged surface the pressure was 0.142 bar(g), compared with 0.128 bar(g) at MESG for the undamaged gap surface.

#### **4.2.3.2 Discussion**

The torque used for fastening the gap in the PRSA is only 20 *cNm* (see Section 3.5.1 and Appendix A-2.4), in the PCFA the torque is 10 Nm. The motive for using a lower torque in the PRSA was because of a suspicion that the gap opening in the PCFA may be smaller than the distance "shims" used, due to the compressible iron oxide on the rusted surface, and that this reduces the actual gap opening when the primary chamber is mounted and the bolts are fastened with torque. This compression can explain the increase in MESG in the PCFA because the gap opening actually is smaller than the value reported after placing the distance "shims" for setting the gap. This can also be explained by taking into consideration that the maximum explosion pressure for the rusted gap surface was higher when the gap opening was set to be the same as the MESG for the undamaged gap surface. But as discussed for the sandblasted gap surface, it can also be a result from the increased roughness that gives larger resistance in the gap opening for the flowing combustion products.

The experiments with rusted gap surfaces in the PRSA did not give an increase in the MESG value as was the case for the experiments in the PCFA. The difference in the MESG can descend from the difference in the torque used for fastening the gap opening. The distance "shims" will not be compressed into the gap surface in the same way as in the PCFA. The results from the experiments on rusted gap surfaces in the PRSA showed that no re-ignition occurred in the external chamber in the first test when the gap opening was the same as the MESG opening for the undamaged gap surface. This implies that for flame gap surfaces that are rusted there is no danger for re-ignition before a second explosion in the primary chamber. After the first test, the gap opening increased because the flow of combustion products through the gap blew away some of the porous rust on the gap surface.

More experiments are needed to be sure of the effect rust will have on the efficiency of flame gaps of Ex "d" equipment. It would be interesting to do experiments on flame gap surfaces with different degree of rust formation, in order to find out how much rust formation a flame

gap can have on the surface before this influences the efficiency of the gap significantly, thus constituting a danger for re-ignition in the external atmosphere. This work is being continued at the University of Bergen. Experiments with gap surfaces that are set to a given gap opening before they are introduced to a corrosive environment are being performed. This is more realistic when comparing to how rust formation of Ex "d" equipment installed in the industry will develop. The results from these experiments will be presented in December 2010 by (Solheim 2010).

From the experiments it is found that rust formation of a flame gap surfaces poses a danger first when the second explosion test is performed. In the industry it is an extremely low probability for this to happen with installed Ex "d" equipment.

#### 4.2.4 Results and discussion from experiments on Plexiglas flame gap surfaces

Flame gap surfaces made of the material Plexiglas or Poly(methyl methacrylate) (PMMA) was tested in the two different apparatuses. The results from these experiments are summarized in table 4-7 and 4-8. The specifications for the Plexiglas gap surfaces can be found in Section 3.4.4.1 table 3-6, and Section 3.5.4.2 table 3-12.

##### 4.2.4.1 Results

**Table 4-7** *MESG values from experiments on Plexiglas flame gap surfaces in the different apparatuses*

Apparatus	Gap surface Configurations	Ignition distance[mm]	MESG [mm]	MESG Undamaged gap surface [mm]
PRSA	Plexi	14	0.98	0.98
PCFA	Plexi	14	N/A	0.95

**Table 4-8** *Mean pressures obtained at MESG for Plexiglas gap surfaces, pressure from Plexiglas surface at the same opening as MESG opening for undamaged gap surface.*

Apparatus	Gap surface Configurations	Mean pressure MESG [barg]	Pressure at MESG for undamaged surface [barg]	Pressure MESG undamaged [barg]
PRSA	Plexi	3.154	3.154	3.157
PCFA	Plexi	N/A	N/A	0.128

As shown in table 4-7 the slit with Plexiglas gap surface gave equal MESG value as the slit with undamaged gap surface in the PRSA.

When the flange with Plexiglas surface was mounted in the PCFA it was discovered some problems with the apparatus which lead to the modification of the equipment (see Section 3.4.6). Plexiglas is a more bendable material and not as stiff a material as steel, the flanges was observed to be pressed together when torque was used for assembling the flanges in the

PCFA. Therefore the gap opening became much smaller than the distance "shims" used to set the gap opening, and the experiments gave invalid data for MESG determination with Plexiglas surface in the PCFA.

As there was no change in the MESG for the gap surface of Plexiglas compared to the undamaged gap surface, there was no change in the resulting explosion pressure obtained from experiments on Plexiglas gap surface either as shown in table 4-8.

#### **4.2.4.2 Discussion**

Most Ex "d" equipment are metallic; usually cast iron, aluminium or formed steel. From the literature there is no evidence that metallic construction is essential for the Ex "d" equipment to function properly. Smith did in (Smith 1953), refer to the work of Staples who showed experimentally that the MESG with bronze gaps is almost equal to the MESG value obtained from gaps made from Bakelite (a type of plastic), despite the large differences in the thermal properties of the two materials. This can be compared with Redekers work in (Redeker 1981), which showed that when the width of the flame gap was increased above a given size ( $\approx 25$  mm), the effectiveness of the flame gap was not increased. The results found from the experiments in this thesis with Plexiglas gap surfaces are in accordance with the literature. Therefore it is believed that the cooling of the combustion gases in the gap is a secondary parameter when considering the importance of the mechanisms involved for preventing transmission of an explosion through a narrow gap to the external surroundings. This is also further evidence for the assumption that the pressure and hence the velocity through the gap, which increases the rate of entrainment of cool unburned gas, is the parameter of greatest importance for cooling of the hot combustion jet.

## 4.2.5 Results and discussion from experiments on gap surfaces with crosswise grooves on the flame gap surfaces

Multiple crosswise grooves (see section 3.3) of 2.0 mm width and depth 3.0 mm were milled into gap surfaces which in basis had the same specifications as the undamaged flame gap surface. Gap surfaces which had approximately the same configuration are tested in the PCFA and the PRSA. In the PCFA eight grooves follow the circular slit around the surface but do not make a “channel” that perforates the slit in relation to the direction of flow/reaction (see figure 3-15 and 3.16 in Section 3.4.5). Approximately the same kind of gap configuration was made on a slit used in the PRSA, seven grooves were milled into this gap surface (see figure 3.31 and 3-32 in Section 3.5.4.4).

### 4.2.5.1 Results

**Table 4-9** *MESG values from experiments on flame gap surfaces with crosswise grooves in the different apparatuses*

Apparatus	Gap surface Configurations	Ignition distance[mm]	MESG [mm]	MESG undamaged gap surface [mm]
PRSA	PH-7.2.3	14	1.10	0.98
PCFA	CH-8.2.3	14	1.14	0.95

**Table 4-10** *Mean pressures obtained at MESG for gap surfaces with multiple crosswise grooves, pressure from the same surfaces at the same opening as MESG opening for undamaged gap surface*

Apparatus	Gap surface Configurations	Mean pressure MESG [barg]	Pressure at MESG for undamaged surface[barg]	Pressure MESG undamaged [barg]
PRSA	PH-7.2.3	4.209	4.331	3.157
PCFA	CH-8.2.3	0.286	0.735	0.128

As shown in table 4-9, slits with crosswise orientated grooves on the flame gap surface had a better ability to prevent re-ignition in the secondary chamber than the undamaged gap surfaces. Gap surfaces tested in both apparatuses gave a relative large increase in the MESG value. The slit tested in the PRSA gave an increase of the MESG by 12.2%. In the PCFA the increase was even larger, and gave an increase in MESG of 20% compared to the MESG for undamaged gap surfaces.

From table 4-10 and figure 4-5, it is shown that the pressure build up from the surfaces with crosswise grooves is significantly higher when comparing with same gap opening for the undamaged surfaces. The pressure development in the start is similar for the undamaged and the gap surface with seven crosswise grooves investigated in the PRSA, shown in figure 4-5. The pressure when the MESG value is reached is also higher for the gap surfaces with crosswise grooves, compared to the pressures from MESG opening for the undamaged gap surface.



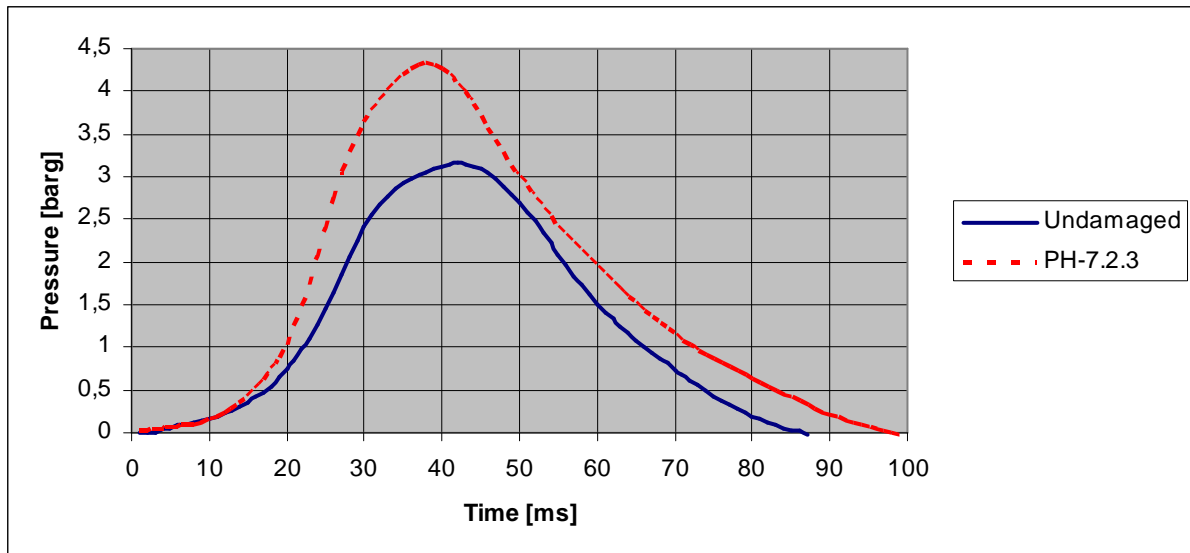


**Figure 4-5** Pressure development with a gap opening of 0.98 mm and ignition position  $Z_i$ : 14 mm, the solid line shows the pressure build up for a undamaged gap surface, and the dotted line shows the pressure build up for a gap surface with seven crosswise grooves (PH-7.2.3) tested in the PRSA. Maximum pressure for gap surface PH-7.2.3 is approximately 4.3 bar(g), and for the undamaged gap surface approximately 3.1 bar(g)

An interesting observation was done when experiments for finding the gap opening that gave 100% re-ignition was performed in the PRSA. For a gap opening that gave both re-ignition and no re-ignition in the secondary chamber, gap opening  $Y_i = 1.14$ mm, ignition distance  $Z_i = 14$  mm, it was observed that the pressure build up in the primary chamber was significantly higher when no re-ignition in the secondary chamber was initiated, shown in table 4-11.

**Table 4-11** Measurement data from experiments for finding the gap opening that gave 100% re-ignition. Note the significant rise in pressure when no re-ignition in the secondary chamber was observed, compared to the pressures when re-ignition in the secondary chamber was initiated

<b>Date:</b>	09.12-16.12.2009		
<b>Surface configuration:</b>	PH-7.2.3		
<b>Apparatus:</b>	PRSA		
<b><math>Y_i</math> [mm]</b>	<b><math>Z_i</math> [mm]</b>	<b>Pmax [barg]</b>	<b>Re-ignition</b>
1.14	14	3.977	Yes
1.14	14	4.018	Yes
1.14	14	3.972	Yes
1.14	14	3.908	Yes
1.14	14	3.906	Yes
1.14	14	N/A	Yes
1.14	14	N/A	Yes
1.14	14	3.977	Yes
<b>1.14</b>	<b>14</b>	<b>4.598</b>	<b>No</b>

The same effect was also observed for the gap surface CH-8.2.3 tested in the PCFA, but the difference in the pressure was not as significant as the one found in the PRSA.

#### 4.2.5.2 Discussion

The experiments with multiple crosswise grooves on the flame gap surfaces gave a significant increase in the MESG compared to undamaged flame gap surfaces. From the results it can be seen that the maximum pressure build up is larger when the gap surfaces with crosswise grooves are tested. This indicates that it is more resistance on the flowing gases through the gap, and the pressure is larger before the gases are ejected through the gap and into the external chamber. As discussed in Section 4.2.1.2, it is assumed that the first jet of hot combustion gases is the one most favourable for re-ignition in the external chamber. From figure 4-5 it can be seen that the pressure rise in the start of the explosion is similar for the undamaged gap surface and the gap surface with seven crosswise grooves (PH-7.2.3) tested in the PRSA. After about 15 ms the pressure rise ( $dp/dt$ ) for the PH-7.2.3 gap surface exceeds the pressure rise for the undamaged gap surface. It is then assumed that the flame front has reached the entrance of the gap, and gets "quenched" in the gap. The first jet of hot combustion products are being "pushed" out through the gap opening, because there is more resistance in the gap from the crosswise grooves, the pressure increases more in the experiments with the gap surface with crosswise grooves. The first jet in the experiments with gap surfaces with crosswise grooves will therefore be ejected at a higher pressure and hence higher velocity compared to the first jet in the experiments with undamaged gap surfaces.

The reason for the increase in MESG for gap surfaces with crosswise grooves is in accordance with the literature reviewed in chapter 2. Even though there isn't found any literature that describes experimental testing of the effect different gap surface configurations will have upon the re-ignition phenomena by a hot combustion jet. It can be correlated with the experiments done on quenching distance by (Ballal and Lefebvre 1977) and the work from (Thibault, Liu et al. 1982). Both pointed out that increased pressure, velocity and turbulence intensity gives a higher quenching distance and minimum ignition energy. This is also supported by the Phillips theory discussed in chapter 2, and figure 2-13 from (H.Phillips 1988) which show that the MESG increases with an increase in initial pressure. The Schlieren and OH-PLIF images shown in figure 2-26 and 2-27 from (Sadanandan, Markus et al. 2009) visualized the effect higher velocity of hot combustion products will have upon the rate of "cooling" by mixing and entrainment with the "cold" unburned gas. This creates a flow regime that is less favourable for re-ignition of the gas in the external chamber. The crosswise grooves will have the same effect upon the flow as an initial increase in pressure and turbulence.

Let us consider the effect these crosswise grooves will have on the flow before and after the first jet of combustion products is ejected through the gap and into the external chamber, and the effect this will have upon the re-ignition of the explosive gas atmosphere in the external chamber. When the explosion is initiated in the primary chamber, the flame front starts to propagate towards the walls and the entrance of the gap in the primary chamber. This creates a pressure front which will create movement in the unburned gas and start to "push" unburned gas through the gap with crosswise grooves. These grooves will create fluctuations and turbulence in the flow of the unburned gas when they are "pushed" through the gap and meet the external mixture. This means that there is already created a turbulent state in the external chamber before the first jet of hot combustion gases is ejected into the external chamber. When the flame front reaches the gap opening inside the primary chamber and gets "quenched", the pressure is higher than for an undamaged surface as discussed above, and the grooves create turbulence of the flow of hot combustion products which then is ejected into the already turbulent unburned gas. This gives rise to an efficient cooling of the hot

combustion jet by entrainment and mixing with cold unburned gas, and the heat generation by the reaction of hot gas with unburned gas is too slow to counteract the heat loss from entrainment and mixing with the unburned gas. When the jet moves further away from the gap opening the velocity and turbulence will decrease, but the jet has already become so deformed and its energy so dissipated that the entrained mixture never reaches the temperature necessary for ignition. Therefore the MESG is increased for gap surfaces with crosswise grooves, to get re-ignition of the external gas atmosphere, the gap opening has to be increased to a gap opening so large that the gases get a low enough velocity and turbulence intensity which decreases the rate of cooling by mixing and entrainment of the hot jet of combustion products. When the velocity is decreased the heat transfer to the gap increases because the time the gas is inside the gap is increased.

The above suggested theory is only based on the influence the crosswise grooves is thought to have on the flow through the gap, found from literature review on the subject. Due to the lack of relevant theory of the influence of gap surface structure on the re-ignition phenomena, more experiments should be done where the flow through the gap is visualized for example by use of Schlieren and OH-LIF images, as used by (Sadanandan, Markus et al. 2009), discussed in Section 2.4.7. First then a final quantitative conclusion of how the crosswise grooves affect the flow and re-ignition by hot combustion jets can be given. Experiments where the effect by crosswise grooves is examined by use of high speed camera and temperature measurements, is in progress at the University of Bergen, and will be submitted in December by (Solheim 2010).

From the experiments and from the literature reviewed, it is shown that crosswise grooves that do not perforate the gap in the direction of flow cause the gap to be less efficient. In fact crosswise grooves create a flow regime out from the flame gap that reduces the probability for re-ignition of the external atmosphere and makes the gap more efficient. These results may be used for designing safer Ex "d" equipment, and when considering what kind of damage of the flame gap that constitute a danger for the integrity of the equipment. As mentioned above more experiments are needed to reach a final conclusion. It can furthermore be the case that if crosswise grooves without the same width and depth are applied on the gap surface, they can in fact create a flow regime that will be more favourable for re-ignition, because the turbulence and velocity is decreased with less significant grooves. This work is being continued at the University of Bergen and is to be presented in December by (Solheim 2010).

## 4.2.6 Results and discussion from experiments on slits with lengthwise grooves on the flame gap surfaces

Multiple lengthwise grooves (see Section 3.3) of 1.0 mm width and depth 4.0 mm were milled into gap surfaces which in basis had the same specifications as the undamaged flame gap surface. Gap surfaces which had approximately the same configuration were tested in the PRSA and the MPCFA. These gap surfaces are described in detail in Section 3.4.7, table 3-9, figure 3-19 and 3-20, and Section 3.5.4.4, table 3-16, figure 3-33 and 3-34.

### 4.2.6.1 Results

**Table 4-12** *MESG values from experiments on flame gap surfaces with lengthwise grooves in the different apparatuses*

Apparatus	Gap surface Configurations	Ignition distance[mm]	MESG [mm]	MESG undamaged gap surface [mm]
PRSA	PV-10.1.4	14	1.12	0.98
MPCFA	CV-20.1.4	14	0.93	0.91

**Table 4-13** *Mean pressures obtained at MESG for gap surfaces with multiple lengthwise grooves, pressure from the same surfaces at the same opening as MESG opening for undamaged gap surface.*

Apparatus	Gap surface Configurations	Mean pressure MESG [barg]	Pressure at MESG for undamaged surface [barg]	Pressure MESG undamaged [barg]
PRSA	PV-10.1.4	1.783	1.837	3.157
MPCFA	CV-20.1.4	0.118	N/A	0.128

As shown in table 4-12, the slits with lengthwise orientated grooves on the flame gap surface examined in the present work, had a better ability to prevent re-ignition in the secondary chamber than the undamaged gap surfaces. Gap surfaces tested in both apparatuses gave an increase in the MESG value compared to the MESG value for the undamaged gap surface. The gap surface tested in the PRSA gave an increase of MESG by 14.3%. In the MPCFA the increase was 2.2%. It should be pointed out that the CV-20.1.4 slit is compared with the undamaged slit tested in the MPCFA.

Gap surfaces with lengthwise grooves increases the ventilation area of the gap, this is verified by the results from pressure measurements in the primary chamber, shown in table 4-13. The pressure build up is significantly lower in the PRSA when the gap opening is set to be the same as the MESG opening for the undamaged gap surface. The pressure when the MESG value is reached for these surfaces is also lower compared to the pressure obtained at MESG for undamaged gap surface.

#### 4.2.6.2 Discussion

Lengthwise grooves (see Section 3.3) that perforate the gaps through the whole gap-width are the kinds of damage thought to be most critical for the efficiency of a flame gap. Results from single lengthwise grooves discussed in Section 4.2.5, showed that lengthwise grooves had to have a width as large as 3 mm before they started to influence the efficiency of the flame gap in a negative way. No decrease in the MESHG was found when the grooves were 1 mm wide and 4mm deep. Experiments with multiple lengthwise grooves were performed to see if grooves with these dimensions would affect the efficiency of the flame gap if a large number of these grooves were applied on the gap surface. From the results reported above it can be seen that this was not the case.

The results show that these grooves influence the flow through the gap in another way than crosswise grooves. The maximum pressure is lower in the PRSA because there is a larger venting area for the combustion products. This reduces the velocity of the gases through the gap; in this case it gave an increase in the MESHG value. It can be a result of the increased time the hot combustion products are inside the narrow gap. The heat transfer from the hot gas to the gap walls can cause the hot jet to be more cooled down, before the jet is ejected into the external chamber, compared with the undamaged gap surface. But as discussed earlier it is not believed that the "cooling" in the gap is of a high order, and therefore this theory is not in accordance with the literature and the theory discussed for the other surface configurations in this thesis. The rate of cooling by entrainment and mixing will decrease because the velocity through the gap and into the external atmosphere is decreased, this should decrease the MESHG. The grooves are only 1 mm wide which is almost the same as the MESHG for the PRSA which is 0.98 mm for undamaged gap surfaces, the reason for the increase of MESHG in the PRSA can arise from turbulence formation from the grooves, despite the decreased pressure and velocity through the gap.

The change in MESHG with gap surfaces with lengthwise grooves was only significant in the PRSA. In the MPCFA the MESHG was almost equal to the MESHG for the undamaged gap surface. The reason for this is thought to be because the venting area in the MPCFA already is large with undamaged gap surface. The pressures are almost equal for the undamaged gap surface and for the gap surface with lengthwise grooves, this indicates that the velocity of the gas through the gap is almost equal and hence the MESHG value is equal. This shows that there most likely is not an increased heat transfer in the gap, even though the gap surface area is increased by the grooves. This again underpins the fact that "cooling" of the hot combustion products in the gap is only of second order importance when considering which mechanisms that has the largest effect on reducing the temperature in the hot combustion gases and preventing re-ignition outside the flame proof enclosure. The dominant mechanism is the rate of "cooling" by mixing and entrainment with "cold" unburned gas outside the gap. Hence the velocity and turbulence through the gap into the external mixture is the dominant parameter.

Despite the insufficient explanation of why the MESHG in the PRSA increased for gap surfaces with multiple lengthwise grooves, the results indicate that single grooves that do not constitute a danger for reducing the efficiency of the gap do not constitute a danger even if a large number of these grooves are applied on the gap.

### 4.3 Results and discussion from experiments with single lengthwise grooves performed in the PRSA

A total of eleven different slits with single grooves with different width and depth that perforates the slit lengthwise (see Section 3.3) in relation to the flow direction is examined in the PRSA. The slits had in basis the same quality and roughness as the undamaged gap surface before applying the grooves. In table 4-14 an overview of the MESG values found from experiments on slits with single lengthwise grooves on the gap surface with different width and depth that perforates the slit in the direction of flow is listed (see Section 3.5.4.5 for specifications of the gap surfaces with single lengthwise grooves).

#### 4.3.1 Results

**Table 4-14** Overview of the MESG values found on slits with single grooves with different width and depth that perforates the slit lengthwise in relation to the direction of flow. Experiments in the PRSA

Apparatus	Name	Depth	Width	MESG 14 mm
PRSA	1.4	4	1	1.01
PRSA	2.01	0.1	2	0.97
PRSA	2.02	0.2	2	0.95
PRSA	2.05	0.5	2	0.95
PRSA	2.1	1	2	0.95
PRSA	3.01	0.1	3	0.95
PRSA	3.02	0.2	3	0.88
PRSA	3.05	0.5	3	0.88
PRSA	3.1	1	3	0.4
PRSA	4.01	0.1	4	0.93
PRSA	4.05	0.5	4	0.63

The results are also presented in figure 4.6, it is illustrated how larger depth of the grooves affect the MESG value with a given width of the groove. Note that there is a slight improvement in the MESG for slit 1.4, which has a groove with width of 1mm and depth of 4mm. This is the largest depth tested. For grooves with width 2mm there is a small decrease in the MESG from 0.98 to 0.97 mm when the depth is 0.1 mm, and to 0.95 mm when the depth is 0.2, 0.5, and 1mm. When the width of the groove is increased to 3mm the MESG value decreased more rapidly, when the depth of the groove was increased. For grooves with groove width 4mm a significant decrease was found when the depth was increased to 0.5mm.

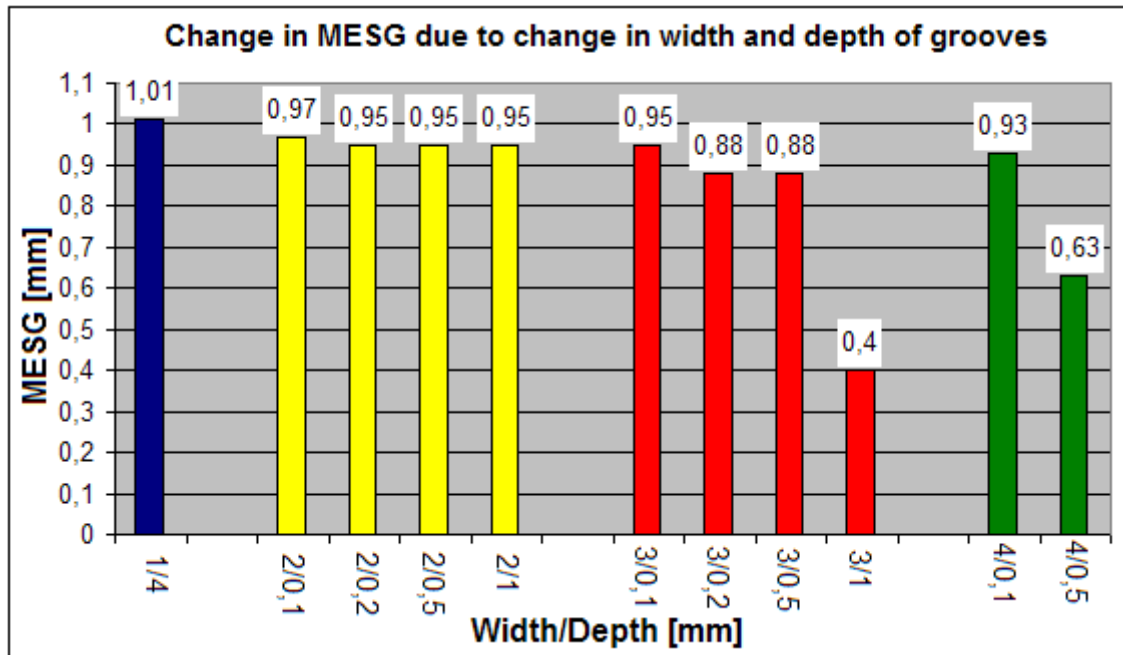


**Figure 4-6** Change in MESG due to change in width and depth of single lengthwise grooves in the flow direction through the whole gap length

#### Discussion

The results indicate that the width and depth of the groove determines whether a groove is "dangerous", which may negatively influence the efficiency of the flame gap in Ex "d" equipment. It is found that the grooves must have a width of 3mm and a depth of 1 mm before single lengthwise grooves in the midpoint of the gap gives a significant decrease of the MESG and hence of the efficiency of the gap. For grooves with widths and depths below this size, the grooves are not large enough to create jets of hot combustion products with enough energy and high enough temperatures to ignite the gas in the external chamber. The combustion products are cooled down inside the gap with the same efficiency as for the undamaged gap surface, and are ejected into the external chamber with equal velocities and flow conditions.

When the width of the groove is increased to 3 mm the groove approaches a size which is so large that the small volume of gas that is "pushed" through just in the "channel" made by the groove, reaches a condition which has large enough energy and temperature, to create conditions more favourable for re-ignition. The cooling of the hot combustion products is reduced just in the groove "channel" and the velocity of the hot combustion gases are decreased and the MESG and efficiency of the gap is reduced.

From these experiments it is shown that single lengthwise grooves have to be relatively large to influence the efficiency of the flame gap in Ex "d" equipment. This can be used when considering what kind of damage of the flame gap is large enough to constitute a danger for the integrity of the equipment.

The reason for not testing grooves with larger depths than 1 mm for grooves with width 2-4 mm is from the assumption that larger grooves is not likely to occur on Ex "d" equipment.





## 5 Conclusions

1. International standards (IEC) require that the average permissible roughness of any flame gap surface in flameproof electrical apparatuses has to be  $< 6.3 \mu\text{m}$ . The standards also require that any damaged joint surface has to be restored to this quality, but they do not provide any guidance as to what level of damage is considered significant. As a result even minor mechanical or corrosive damage of flame path surfaces calls for expensive overhaul and repair. This is mandatory despite the fact that a generous safety factor is included in the requirements to maximum permissible gap widths. For example, for the plane-flange configuration and explosive gas (propane) used in the present investigation, the maximum permissible width in a flameproof apparatus is only 0.4 mm, whereas the real limiting value (MESG) is 0.92 mm.
2. Normally the purpose of MESG experiments is to compare MESGs of different gases and vapours, using the same smooth flame gap surface in all experiments. However, in the present investigation MESG has been used as a parameter for judging whether a given type of damage of the gap surface had any noticeable effect on the ability of the flame gap to prevent flame transmission. Hence, a significant reduction of MESG compared with that obtained with a standard undamaged surface would mean that the particular type of damage under test had destroyed the gap efficiency significantly. On the other hand a significant increase of MESG compared with that for the undamaged surface would mean the damage had in fact significantly increased the gap efficiency.
3. In the experiments performed in the present work premixed 4.2 vol. % propane in air was used as the test gas mixture in all the experiments. Two different apparatuses were used, viz. a plane circular-flange apparatus (PCFA) and a plane rectangular-slit apparatus (PRSA). The flame gap surfaces were damaged mechanically by milling grooves of various depths and widths, either lengthwise or crosswise in relation to the flow direction of the gas through the gap. In one test series the gap surface (steel) was exposed to severe outdoor rusting before being exposed to explosion experiments. In another test series the steel surface was sandblasted. In one test series gap surfaces of Plexiglas were tested.
4. It was important to make sure that the MESG results were obtained at worst-case conditions. Therefore, since MESG obtained with a given apparatus depends strongly on the distance between the ignition point in the primary chamber and the flame gap entrance, the optimal distance for re-ignition had to be determined. An optimal distance of 14 mm had been confirmed experimentally for the PCFA by Opsvik (2010). In the present investigation a similar study was undertaken for the PRSA, and it was found that even for this apparatus 14 mm was the optimal distance for flame transmission. Consequently this distance was used in all the experiments also with the PRSA.
5. Three main series of experiments were conducted, viz. a first series using the plane circular-flange apparatus (PCFA), a second series of similar experiments using the plane rectangular-slit apparatus (PRSA), and finally a third series using the PRSA only. The findings from the three series were as follows (the underlying reasons for the various findings are discussed in Chapter 4:

- For undamaged gap surfaces ( $< 6.3 \mu\text{m}$ ) experiments in the PCFA gave an MESG of 0.95 mm, whereas experiments in the PRSA gave 0.98 mm, i.e. the two values were close to identical.
  - For sandblasted gaps with twice the allowed average roughness, MESG was 0.91 mm with the PCFA and 0.93 with the PRSA. These results are only marginally lower than those obtained with the undamaged surfaces.
  - For rusted gaps in the PCFA Opsvik (2010) had found that the rust formation increased MESG to 1.00 – 1.07 mm and hence improved the gap performance slightly. In the present investigation with the PRSA a reduction of MESG to 0.82 – 0.83 mm was found. Further experiments to resolve this puzzle are in progress at the University of Bergen.
  - In the single test series with undamaged Plexiglas gap surface ( $< 6.3 \mu\text{m}$ ) it was found that MESG was identical with that obtained with undamaged steel surfaces.
  - With multiple parallel crosswise rectangular grooves milled into one of the two surfaces of the gap there was in fact a significant improvement of the gap performance. Hence, in the PCFA MESG increased from 0.95 mm for the undamaged gap to 1.14 mm for the gap with grooves. For the PRSA the corresponding figures were 0.98 mm and 1.10 mm.
  - For multiple lengthwise milled rectangular grooves of 1 mm width and depth 4 mm a slight improvement of the gap performance was found (slight increase in MESG) with both the PCFA and the PRSA.
  - For single lengthwise grooves located in the middle of the gap a groove width of 1 mm had no influence on the gap performance even with a groove depth of 4 mm. With groove widths from 3 mm and upwards a gradual reduction of the gap performance with increasing width was found. The extent of this reduction increased with the groove depth in the investigated range 0.1 to 1.0 mm.
6. The overall conclusion from this investigation is that even very significant mechanical damage of surfaces of flame gaps in flameproof apparatus does not reduce the gap efficiency. In fact, in some cases significant improvement was observed. This in particular applies to crosswise grooves (e.g. accidental scratches). It is expected that these findings may trigger a discussion of possible revisions of national and international standards for both design and maintenance of flameproof enclosures.

## 6 Recommendations for further work

The experimental investigations in the present thesis have successfully showed the effect some different damages of the flame gap surface of Ex "d" equipment will have upon the efficiency of the gap. Both verification experiments and experiments with other damages are needed to be able to provide final quantitative conclusions. Suggestion for further work is listed below.

- Establish systems which can quantify the different conditions outside the gap exit created by the different flame gap configurations investigated in this thesis, e.g.: velocity measurements, turbulence measurements, Schlieren system, high speed camera, high speed laser-induced fluorescence (LIF) images of the hydroxyl-radical (OH), temperature measurements etc.
- More experiments are needed on gap surfaces with grooves. The experiments performed in this thesis with crosswise grooves on the flame gap surfaces are grooves with a relative large depth. Experiments with crosswise grooves which have a smaller depth would be useful, when considering that these grooves will create less initial turbulence, and maybe create conditions outside the gap opening more favourable for re-ignition than the large crosswise grooves.
- For the single lengthwise grooves it is only done experiments with single grooves in the midpoint of the slit surface. Experiments with single lengthwise grooves on other positions on the slit, and how these grooves influences the gap efficiency would be useful. This can be used to give guidance of the degree of damage and grooves/scratches that is critical for the efficiency of a flame gap in Ex "d" equipment, and damage that are not.
- Other damage of the gap surface should be tested, e.g. experiments with lengthwise grooves turned with different angels, shown in figure 6-1.

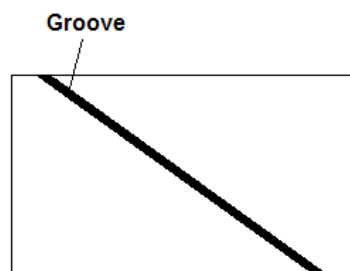


**Figure 6-1** *Illustration of a single groove milled into a gap surfaces with a given angle.*

- Experiments with single lengthwise grooves in the PCFA could be performed, to compare the results found with single lengthwise grooves in the PRSA.
- Investigate the effect of different dusts inside the flame gap, and the influence the dust will have upon re-ignition of the external atmosphere.

- Experiments with damage of flame gaps of commercial available Ex "d" equipment, to verify the results found in the apparatuses designed and built at the University of Bergen.
- Further investigation of rusted flame gap surfaces is needed.
- Investigate the effect obstructions just outside the flame gap will have on re-ignition of the external atmosphere.
- Numerical simulations on explosion transmission through narrow gaps, and re-ignition by hot combustion jets.
- Experiments with more reactive gases, in the present work it is only done experiments with 4.2 vol. % Propane in air
- A new gas analyzer is bought for the gas laboratory at the University of Bergen, this is a more accurate system, and the composition of the gas mixture will be more accurate, experiments should be carried out with this new equipment. Further modification of the experimental apparatuses could also be done, to make them more realistic compared to commercial available Ex "d" enclosures.
- A large number of experimental data is obtained from the work with the present thesis; these results could be further investigated and discussed.
-

# References

- Ballal, D. R. and A. H. Lefebvre (1975). "The influence of flow parameters on minimum ignition energy and quenching distance." Symposium (International) on Combustion 15(1): 1473-1481.
- Ballal, D. R. and A. H. Lefebvre (1977). "Flame quenching in turbulent flowing gaseous mixtures." Symposium (International) on Combustion 16(1): 1689-1698.
- Beyer, M. (1996). Über den Zünddurchschlag explodierender Gasgemische an Gehäusen der Zündschutzart 'Druckfeste Kapselung'. VDI Reiche.
- Beyling, C. (1906). Versuche zwecks Erprobung der Schlagwettersichercherheit besonders geschutzer elektrischer Motoren und Apparate. Glückaf: 42.
- Boust, B., J. Sotton, et al. (2007). "Unsteady heat transfer during the turbulent combustion of a lean premixed methane-air flame: Effect of pressure and gas dynamics." Proceedings of the Combustion Institute 31(1): 1411-1418.
- Çengel, Y. A. and M. A. Boles (2007). Thermodynamics: an engineering approach. Boston, McGraw-Hill.
- Drysdale, D. (1999). An introduction to fire dynamics. Chichester, Wiley.
- Eckhoff, R. K. (2005). Explosion hazards in the process industries. Houston, Tex., Gulf Publishing.
- Einarsen, R. I. (2001). Experimental determination of holes and slits in flameproof enclosures, for preventing transmission to external explosive gas clouds. Department of Pyhsics programme of process safety. Bergen, University of Bergen. Cand.Scient.
- Fenn, J. B. C., H.F. (1953). Activation energies in high temperature combustion. Fourth symposium (International) on combustion. Baltimore, Williams and Williams.
- Fox, R. W. and A. T. McDonald (1994). Introduction to fluid mechanics. New York, Wiley.
- Frank-Kameneckij, D. A. (1955). Diffusion and heat exchange in chemical kinetics. Princeton, Princeton University Press.
- Friedman, R. and W. C. Johnston (1950). "The Wall-Quenching of Laminar Propane Flames as a Function of Pressure, Temperature, and Air-Fuel Ratio." Journal of Applied Physics 21(8): 791-795.
- Groh, H. (2004). Explosion protection: electrical apparatus and systems for chemical plants, oiland gas industry, coal mining. Amsterdam, Elsevier/Butterworth Heinemann.
- H.Phillips (1971). The Mechanism of flameproof protection. Reasearch report 275. SMRE.

- H.Phillips (1972). "Ignition in a transient turbulent jet of hot inert gas." Combustion and Flame **19**: 8.
- H.Phillips (1987). The Physics of the Maximum Experimental Safe Gap. Proceedings of the International Symposium on the Explosion Hazard Classification of Vapors, Gases and dusts, Washington, D.C, National Academy press.
- H.Phillips (1988). The Safe Gap: Effect of explosion Pressure. IEE Conference Publication London: 5.
- IEC (1996). IEC (1996): 60079-20:1996 Explosive atmospheres Part 20: Data for flammable gases and vapours, relating to the use of electrical apparatus, Central Office of International Electrotechnical Commission, Geneva,Switzerland.
- IEC (2002). IEC (2002): 60079-1-1:2002 Electrical apparatus for explosive gas atmospheres Part 1-1: Flameproof enclosures 'd' Method of test for ascertainment of maximum experimental safe gap, Central Office of International Electrotechnical Commission, Geneva,Switzerland.
- IEC (2007a). IEC(2007a):60079-1:2007 Explosive atmospheres. Part 1: Equipment protection by flame proof enclosures "d".
- IEC (2007b). 60079-19:2007 Explosive atmospheres - Part 19: Equipment repair, overhaul and reclamation.
- IEC (2007c). IEC(2007c):60079-17:2007 Explosive atmospheres. Part 17: Electrical installations inspection and maintenance.
- Kanury, A. M. (1975). Introduction to combustion phenomena: (for fire, incineration, pollution, and energy applications). New York, Gordon and Breach.
- Larsen, Ø. (1998). A Study of Critical Dimensions of Holes for Transmission of Gas Explosions and development & Testing of a Schlieren System for studying Jets of Hot Combustion Products. Department of Physics and Technology. Bergen, University of Bergen. Cand.Scient.
- Lewis.B, Von Elbe. G. (1987). Combustion, flames and explosions of gases. Orlando, Academic Press.
- McCabe, W. L., P. Harriott, et al. (2005). Unit operations of chemical engineering. Boston, McGraw-Hill.
- Norris, R. H. a. S., DD (1940). "Laminar-Flow heat-transfer coefficients for ducts." Transactions of the American Society of Mechanical Engineers 62.
- Opsvik et.al, H., Grov., Eckhoff, R.K. (2010). MESG for propane/air in standard circular - flange experiments. Influence of sandblasting and corrosion of flame gap surfaces. Sixth International Seminar on Fire and Explosion Hazards. Weetwood Hall, Leeds, UK.

- Opsvik, H. E. Z. (2010). Experimental investigation of the influence of mechanical and corrosion damage of gap surfaces on the efficiency of flame gaps in flameproof apparatus. Department of physics and technology. Bergen, University of Bergen. Master Sc.
- Petroleum Safety Authority Norway, P. (2009). Trends in Risk Level in the Petroleum Activity on the Norwegian Continental Shelf. Ø. Tuntland: 36.
- Redeker, T. (1981). Classification of flammable gases and vapours by the flameproof safe gap and the incendivity of electrical sparks, Physikalisch Technische Bundesanstalt, Heat Division, Braunschweig.
- Sadanandan, R., D. Markus, et al. (2007). "Detailed investigation of ignition by hot gas jets." Proceedings of the Combustion Institute **31**(1): 719-726.
- Sadanandan, R., D. Markus, et al. (2009). Observation of the transmission of gas explosions through narrow gaps using time-resolved laser/Schlieren techniques, University of Karlsruhe.
- Servomex (1991). Servomex 1410B. Infrared Analyser. Instruction Manual.
- Smith, P. B. (1953). The role of flanges in conferring on protection on flameproof electrical enclosures. Safety in Mines Research Establishment
- Solheim, F. (2010). Master thesis. Bergen, Department of physics and technology, University of Bergen Norway.
- Tennekes, H. a. L., J.L. (1994). A first course in turbulence London, England, The MIT Press.
- Thibault, P., Y. K. Liu, et al. (1982). "Transmission of an explosion through an orifice." Symposium (International) on Combustion **19**(1): 599-606.
- Toney, M. K., T. Griffith, et al. (2000). A history of electrical area classification in the United States. Petroleum and Chemical Industry Conference, 2000. Record of Conference Papers. Industry Applications Society 47th Annual.
- VDE (1935). Guiding Principles on the Installation of Electrical Systems in Potentially Explosive Production Areas and Storage rooms. E. E. Protection. Berlin.
- Wolfhard, H. G. and A. E. Bruszak (1960). "The passage of explosions through narrow cylindrical channels." Combustion and Flame **4**: 149-159.





# APPENDIX

# Appendix A – Experimental apparatuses and procedures

## A.1 Equipment list

Table A-1-1 *Equipment list*

Equipment	Type
Gas Analyzer	Servomex 1400B4 SPX
Computer	Dell Latitude D630
DAQ	NI USB 6009
Pressure Transducer	Kistler 701A
Charge Amplifier	Kistler 5073
Test gas	Propane (99.95 %)
Calibration gas	5 % propane, Nitrogen (95%)
Spark Generator	Taylor made. Se appendix A.2
Roughness analyzer	Mitutoyo SJ-400
Roghness analyzer	Diavite DH-5
Experimental Apparatus	Plane Circular Flange Apparatus
Experimental Apparatus	Plane Rectangular Slit Apparatus

## A.2 Experimental Procedures

### A 2.1 Adjusting Procedure - gap opening in the Plane Circular Flange Apparatus

From (Opsvik 2010)

- 1 Remove the primary chamber from the secondary chamber by loosing the disparate cables and gas supply
- 2 Dismount the two flanges which the primary chamber consists of - by loosen the connecting nuts and screws

- 3 Clean the flange surfaces with a suitable solvent and a soft rag
- 4 Locate the calibration plates (4 pieces) as indicated at the drawing and photo underneath

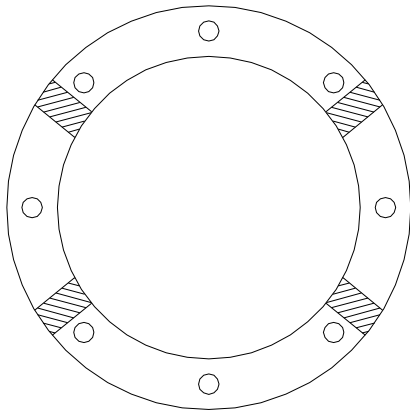


**Figure A-2.1a** Drawing of apparatus flange (flame path) with the distance "shims" in correct position

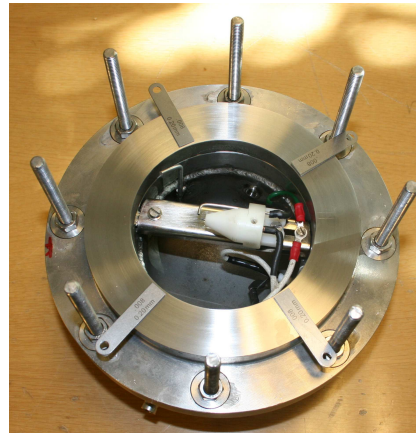


**Figure A-2.1b** Picture of apparatus flange (flame path) with the distance "shims" in correct position

- 5 Assembly the two flanges and gain a centric location by using the special made gauge tool while tightening up the bolts. Centricity is important when it comes to ascertain the characteristic criterion connected to the appurtenant flange setup. The pictures and sketch below shows the centricity tool

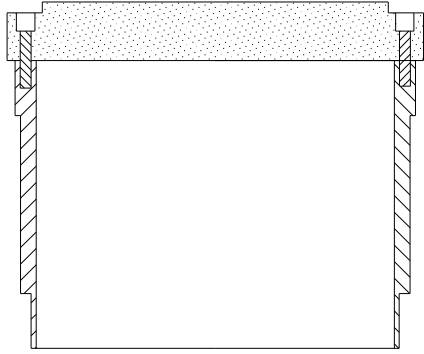


**Figure A-2.2a.** Section drawing of the assembly centring tool

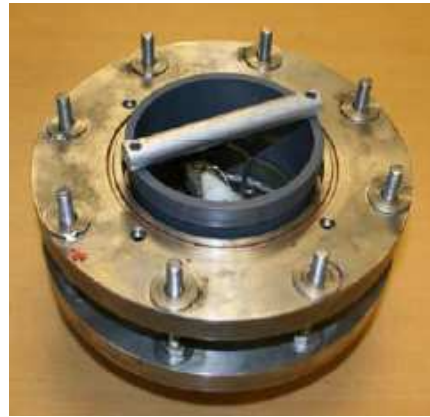


**Figure A-2.2b** Photo of the assembly centring tool

- 6 To ensure the same applied forces for each opening/experiment (provide reproducibility) the bolts were mounted with a torque set to 10 Nm

In general the opening is to be adjusted in steps of 0,1 mm adjusted by means of distance plates. When identifying the MESG the increments were set to 0,01 mm.



**Figure A-2.3** Distance plates used to adjust the gap between the flame paths

When changing the flanges on the primary chamber parts of this procedure may be used. After the experimental apparatus is dismantled the replaceable flanges can be exchanged by loosening the four Allen screws in the upper part, and the three Allen screws in the lower part

## A 2.2 Experimental procedure - The Plane Circular Flange Apparatus (PCFA)

From (Opsvik 2010)

After the gas analyzer is calibrated it has to be powered in the period the experiments are performed. A power off situation requires a new calibration. When starting the gas analyzer in

the morning, or after a longer brake, it's not mandatory, but prudent, to perform a zero point calibration, ref. point A.2.6 - Setting the zero.

The reference values in the procedure, with respect to flow, are based on experiences with a gas concentration of 4,2 % propane in air.

With reference to the schematic in Figure A-2.4 the following steps has to be accomplished:

- 1.) Install the plastic membrane on the top of the apparatus
- 2.) Turn on the spark generator
- 3.) Open utility valves (1, 2, 3 and 4). Close evacuating valve (7) and ensure that the 3 way valve (8) is in supply position
- 4.) Open the valve for air supply (5). Air pressure set to 0,5 barg
- 5.) Start the gas analyzer pump
- 6.) Open the valve for the gas supply (6). Gas pressure set to 0,5 barg
- 7.) Adjust the air and gas flow preliminary to 75% and 15% respectively on the analyzers flow meters
- 8.) Maximum gas flow is 1000 ml/minute
- 9.) Monitor the gas concentration level on inlet and outlet from the apparatus, and adjust up/down on the air supply to achieve 4,2 % propane in air. Allow the analyzer to stabilize at least 60 seconds before reading out measurements
- 10.) When the gas concentration level on the outlet reaches set point, start monitoring the gas concentration on the inlet of the experimental apparatus. Open the evacuating valve (7) and set the 3 way valve (8) to monitor the outlet. Close the utility valves (1, 2, 3 and 4)
- 11.) Secure the area
- 12.) Wear ear protection
- 13.) Activate the Labview program
- 14.) Store the measurements by means of specifying a filename in Labview
- 15.) Flush with air prior to new experiments
- 16.) When the experiments are completed remember to close the gas- (6) and air supply (5)

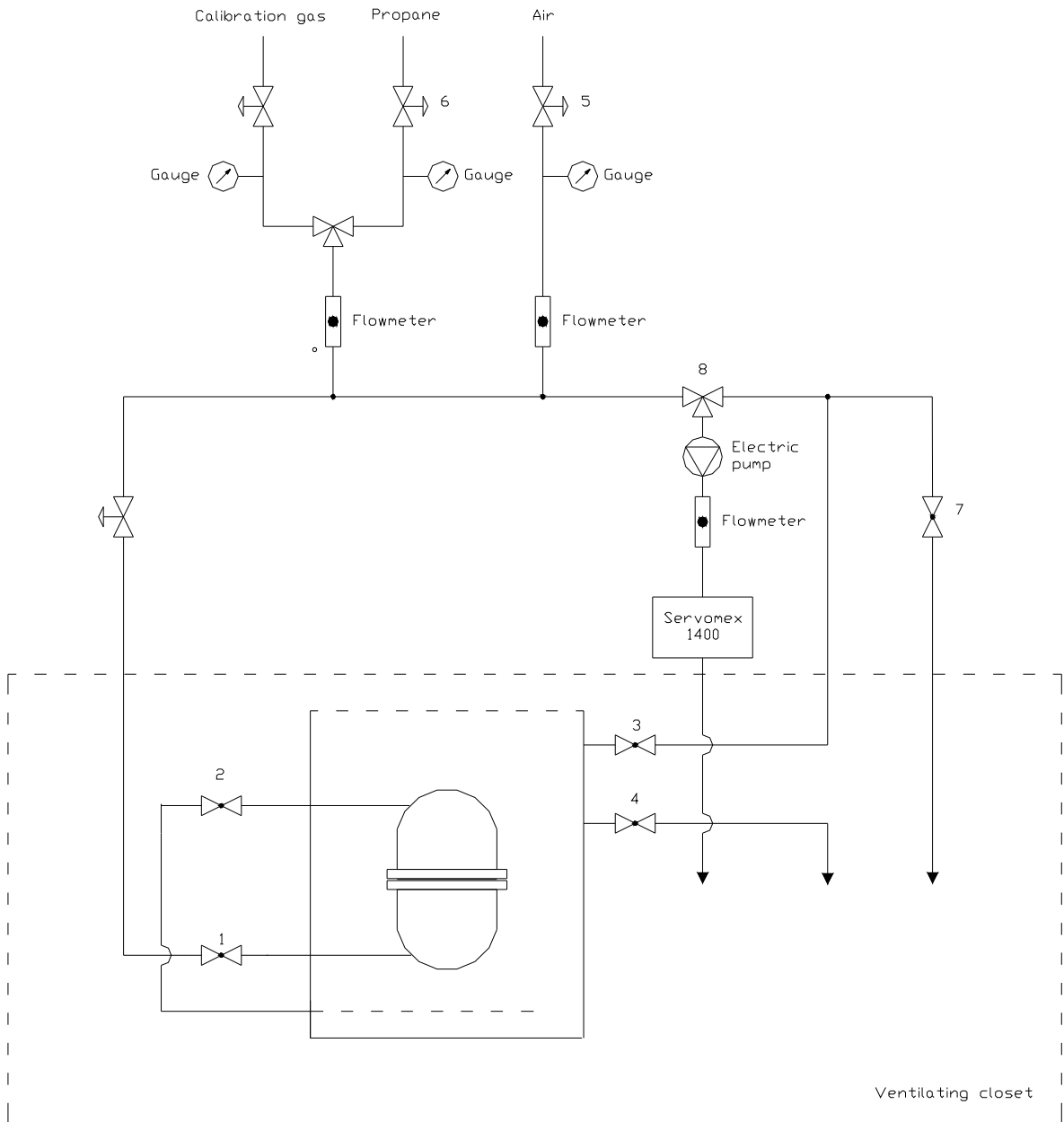


**Figure A-2.4** The PCFA with appurtenant tubing

## A 2.3 Checklist

From (Opsvik 2010)

In Table A-2, a checklist for experiments in the PCFA and PRSA is shown. This checklist is a tool for remembering the most important things in terms of safety and measurements when performing experiments.

**Table A-2.1** *Checklist for the experimental procedure for experiments in the experimental apparatus*

<b>What to check</b>	√
Spark generator on	
Data acquisition system is turned on	
Valves in correct position	
Secure area	
Ear Protection	
Activate experiment	
Measurement data saved with a proper address and filename	
Check test area after secondary explosions	

## A 2.4 Adjusting Procedure - gap opening in the PRSA

1. Remove the external chamber, by turning the whole chamber counter clockwise.
2. Remove the top of the primary chamber where the flame gap is located.
3. Locate the distance "shims" in both sides through the gap (shown in figure), make sure that the distance "shims" are through the whole gap width, to ensure uniform gap opening.
4. Fasten the two screws in the top of the gap (shown in figure A-2.5a and b), with a torque of 20 cNm.
5. Fasten the four screws at the start of the gap with a torque of 20 cNm (shown in figure A-2.6a and b).
6. Fasten the six screws on the bottom of the gap with a torque of 1 Nm.



**Figure A-2.5a** Photograph of the upper part of the flame gap in the PRSA, with distance "shims" placed, the gap is fastened with a small torque applied on the screws seen in the photograph

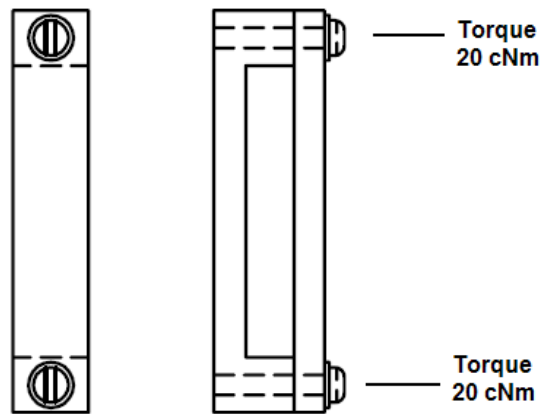


**Figure A-2.5b** Drawing of the clamp in the upper part of the flame gap, with the two screws that must be fastened with a torque of 20 cNm



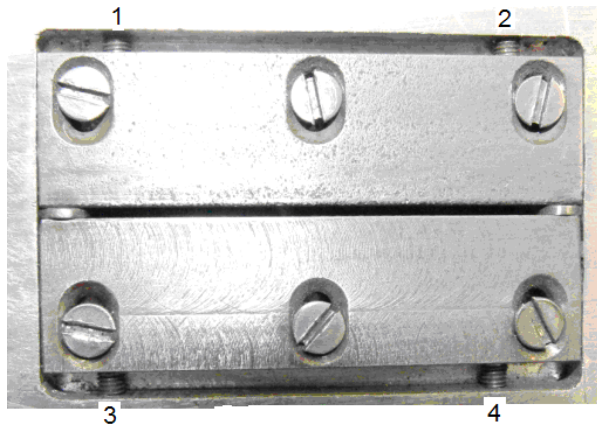


**Figure A-2.6a** Photograph of the lower part of the flame gap in the PRSA, this is the part which is inside the primary chamber. The numbers 1-4 on the photograph is the screws which are tightened with the same torque as the screws in the upper part of the flame gap, ensuring a uniform gap opening over the whole width of the gap. On the sides of the flame gap the distance "shims" can be seen

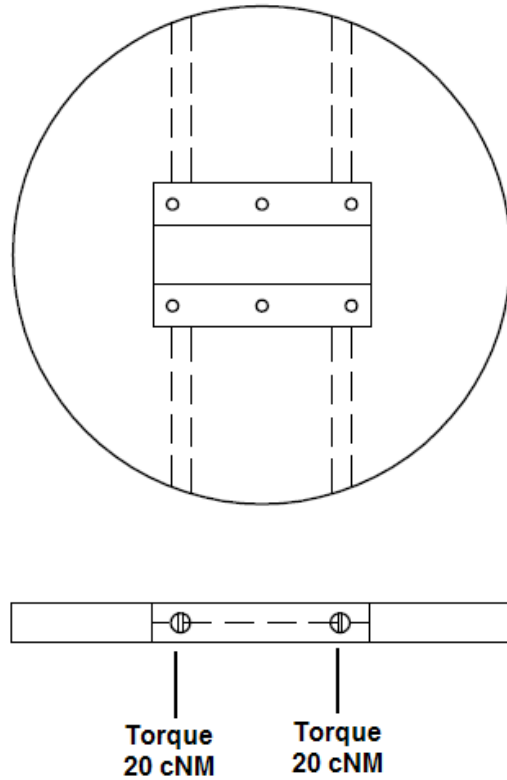


**Figure A-2.6b** Drawing of the lower part of the flame gap inside the primary chamber of the PRSA. The drawing shows where the screws clamp the gap together on the position where the distance "shims" are located

## **A 2.5 Experimental procedure – The Plane Rectangular Slit Apparatus (PRSA)**

After the gas analyzer is calibrated it has to be powered in the period the experiments is been performed. A power off situation requires a new calibration. When starting the gas analyzer in the morning, or after a longer brake, it's not mandatory, but prudent, to perform a zero point calibration, ref. point A.2.6 - Setting the zero.

The reference values in the procedure, with respect to flow, are based on experiences with a gas concentration of 4.2 % propane in air.

With reference to the schematic in Figure A-2.7 the following steps has to be accomplished:

- 1.) Install the plastic membrane on the top of the apparatus.
- 2.) Turn on the spark generator.
- 3.) Open utility valves (1, 2, 4 and 5). Close evacuating valve (7) and ensure that the 3 way valve (8) is in supply position. Service valve (6) shall be closed at all times during the experiments.
- 4.) Open the valve for air supply (9). Air pressure set to 0,5 barg.
- 5.) Start the gas analyzer pump.
- 6.) Open the valve for the gas supply (10). Gas pressure set to 0,5 barg.
- 7.) Adjust the air and gas flow preliminary to 75% and 15% respectively on the analyzers flow meters.
- 8.) Maximum gas flow is 1000 ml/minute.
- 9.) Monitor the gas concentration level on inlet and outlet from the apparatus, and adjust up/down on the air supply to achieve 4,2 % propane in air. Allow the analyzer to stabilize at least 60 seconds before reading out measurements.
- 10.) When the gas concentration level on the outlet reaches set point, start monitoring the gas concentration on the inlet of the experimental apparatus. Open the evacuating valve (7) and set the 3 way valve (8) to monitor the outlet. Close the utility valves (1, 2, 4 and 5).
- 11.) Secure the area.
- 12.) Wear ear protection.
- 13.) Activate the Labview program.
- 14.) Store the measurements by means of specifying a filename in Labview.
- 15.) Flush with air prior to new experiments.
- 16.) When the experiments are completed remember to close the gas- (10) and air supply (9).

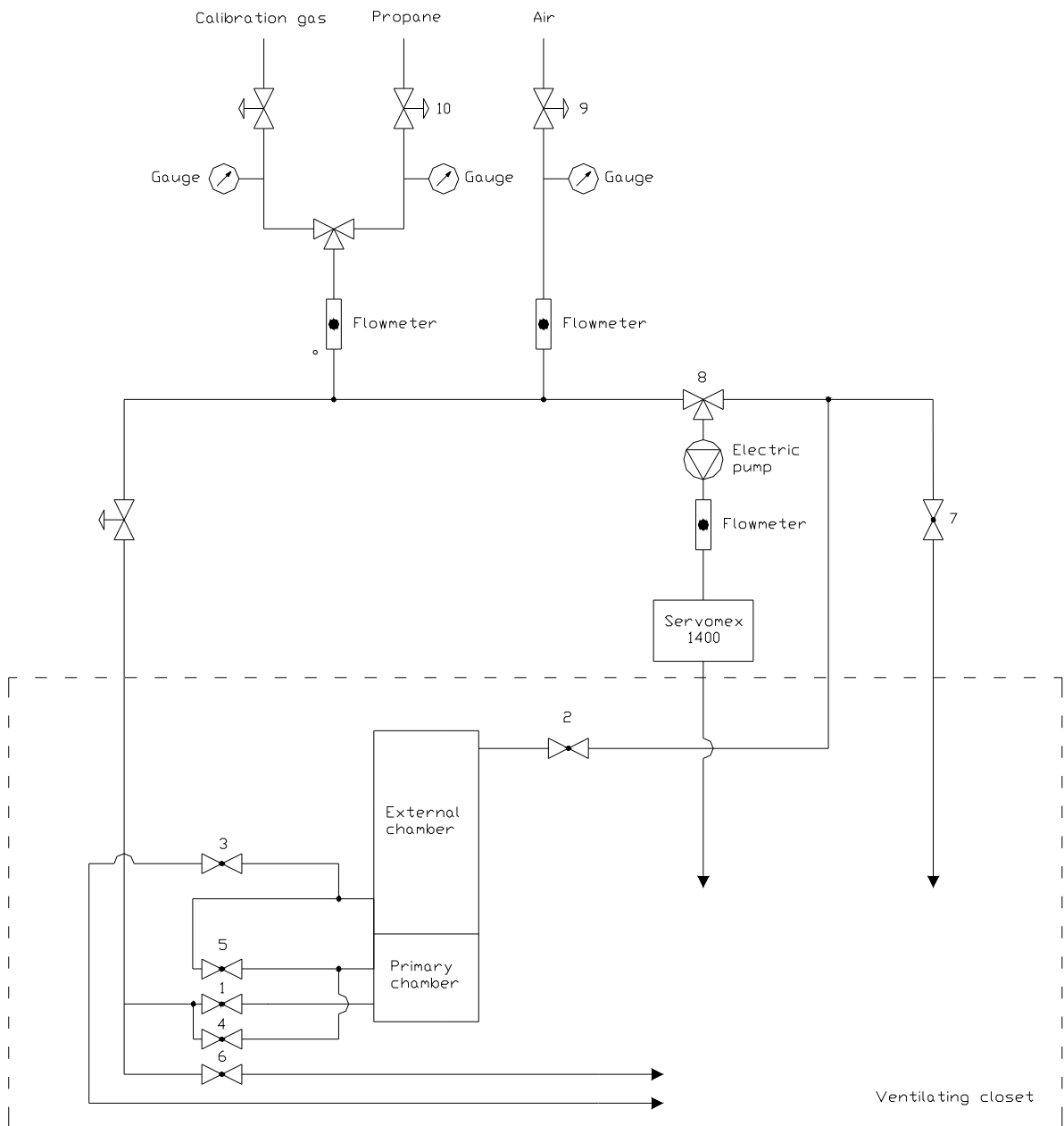


**Figure A-2.7** PRSA with appurtenant tubing

## A 2.6 Calibration procedure - Gas Analyzer

From (Opsvik 2010)

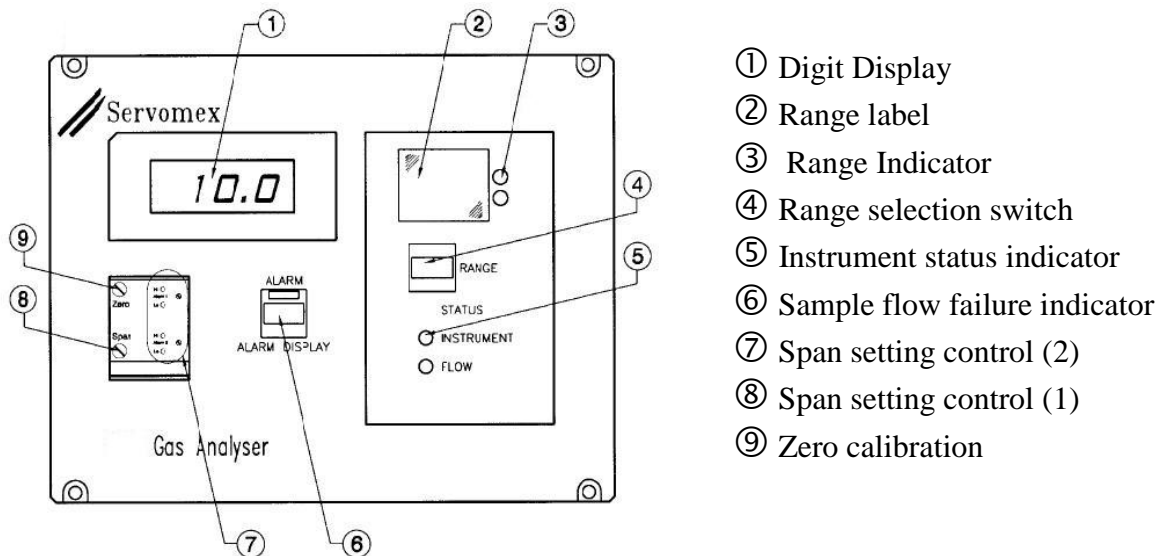


**Figure A-2.7** Servomex 1410 B - Infrared Gas Analyzer

For optimum accuracy allow a minimum of four hours from power on for the monitor to stabilise before performing a calibration.

When connecting the calibration gases allow at least 60 seconds for the internal pipe work and cell to flush out completely before making adjustments to the calibration. The analyzer should be calibrated at the temperature at which it will operate.

Servomex recommendations with respect to calibration intervals:

Weekly: Check Zero

Monthly: Check Zero and span. Adjust as necessary

### Setting the Zero

- i) Open the air supply valve. Adjust air pressure to 0,5 barg and flow to 1,0 litre/minute
- ii) Ensure that gas supply valve is closed
- iii) Start pump. Allow operation for approximately two minutes
- iv) Adjust display to 0,00 - if necessary. Use the Zero calibration potentiometer in the front of the analyzer, indicated as number ⑨ in figure A-4.2.1. Turning the potentiometer clockwise gives a increase in the display and vice versa

### Setting the span

- i) Close the air supply
- ii) Open the calibration gas supply. The calibration gas consists of 5% propane and 95% Nitrogen

- iii) Adjust gas pressure to 0,5 barg and flow to 1 litre/minute
- iv) Adjust display to 5,00% - if necessary. Use the Span calibration potentiometer in the front of the analyzer, indicated as number ⑧ in figure A-4.2.1. Turning the potentiometer clockwise gives a increase in the display and vice versa

The span potentiometer to the right is only in use if a second span gas is introduced. The method would be precisely the same as described in point iv) above.

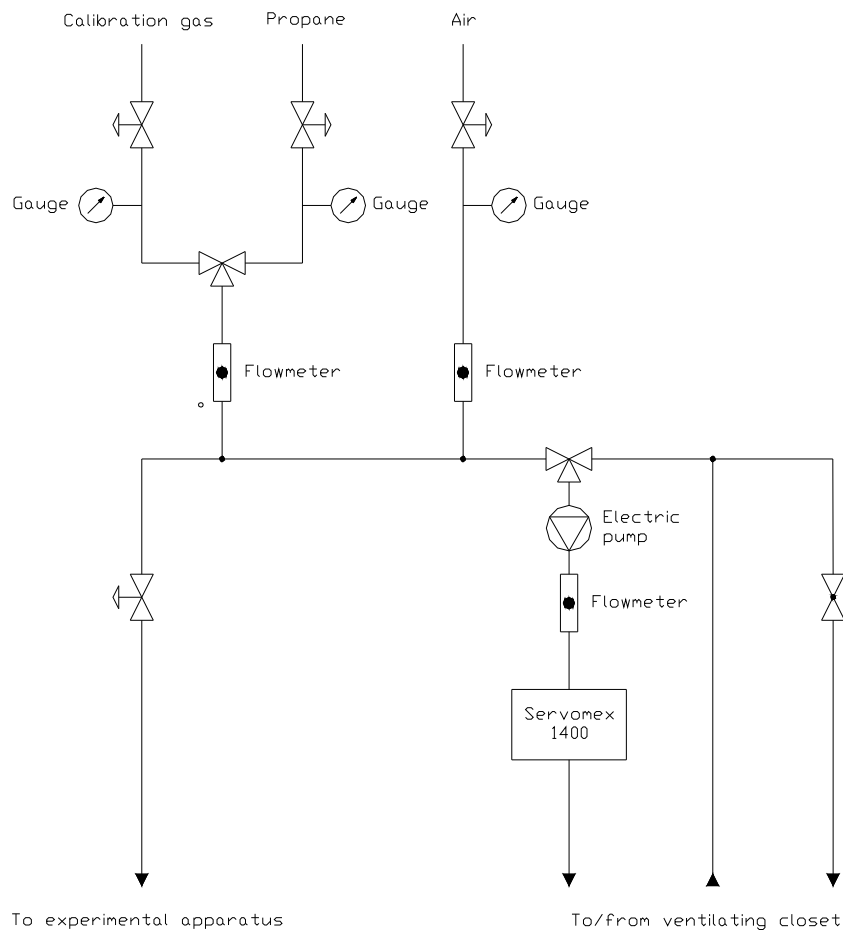


**Figure A-2.8** Servomex 1410 B - Infrared Gas Analyzer with appurtenant pipe work and fixtures

## A 2.7 Data Acquisition System

From (Opsvik 2010)

### A simplified user guide for the Labview program for running the experiment

A program was made, based on Labview, in order to run the experiment. In the front panel of the program, shown in Figure A-2.9 and A-2.10, the experiments it's getting controlled. In the block diagram, shown in the same figure, input/output-channel settings can be chosen by the use of the data acquisition (DAQ) assistants. To activate the experiment, press the arrow button in the upper left corner of the front panel. After every experiment it is important that the file name for the logging file is saved. This is done via the file path dialog box.

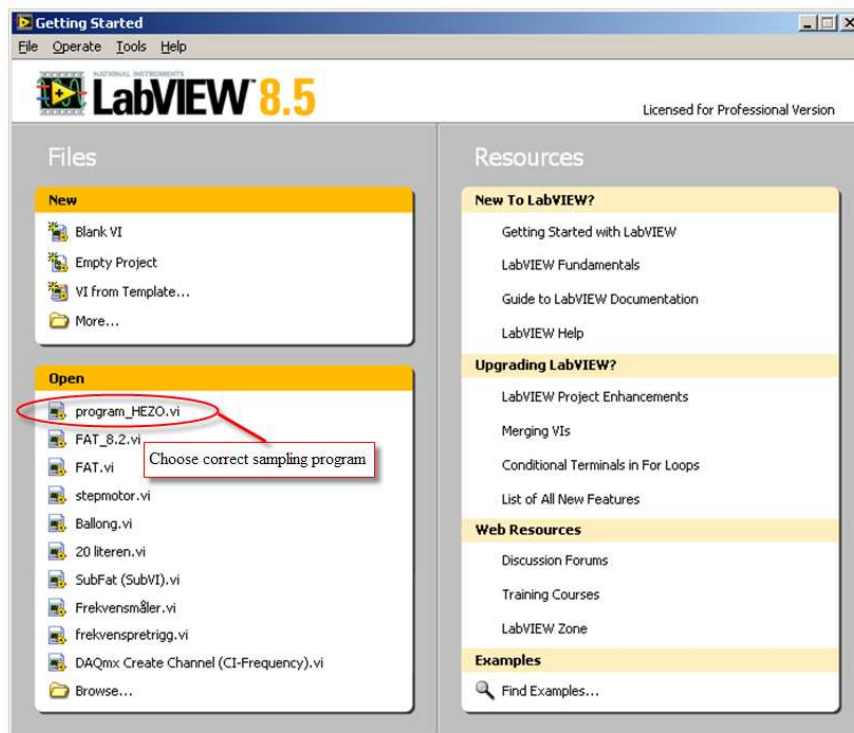
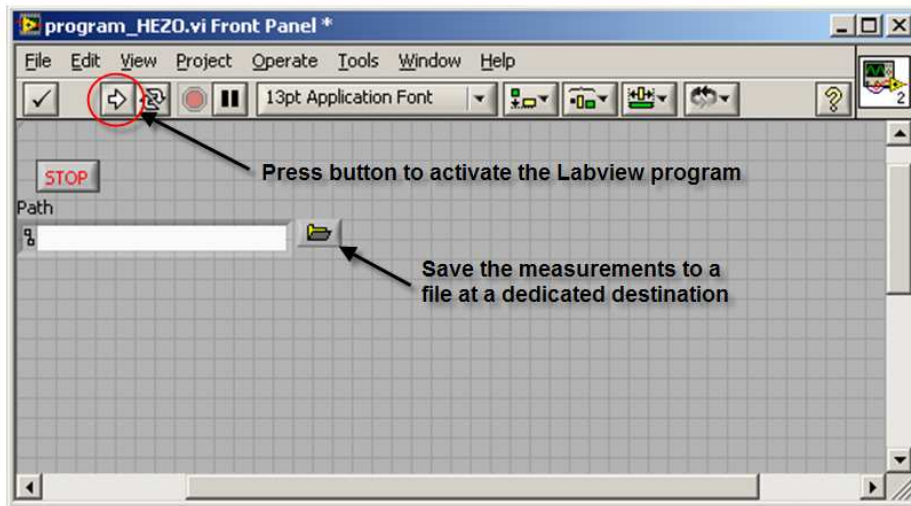


Figure A-2.9 Initial Labview dialog box



**Figure A-2.10** *Main Labview dialog box*

## Appendix B – Spark Generator

From (Kalvatn 2009)

An electric spark generator has been made for preliminary experiments for both this project and others e.g. the modified balloon experiment. However, it did not generate enough energy to ignite pure dust clouds and was therefore only used for gas mixtures and hybrid mixtures with gas and dust. The energy generated has been estimated at around 50 mJ. Figure A-3 shows the schematic for the generator. The part list is shown in Table B-1 The electronics of the generator is built into a cabinet with the size of 25 x 20 x 11 cm (L x W x H) and a handle on the top. The electrical circuit board within the spark generator has been made at the UiB. The basic principle of the generator is to discharge a capacitor that has been loaded by electricity from the regular power net. Either a negative or a positive flank of voltage can manually, or externally trigger the spark generator. The desired setting is chosen on the front panel of the spark generator. The possibility to externally trigger the spark discharge makes it easy to trigger the spark from a computer, thus it is implemented in the Labview program for running the FAT experiment. Figure B-1 below shows the inner parts of the generator.

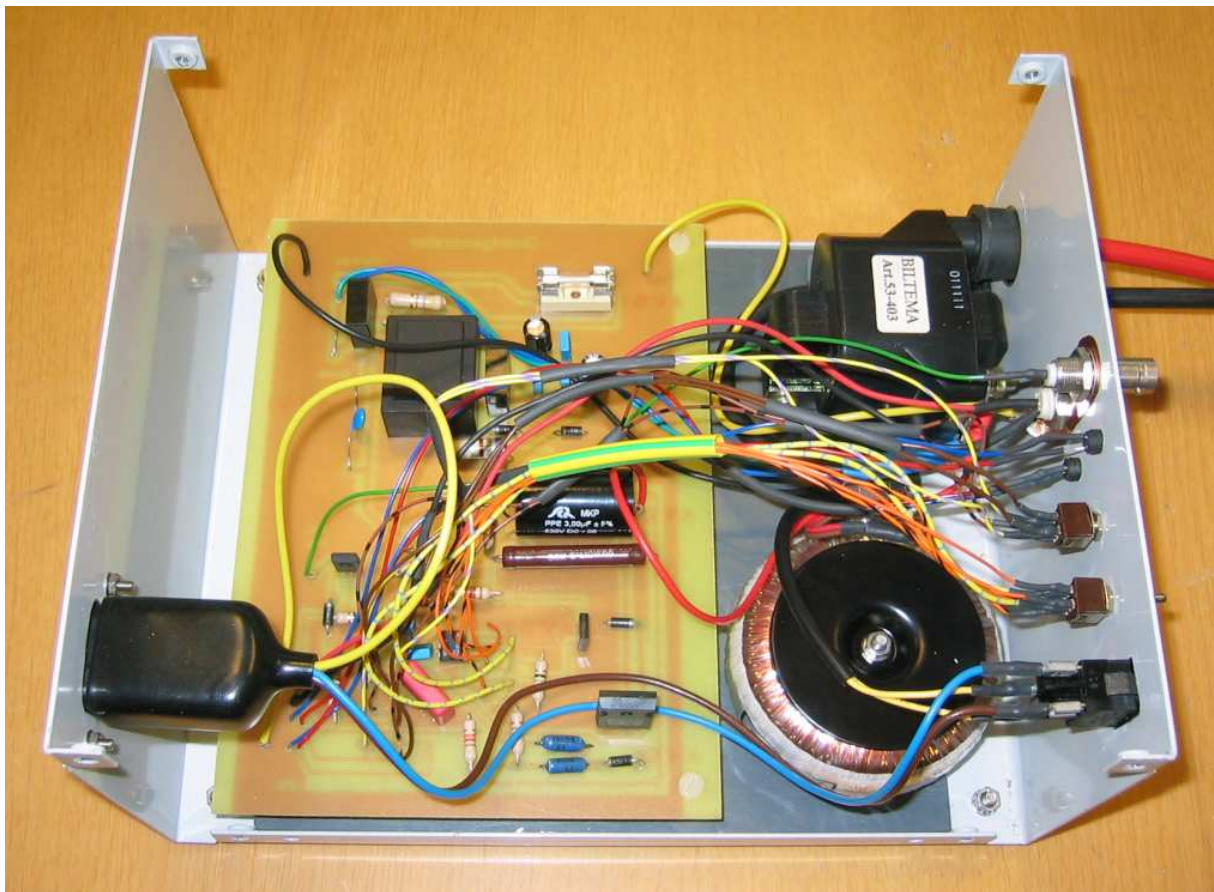


**Figure B-1** Inner parts of the electric spark generator



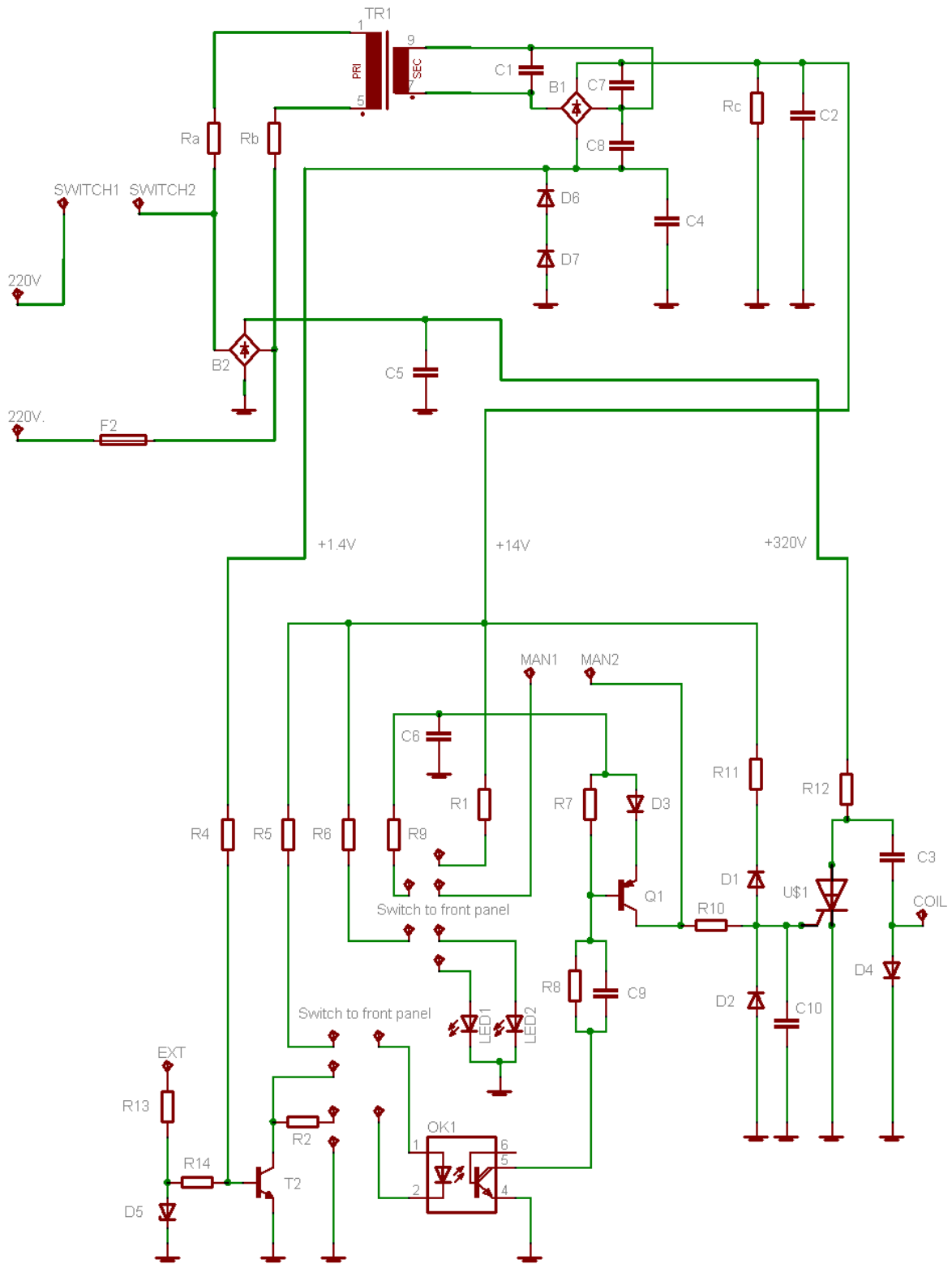


**Figure B-2** *Electrical circuit for spark generator*

**Table B-1** Part list for spark generator

Part	Value	Device	
C3	1u/500V	C-EU275-113X316	capacitor
C6	2.2u	C-EU050-025X075	capacitor
C9	0.1u	C-EU025-024X044	capacitor
C10	0.1u	C-EU050-025X075	capacitor
D1	1N4004	1N4004	diode
D2	1N4004	1N4004	diode
D3	1N4004	1N4004	diode
D4	1N4004	1N4004	diode
D5	1N821	1N821	diode
LED1		LED5MM	led
LED2		LED5MM	led
OK1	4N33	4N33	optocoupler
Q1	BD140	BD140	transistor-pnp
R1	100	R-EU_0207/10	resistor
R2	15	R-EU_0207/10	resistor
R4	10k	R-EU_0207/10	resistor
R5	680	R-EU_0207/15	resistor
R6	1.2k	R-EU_0207/10	resistor
R7	1.2k	R-EU_0207/10	resistor
R8	1.2k	R-EU_0207/10	resistor
R9	220	R-EU_0207/10	resistor
R10	15	R-EU_0207/10	resistor
R11	100	R-EU_0207/10	resistor
R12	58k/2w	R-EU_0617/22	resistor
R13	470	R-EU_0207/10	resistor
R14	120	R-EU_0207/10	resistor
T2	BD139	BD139	transistor
U\$1	30TPS08	30TPS08	triac
B1		SKB	rectifier
B2		SKB	rectifier
C1	0.1u	C-EU050-025X075	capacitor
C2	100u	C-EU050-025X075	capacitor
C4	100u	C-EU050-025X075	capacitor
C5	0.01u/400V	C-EU275-093X316	capacitor
C7	0.1u	C-EU050-025X075	capacitor
C8	0.1u	C-EU050-025X075	capacitor
D6	1N4004	1N4004	diode
D7	1N4004	1N4004	diode
F2		SH22,5A	fuse
Ra	470/1w	R-EU_0411/15	resistor
Rb	470/1w	R-EU_0411/15	resistor
Rc	680/1w	R-EU_0411/15	resistor
TR1		EI30-1	trafo
coil		Art.53-403	Biltema

## **Appendix C – Measurement data from experiments**

Some of the measurements data around and at the MESG opening for the different gap surfaces are given in this appendix.

<b>Date:</b>	07.12.2009		
<b>Surface configuration:</b>	New/Undamaged		
<b>Apparatus:</b>	PRSA		
<b>Yi [mm]</b>	<b>Zi [mm]</b>	<b>Pmax [barg]</b>	<b>Re- ignition</b>
0,99	14	3,130	Yes
0,99	14	3,129	Yes
0,99	14	3,127	No
<b>Mean: 3,12866667</b>		<b>Max:</b>	3,13
0,98	14	3,108	No
0,98	14	3,156	No
0,98	14	3,109	No
0,98	14	3,157	No
0,98	14	3,144	No
0,98	14	N/A	No
0,98	14	N/A	No
0,98	14	3,155	No
0,98	14	3,155	No
0,98	14	3,109	No
<b>Mean: 3,136625</b>		<b>Max:</b>	3,157
1,00	14	3,014	Yes
1,00	14	2,970	Yes
1,00	14	2,909	Yes
1,00	14	3,014	Yes
1,00	14	3,016	Yes
1,00	14	3,072	Yes
1,00	14	3,049	Yes
1,00	14	3,031	Yes
1,00	14	2,996	Yes
1,00	14	3,054	Yes
<b>Mean: 3,013</b>		<b>Max:</b>	3,072

<b>Date:</b>	09.12-16.12.2009		
<b>Surface configuration:</b>	PH-7,2,3		
<b>Apparatus:</b>	PRSA		
<b>Yi [mm]</b>	<b>Zi [mm]</b>	<b>Pmax [barg]</b>	<b>Re- ignition</b>
0,98	14	4,331	No
<b>Mean: 4,302</b>		<b>Max:</b>	4,331
0,99	14	4,273	No
<b>Mean: 4,273</b>		<b>Max:</b>	4,273
1,00	14	4,166	No
<b>Mean: 4,166</b>		<b>Max:</b>	4,166
1,01	14	4,204	No
<b>Mean: 4,204</b>		<b>Max:</b>	4,204
1,02	14	4,288	No
1,03	14	4,132	No
<b>Mean: 4,132</b>		<b>Max:</b>	4,132
1,04	14	4,155	No

	<b>Mean: 4,155</b>	<b>Max:</b>	4,155
1,05	14	4,148	No
	<b>Mean: 4,148</b>	<b>Max:</b>	4,148
1,06	14	4,028	No
	<b>Mean: 4,028</b>	<b>Max:</b>	4,028
1,07	14	N/A	No
	<b>Mean: N/A</b>	<b>Max:</b>	N/A
1,08	14	4,049	No
	<b>Mean: 4,049</b>	<b>Max:</b>	4,049
1,13	14	3,438	No
	<b>Mean: 3,438</b>	<b>Max:</b>	3,438
1,18	14	N/A	Yes
	<b>Mean: N/A</b>	<b>Max:</b>	N/A
1,17	14	3,913	Yes
	<b>Mean: 3,913</b>	<b>Max:</b>	3,913
1,16	14	3,819	Yes
	<b>Mean: 3,819</b>	<b>Max:</b>	3,819
1,15	14	3,901	Yes
	<b>Mean: 3,901</b>	<b>Max:</b>	3,901
1,14	14	3,980	Yes
1,14	14	3,977	Yes
1,14	14	4,018	Yes
1,14	14	3,972	Yes
1,14	14	3,908	Yes
1,14	14	3,906	Yes
1,14	14	N/A	Yes
1,14	14	N/A	Yes
1,14	14	3,977	Yes
1,14	14	4,598	No
	<b>Mean: 4,042</b>	<b>Max:</b>	4,598
1,15	14	3,985	Yes
1,15	14	3,824	Yes
1,15	14	3,883	Yes
1,15	14	3,855	Yes
1,15	14	3,916	Yes
1,15	14	3,900	Yes
1,15	14	3,908	Yes
1,15	14	3,875	Yes
1,15	14	4,548	No
	<b>Mean: 3,966</b>	<b>Max:</b>	4,548
1,16	14	3,918	Yes
1,16	14	N/A	Yes
1,16	14	N/A	Yes
1,16	14	3,880	Yes
1,16	14	3,845	Yes
1,16	14	3,839	Yes
1,16	14	3,804	Yes
1,16	14	4,469	No
	<b>Mean: 4,137</b>	<b>Max:</b>	4,469
1,17	14	3,804	Yes
1,17	14	N/A	Yes

1,17	14	3,885	Yes
1,17	14	3,962	Yes
1,17	14	3,842	Yes
1,17	14	4,588	No
<b>Mean: 4,215</b>		<b>Max:</b>	4,588
1,18	14	3,999	Yes
1,18	14	4,596	No
<b>Mean: 4,298</b>		<b>Max:</b>	4,596
1,19	14	3,862	Yes
1,19	14	3,832	Yes
1,19	14	3,868	Yes
1,19	14	3,863	Yes
1,19	14	N/A	Yes
1,19	14	3,806	Yes
1,19	14	3,878	Yes
1,19	14	N/A	Yes
1,19	14	3,808	Yes
1,19	14	N/A	Yes
<b>Mean: 3,845</b>		<b>Max:</b>	3,878
1,13	14	N/A	Yes
<b>Mean: N/A</b>		<b>Max:</b>	N/A
1,12	14	4,048	Yes
<b>Mean: 4,048</b>		<b>Max:</b>	4,048
1,11	14	N/A	No
1,11	14	N/A	Yes
<b>Mean: N/A</b>		<b>Max:</b>	N/A
1,10	14	4,199	No
1,10	14	4,176	No
1,10	14	4,100	No
1,10	14	4,048	No
1,10	14	4,129	No
1,10	14	4,188	No
1,10	14	4,135	No
1,10	14	4,140	No
1,10	14	4,790	No
1,10	14	4,183	No
<b>Mean: 4,209</b>		<b>Max:</b>	4,790

<b>Date:</b>	11.11-12-11.2009		
<b>Surface configuration:</b>	Sandblasted		
<b>Apparatus:</b>	PRSA		
<b>Yi [mm]</b>	<b>Zi [mm]</b>	<b>Pmax [barg]</b>	<b>Re- ignition</b>
0,97	14	3,220	Yes
0,97	14	3,157	Yes
0,97	14	3,122	Yes
0,97	14	3,129	Yes
0,97	14	3,149	Yes
0,97	14	N/A	Yes
0,97	14	3,149	Yes

0,97	14	3,146	Yes
0,97	14	3,152	Yes
0,97	14	3,156	Yes
<b>Mean: 3,153</b>		<b>Max:</b>	3,220
0,96	14	N/A	Yes
<b>Mean: N/A</b>		<b>Max:</b>	N/A
0,95	14	3,129	Yes
<b>Mean: 3,129</b>		<b>Max:</b>	3,129
0,94	14	N/A	No
0,94	14	N/A	Yes
<b>Mean: N/A</b>		<b>Max:</b>	N/A
0,93	14	3,921	No
0,93	14	3,967	No
0,93	14	3,934	No
0,93	14	3,938	No
0,93	14	3,212	No
0,93	14	N/A	No
0,93	14	N/A	No
0,93	14	3,916	No
0,93	14	N/A	No
0,93	14	N/A	No
<b>Mean: 3,815</b>		<b>Max:</b>	3,967

<b>Date:</b>	3.2-5.2.2010		
<b>Surface configuration:</b>	Corroded 1		
<b>Apparatus:</b>	PRSA		
<b>Yi [mm]</b>	<b>Zi [mm]</b>	<b>Pmax [barg]</b>	<b>Re- ignition</b>
0,98	14	3,108	No
0,98	14	2,909	Yes
<b>Mean: 3,009</b>		<b>Max:</b>	3,108
0,97	14	2,897	Yes
<b>Mean: 2,897</b>		<b>Max:</b>	2,897
0,96	14	2,877	Yes
<b>Mean: 2,877</b>		<b>Max:</b>	2,877
0,95	14	3,190	No
0,95	14	3,126	Yes
0,95	14	3,046	Yes
<b>Mean: 3,120</b>		<b>Max:</b>	3,190
0,94	14	3,192	Yes
<b>Mean: 3,192</b>		<b>Max:</b>	3,192
0,93	14	3,109	Yes
0,93	14	3,06078	Yes
<b>Mean: 3,085</b>		<b>Max:</b>	3,109
0,91	14	N/A	Yes
0,91	14	3,10917	Yes
<b>Mean: 3,109</b>		<b>Max:</b>	3,109
0,9	14	3,0748	Yes
0,9	14	3,08879	
<b>Mean: 3,082</b>		<b>Max:</b>	3,089

0,89	14	3,11935	Yes
<b>Mean: 3,119</b>		<b>Max:</b>	3,119
0,87	14	3,18186	Yes
<b>Mean: 3,182</b>		<b>Max:</b>	3,182
0,86	14	3,215	No
0,86	14	3,21754	Yes
<b>Mean: 3,216</b>		<b>Max:</b>	3,218
0,85	14	3,21868	No
0,85	14	N/A	Yes
<b>Mean: 3,219</b>		<b>Max:</b>	3,219
0,84	14	3,13089	Yes
<b>Mean: 3,131</b>		<b>Max:</b>	3,131
0,83	14	3,12579	No
0,83	14	3,15893	No
0,83	14	3,14109	No
0,83	14	3,17167	No
0,83	14	3,14109	No
0,83	14	3,14109	No
0,83	14	3,14109	No
0,83	14	3,13854	No
0,83	14	3,09011	No
0,83	14	3,11681	No
<b>Mean: 3,137</b>		<b>Max:</b>	3,172
0,87	14	3,13463	Yes
0,87	14	3,06842	Yes
0,87	14	3,06972	Yes
0,87	14	3,06078	Yes
0,87	14	3,09643	Yes
0,87	14	3,07737	Yes
0,87	14	3,0643	Yes
0,87	14	3,06892	Yes
0,87	14	3,07606	Yes
<b>Mean: 3,080</b>		<b>Max:</b>	3,135

<b>Date:</b>	8.2-10.2.2010		
<b>Surface configuration:</b>	Corroded 2		
<b>Apparatus:</b>	PRSA		
<b>Yi [mm]</b>	<b>Zi [mm]</b>	<b>Pmax [barg]</b>	<b>Re- ignition</b>
0,98	14	3,118	No
0,98	14	2,974	Yes
<b>Mean: 3,046</b>		<b>Max:</b>	3,118
0,82	14	3,197	No
0,82	14	3,233	No
0,82	14	3,146	No
0,82	14	3,233	No
0,82	14	3,208	No
0,82	14	3,160	No
0,82	14	3,201	No
0,82	14	3,304	No



0,82	14	3,248	No
0,82	14	3,243	No
<b>Mean: 3,217</b>		<b>Max:</b>	<b>3,304</b>
0,89	14	3,107	Yes
0,89	14	N/A	Yes
0,89	14	3,068	Yes
0,89	14	3,089	Yes
0,89	14	3,046	Yes
0,89	14	3,023	Yes
0,89	14	3,079	Yes
0,89	14	3,103	Yes
0,89	14	3,076	Yes
0,89	14	3,007	Yes
<b>Mean: 3,066</b>		<b>Max:</b>	<b>3,107</b>

<b>Date:</b>	11.3-15.3.2010		
<b>Surface configuration:</b>	PV-10.1.4		
<b>Apparatus:</b>	PRSA		
<b>Yi [mm]</b>	<b>Zi [mm]</b>	<b>Pmax [barg]</b>	<b>Re- ignition</b>
1,12	14	1,765	No
1,12	14	1,715	No
1,12	14	N/A	No
1,12	14	1,836	No
1,12	14	1,836	No
1,12	14	1,755	No
1,12	14	1,801	No
1,12	14	1,765	No
1,12	14	1,772	No
1,12	14	1,806	No
<b>Mean: 1,783</b>		<b>Max:</b>	<b>1,836</b>

<b>Date:</b>	24.03.2010		
<b>Surface configuration:</b>	Plexi		
<b>Apparatus:</b>	PRSA		
<b>Yi [mm]</b>	<b>Zi [mm]</b>	<b>Pmax [barg]</b>	<b>Re- ignition</b>
0,98	14	3,377	No
0,98	14	3,252	No
0,98	14	3,152	No
0,98	14	3,165	No
0,98	14	3,076	No
0,98	14	3,007	No
0,98	14	3,663	No
0,98	14	2,992	No
0,98	14	2,933	No
0,98	14	2,923	No
<b>Mean: 3,154</b>		<b>Max:</b>	<b>3,663</b>

Date:		27.1-1.2.2010	
Surface configuration:		CH-8,2,3	
Apparatus:		PCFA	
Yi [mm]	Zi [mm]	Pmax [barg]	Re- ignition
1,14	14	0,264	No
1,14	14	0,279	No
1,14	14	0,274	No
1,14	14	0,285	No
1,14	14	0,274	No
1,14	14	0,274	No
1,14	14	0,271	No
1,14	14	0,317	No
1,14	14	0,310	No
1,14	14	0,312	No
<b>Mean:</b>		0,286	<b>Max:</b> 0,317
1,15	14	0,251	No
1,15	14	0,271	Yes
<b>Mean:</b>		0,261	<b>Max:</b> 0,271
1,16	14	0,269	No
<b>Mean:</b>		0,269	<b>Max:</b> 0,269
1,17	14	0,264	Yes
1,17	14	0,266	No
<b>Mean:</b>		0,265	<b>Max:</b> 0,266
1,18	14	0,236	Yes
1,18	14	0,236	Yes
1,18	14	0,231	Yes
1,18	14	0,256	No
<b>Mean:</b>		0,239	<b>Max:</b> 0,256
1,19	14	0,225	Yes
1,19	14	0,231	Yes
1,19	14	0,241	Yes
1,19	14	0,241	Yes
1,19	14	0,236	Yes
1,19	14	0,246	Yes
1,19	14	0,231	No
<b>Mean:</b>		0,236	<b>Max:</b> 0,246
1,20	14	0,233	Yes
1,20	14	0,219	Yes
1,20	14	0,241	Yes
1,20	14	0,218	Yes
1,20	14	0,241	Yes
1,20	14	0,205	Yes
1,20	14	0,185	Yes
1,20	14	0,233	Yes
1,20	14	0,233	Yes
1,20	14	0,236	Yes
<b>Mean:</b>		0,224	<b>Max:</b> 0,241

<b>Date:</b>	24.03-26.3.2010		
<b>Surface configuration:</b>	New/Undamaged		
<b>Apparatus:</b>	PRSA		
<b>Yi [mm]</b>	<b>Zi [mm]</b>	<b>Pmax [barg]</b>	<b>Re- ignition</b>
0,91	14	0,140	No
0,91	14	0,140	No
0,91	14	0,140	No
0,91	14	0,145	No
0,91	14	0,145	No
0,91	14	0,140	No
0,91	14	0,155	No
0,91	14	0,145	No
0,91	14	0,153	No
0,91	14	0,145	No
<b>Mean:</b>	0,145	<b>Max:</b>	0,155

<b>Date:</b>	24.03.2010		
<b>Surface configuration:</b>	CV-10,1,4		
<b>Apparatus:</b>	PRSA		
<b>Yi [mm]</b>	<b>Zi [mm]</b>	<b>Pmax [barg]</b>	<b>Re- ignition</b>
0,93	14	0,130	No
0,93	14	0,120	No
0,93	14	0,129	No
0,93	14	0,122	No
0,93	14	N/A	No
0,93	14	N/A	No
0,93	14	N/A	No
0,93	14	0,112	No
0,93	14	0,111	No
0,93	14	0,100	No
<b>Mean:</b>	0,118	<b>Max:</b>	0,130

The measurements data for the undamaged, sandblasted and rusted gap surface examined in the PCFA are from (Opsvik 2010)

#### New / undamaged flame paths

Date: 25.07.2009

Yi [mm]	Zi [mm]	Pmax [barg]	Re- ignition	Remarks
0,95	14,0	0,116	No	
0,95	14,0	0,124	No	
0,95	14,0	0,131	No	
0,95	14,0	0,126	No	
0,95	14,0	0,131	No	

0,95	14,0	0,131	No			
0,95	14,0	0,124	No			
0,95	14,0	0,131	No			
0,95	14,0	0,129	No			
0,95	14,0	0,124	No			
0,95	14,0	0,136	No	<b>Mean:</b>	<b>0,128</b>	<b>max 0,136</b>
0,96	14,0	0,139	No			
0,96	14,0	0,139	Yes			
0,96	14,0	0,145	No	<b>Mean:</b>	<b>0,141</b>	<b>max 0,145</b>
0,97	14,0	0,114	Yes			
0,97	14,0	0,118	No	<b>Mean:</b>	<b>0,116</b>	<b>max 0,118</b>
0,98	14,0	0,124	No	<b>Mean:</b>	<b>0,124</b>	<b>max 0,124</b>
0,99	14,0	0,103	No	<b>Mean:</b>	<b>0,103</b>	<b>max 0,103</b>
1,00	14,0	0,108	Yes			
1,00	14,0	0,116	No	<b>Mean:</b>	<b>0,112</b>	<b>max 0,116</b>
1,01	14,0	0,108	Yes			
1,01	14,0	0,109	Yes			
1,01	14,0	0,111	Yes			
1,01	14,0	0,104	Yes			
1,01	14,0	0,113	Yes			
1,01	14,0	0,116	Yes			
1,01	14,0	0,108	Yes			
1,01	14,0	0,111	Yes			
1,01	14,0	0,111	Yes			
1,01	14,0	0,111	Yes	<b>Mean:</b>	<b>0,110</b>	<b>max 0,116</b>

**Abs.max 0,145**

### Corroded flame paths

Date: 12-18.08.2009

Yi [mm]	Zi [mm]	Pmax [barg]	Re-ignition	Remarks
0,95	14,0	0,141	No	superfluous measurement
0,96	14,0	0,135	No	superfluous measurement
0,97	14,0	0,126	No	superfluous measurement
1,07	14,0	0,109	No	
1,07	14,0	0,103	No	
1,07	14,0	0,103	No	
1,07	14,0	0,093	No	
1,07	14,0	0,101	No	
1,07	14,0	0,095	No	
1,07	14,0	0,098	No	
1,07	14,0	0,101	No	
1,07	14,0	0,101	No	
1,07	14,0	0,094	No	<b>Mean: 0,100 max 0,109</b>
1,08	14,0	0,113	Yes	
1,08	14,0	0,093	Yes	
1,08	14,0	0,113	Yes	

1,08	14,0	0,101	Yes		
1,08	14,0	0,101	Yes		
1,08	14,0	0,106	Yes		
1,08	14,0	~	Yes		
1,08	14,0	0,103	Yes		
1,08	14,0	0,104	Yes		
1,08	14,0	0,106	Yes	<b>Mean: 0,104</b>	<b>max 0,113</b>
1,09	14,0	0,103	Yes		
1,09	14,0	0,101	Yes		
1,09	14,0	0,101	Yes		
1,09	14,0	0,094	Yes		
1,09	14,0	0,103	Yes		
1,09	14,0	0,103	Yes		
1,09	14,0	0,108	Yes		
1,09	14,0	0,101	Yes		
1,09	14,0	0,104	Yes		
1,09	14,0	0,095	Yes	<b>Mean: 0,101</b>	<b>max 0,108</b>

**Abs.max 0,113**

### Sand blasted flame paths

Date: 16-17.09.2009

Yi [mm]	Zi [mm]	Pmax [barg]	Re- ignition	Remarks
0,91	14,0	0,136	No	
0,91	14,0	0,157	No	
0,91	14,0	0,141	No	
0,91	14,0	0,146	No	
0,91	14,0	0,136	No	
0,91	14,0	0,139	No	
0,91	14,0	0,136	No	
0,91	14,0	0,141	No	
0,91	14,0	0,157	No	
0,91	14,0	0,149	No	<b>Mean: 0,144</b> <b>max 0,157</b>
0,92	14,0	0,149	Yes	<b>Mean: 0,149</b> <b>max 0,149</b>
0,93	14,0	0,154	Yes	<b>Mean: 0,154</b> <b>max 0,154</b>
0,94	14,0	0,149	No	
0,94	14,0	0,147	No	
0,94	14,0	0,134	Yes	<b>Mean: 0,143</b> <b>max 0,149</b>
0,95	14,0	0,126	No	
0,95	14,0	0,149	Yes	<b>Mean: 0,138</b> <b>max 0,149</b>
0,96	14,0	0,144	Yes	
0,96	14,0	0,144	No	<b>Mean: 0,144</b> <b>max 0,144</b>
0,97	14,0	0,134	Yes	
0,97	14,0	0,126	Yes	
0,97	14,0	0,118	Yes	
0,97	14,0	0,135	Yes	

0,97	14,0	0,123	Yes		
0,97	14,0	0,123	Yes		
0,97	14,0	0,118	Yes		
0,97	14,0	0,118	Yes		
0,97	14,0	0,126	Yes		
0,97	14,0	0,131	Yes	<b>Mean:</b>	<b>0,125</b>
				<b>max</b>	<b>0,135</b>

---

**Abs.max 0,157**

## **Appendix D – Surface roughness measurements**

Report from AGR EmiTeam is attached at the next pages. In addition to the surface roughness measurements performed by AGR, surface roughness measurements were performed at Prototech.

# TEKNIŠK RAPPORT TECHNICAL REPORT



Kunde/Client		Kunde ordren/Client o. No.	IIN3331	Rapport nr /Report No.	AGR-33759-1	Rev.
Adresse/Address		Undersøkelsessted/Test site <b>Straume</b>		Side nr/Page No. <b>1 av/of 1</b>		
Postnummer/Post No.	Poststed/Place	Tegnings nr/Drawing No. --		Antall vedlegg/No. of appendixes <b>6</b>		
Kontaktperson/Supervisor <b>Harald Opsvik</b>				Provedato/Date of test <b>29.09.2009 - 30.09.2009</b>		
Inspeksjon av/Inspection of  <b>Surface roughness measurement.</b>						
Prosedyre/Procedure --		Aksept standard/Accept standard --		Omfang/Extent <b>See appendix</b>	Materiale/Material <b>C/S</b>	
Tilleggsopplysninger/Added information  <b>Utstyr: Mitutoyo Surftest SJ-400</b> <b>Last calibration 22.04.2009</b>						
Anmerkinger/Comments Resultat/Results <b>Surface roughness measurement carried out on:</b>  - <b>8 pcs circular flanges.</b> <b>F1 to F8.</b>  - <b>8 pcs metal bracets.</b> <b>B1 to B8.</b>  <b>For controll areas and measuring result see appendix.</b>						
<b>AGR EmiTeam AS</b>						
Dato/Date	Operatør/Operator	Forfatter/Writer	Dato/Date	Rapport godkjent/Report approved		
01.10.2009	<b>Roy Anders Nilsen</b>	<b>Nilsen, Roy-Anders Bø</b>	01.10.2009			

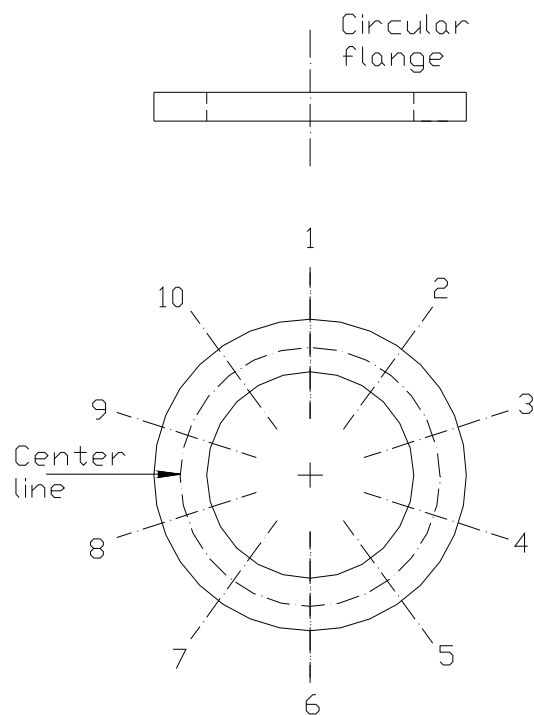


# Inspection report – Surface roughness

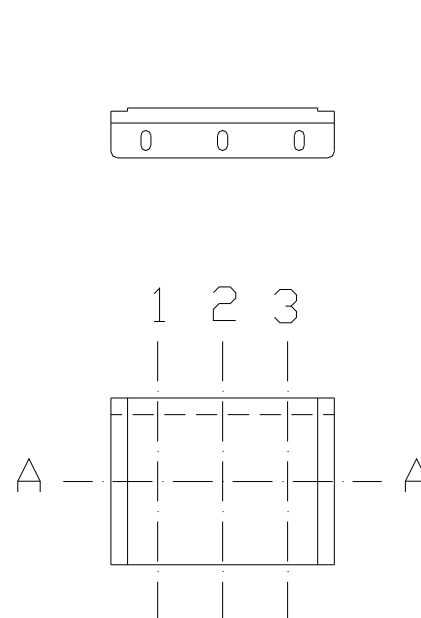
From (Opsvik 2010)

## Scope of inspection

To different types of geometries has been examined. A circular shaped flange and a rectangular metal slit. An inspection program has been described. On the circular flange there have been carried out measurements every  $36^\circ$  as indicated at the figure below. On the metal bracket there where carried out measurements in the three positions indicated below. On the flange the measurements where carried out in the middle but on the bracket the measurements where made along the A-A line. A total of four flange pairs and four brackets where examined. The measurements results are enclosed in the matrixes in chapter 5, Appendix.



Positions examined during roughness measurement on gap surfaces in the PCFA



Positions examined during roughness measurement on gap surfaces in the PRSA

## General theory

Surface finish is, by definition, the allowable deviation from a perfectly flat surface that is made by e.g. some manufacturing process, corrosion or mechanical wear. Whenever any process is used to manufacture a part, there will be some roughness on the surface.

The science of metrology – the study of surface finish/texture/etc. goes into a depth with statistical analysis and complex calculus. This entire math is included in the analyzer and the appurtenant software. Surface texture is generally broken up into three components upon analysis: roughness, waviness, and form. Roughness is generally the marks made on a surface by the machining tool, waviness is the result of the distance between the cutting tool and the work piece changing and finally the form errors arise because the machine tool's ways are not straight or are worn. All three surface finish components exist simultaneously, they just overlap one another. Often each component is examined separately, so the assumption is made that (a correct one, in most cases) roughness has a shorter wavelength than waviness, which in turn has a shorter wavelength than form.

When analyzing surface finish, there are a plenty of different parameters in existence (all in recognized standards) and many more that have been developed for special products and circumstances. Many of these parameters are either redundant or just plain unnecessary. The parameter used for general surface roughness in this report is the Ra. It measures average roughness by comparing all the peaks and valleys to the mean line, and then averaging them all over the entire cutoff length. The cutoff length is the length that the stylus is dragged across the surface; a longer cutoff length will give a more average value, and a shorter cutoff length might give a less accurate result over a shorter stretch of surface.

The parameter most widely used in Europe is Rz, or mean roughness depth. The Rz ISO standard is also called “Ten Point Average Roughness”. It averages the height of the five highest peaks and the depth of the five lowest valleys over the measuring length, using an unfiltered profile. The Rz DIN standard averages the highest point and lowest point over five cutoffs. The newer Japanese standard (JIS) measures the same points, but filters (slightly smoothes) the raw data before creating a profile. In this report the reported values are in accordance with the Rz ISO Standard.

# Measurement equipment

The measurements have been carried out with a Mitutoyo SJ-400. The testing equipment works as follows: a stylus is dragged across a surface, and this will create a profile of the surface. To prevent deflection of the tip when it encounters the tiny bumps on the surface, the stylus on the Mitutoyo SJ-400 is diamond tipped. The surface testers have been calibrated before being used - and periodically thereafter. Its reading is compared to a known value, and adjusted until the tester displays the same reading as the reference specimen.

Apparatus:	Mitutoyo SJ-400
Cut off length	0,8 mm
Calibration specimen (Ra value)	2,95 $\mu$ m
Stylus tip material	Diamond tipped
Stylus tip radius	5 $\mu$ m
Downward force at stylus	4 mN



**Mitutoyo SJ-400 - Apparatus used to measure surface roughness**

## Summary of results

Arithmetical mean values of the Ra and the Rz values of the different work pieces are listed below in table 4.1. The single point from each work piece is listed below.

<b>Id. Number</b>	<b>Geometry</b>	<b>Condition</b>	<b>Ra (<math>\mu\text{m}</math>)</b>	<b>Rz (<math>\mu\text{m}</math>)</b>	<b>Remarks</b>
F1	Circular flange	Sand blasted	11.4	63.7	
F2	Circular flange	Sand blasted	12.2	66.3	
F3	Circular flange	Undamaged	0.2	2.0	
F4	Circular flange	Undamaged	0.2	1.8	
F5	Circular flange	Corroded	7.4	36.1	
F6	Circular flange	Corroded	4.1	22.4	
F7	Circular flange	Needle scaled	5.9	29.1	
F8	Circular flange	Needle scaled	5.9	28.4	
B1	Metal bracket	Sand blasted	12.3	65.5	
B2	Metal bracket	Sand blasted	13.1	76.9	
B3	Metal bracket	Sand blasted	11.6	61.0	
B4	Metal bracket	Sand blasted	13.0	63.4	
B5	Metal bracket	Sand blasted	13.4	69.6	
B6	Metal bracket	Sand blasted	11.2	59.2	
B7	Metal bracket	Needle scaled	8.6	39.7	
B8	Metal bracket	Needle scaled	7.3	39.0	

**Measurement results - surface roughness**

Single point measurements:

d. Nr.	1		2		3		4		5		6		7		8		9		10		Mean value	
	Ra	Rz	Ra	Rz	Ra	Rz	Ra	Rz	Ra	Rz	Ra	Rz	Ra	Rz	Ra	Rz	Ra	Rz	Ra	Rz	Ra	Rz
F1	10,9	65,2	13,6	67,8	13,3	72,0	8,6	49,4	10,1	57,3	11,2	62,5	10,8	62,3	11,2	60,0	11,8	71,0	12,5	69,9	11,4	63,7
F2	12,4	61,3	13,9	73,6	11,8	65,9	10,9	64,6	12,8	71,8	11,6	68,4	11,5	56,9	12,8	74,0	11,2	50,4	13,0	75,9	12,2	66,3
F3	0,2	2,1	0,2	1,7	0,2	1,8	0,2	1,9	0,2	2,1	0,2	1,9	0,2	2,0	0,2	2,3	0,2	2,0	0,2	1,9	0,2	2,0
F4	0,2	1,9	0,2	2,0	0,2	1,7	0,2	1,9	0,2	1,8	0,2	1,8	0,2	1,7	0,2	1,7	0,2	1,7	0,2	2,1	0,2	1,8
F5	6,7	31,9	7,9	35,6	8,4	39,7	5,7	33,6	6,4	31,2	7,4	35,4	6,8	35,5	6,9	31,8	9,2	45,1	8,5	41,0	7,4	36,1
F6	3,6	19,6	2,6	17,1	3,7	23,2	7,8	37,8	3,4	18,7	5,9	29,0	4,0	21,6	2,5	15,1	4,3	22,0	3,2	19,7	4,1	22,4
F7	5,0	20,1	7,9	34,6	7,0	31,1	8,1	29,8	4,8	26,5	4,5	20,6	5,3	29,1	7,7	40,2	5,0	27,6	8,3	31,0	5,9	29,1
F8	5,4	26,5	4,3	23,3	5,3	25,3	5,5	27,5	5,0	26,7	8,1	37,4	6,1	24,8	8,6	36,5	4,7	25,4	6,0	30,1	5,9	28,4

Id. Nr.	1		2		3		Mean value	
	Ra	Rz	Ra	Rz	Ra	Rz	Ra	Rz
B1	9,64	42,30	8,95	41,90	7,20	34,90	8,60	39,70
B2	8,76	46,70	6,73	40,30	6,30	30,00	7,26	39,00
B3	11,21	60,50	12,80	65,90	13,02	70,10	12,34	65,50
B4	13,97	73,90	12,07	80,60	13,21	76,20	13,08	76,90
B5	12,31	61,20	10,86	61,40	11,47	60,30	11,55	60,97
B6	13,85	65,50	11,24	54,70	13,95	70,10	13,01	63,43
B7	10,86	60,70	17,33	77,80	12,01	70,40	13,40	69,63
B8	9,99	52,70	12,20	63,60	11,41	61,30	11,20	59,20



AGR EmiTeam AS  
Postboks 163  
5342 Stramue  
Norge

Er referens

Vår referens  
Per Kedvall

Datum  
2009-04-22

Reparation & funktionskontroll:

Följande ytjämnhetsmätare har genomgått reparation:  
SJ-401 178-956-3D s/n:510340

Därefter har en funktionskontroll genomförts och ytjämnhetsmätaren fungerar OK.

Med vänlig hälsning  
Mitutoyo Scandinavia AB



Per Kedvall  
*Tekniskchef/Kvalitetschef*

**Mitutoyo Scandinavia AB**  
Box 712 \* 194 27 Upplands Väsby  
Tel 08-594 10 974 \* Fax 08-590 924 10  
Org.nr 556210-1138  
E-post: [per.kedvall@mitutoyo.se](mailto:per.kedvall@mitutoyo.se)



SS-EN ISO 9001

## Appendix E – Certificates / Specifications

Certificate	Description
E1	Calibration Gas (Propane and Nitrogen)
E2	Test Gas (Propane)
E3	Pressure Transducers
E4	Pressure Transducers
E5	Charge Amplifier

## E.1 Calibration gas



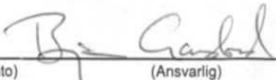
# Sertifikat

Side 1 av 1

Kunde: UIB Institutt for Fysikk og Teknologi	Sertifikat nr.: 4325266-01-K-344061HG	Flaske vannvolum (l): 10	Flaskenummer: K-344061HG	
Kunde referanse: Oddgeir Kleppa	Kvalitetsklasse: 2	Anbefalt trykkregulator: Ultraserien (messing)	Flaskeventilgjenger: DIN 477 No. 1	Fylletrykk v/20°C (bar g): 150

Komponenter	Bestilt sammensetning mol %	Sertifisert sammensetning mol %	Usikkerhet % relativ
Propan Nitrogen	5 Rest	4,90 Rest	2

100 % LEL i luft (vol %):	Konfidens intervall: 95 % (k=2)	Sporbarhet klasse 1: SI-enhet for masse	Kondensasjonstemp. ved fylletrykk (°C) < - 20	Stabilitetstid (måned): 36
Laveste anbefalte brukstrykk (bar g): 5	Anbefalt lager og brukstemp. (°C) 20	Spesielle opplysninger:		
For HMS datablad, se vår hjemmeside <a href="http://www.yarapraxair.com">www.yarapraxair.com</a>		Ved mistanke om utkondensering må flasken lagres horisontalt ved romtemperatur i 14 dager, eller rulles horisontalt i 8 timer ved > 63 omdreininger/min før bruk.		

Rjukan 21/2-08   
(Produksjonssted) (Dato) (Ansvarlig)

Yara Praxair AS Fnr./Reg.No. 945 772 042

Postadr.  
P.O.Box 23, Haugenstua  
N-0915 OSLO

Telefon  
+47 04 27 7

Telefax:  
+47 24 15 64 29



## E.2 Test gas



2

### Salgsspesifikasjon

Dok.id.nr.: SS141  
Gyldig fra: 2004-06-30  
Revisjon: 05  
I alt 2 sider

#### Propan 3.5

##### 1. Spesifikasjon:

Propan(C <sub>3</sub> H <sub>8</sub> )	>	99,95 %
Vann (H <sub>2</sub> O)	<	10 ppm
Oksygen (O <sub>2</sub> )	<	10 ppm
Nitrogen (N <sub>2</sub> )	<	50 ppm
Karbondioksid (CO <sub>2</sub> )	<	20 ppm
Andre hydrokarboner (C <sub>n</sub> H <sub>m</sub> )	<	400 ppm

##### 2. Flasketyper

<u>Størrelse</u>	<u>Innhold</u>	<u>Varenummer</u>
10 liter	4,2 kg	500317
50 liter	21,0 kg	500318

Se også HMS-datablad på vår hjemmeside [www.yara.no](http://www.yara.no)  
(Gass og Kjemikalier -> Produkter og tjenester -> HMS-datablad -> "produktnavn")

Yara Industrial AS forbeholder seg retten til å endre spesifikasjonene uten varsel

**Postadresse**  
Yara Industrial AS  
Postboks 23 Haugenstua  
N-0915 Oslo

**Telefon**  
24 15 76 00

**Telefax**  
24 15 75 50

**Internett**  
[www.yara.no](http://www.yara.no)

## E.3 Pressure transducers



# Kalibrierschein DRUCK Calibration Certificate PRESSURE

Type **701A** Serial No. **1740583**

<b>Kalibriert durch</b> Calibrated by	<b>Datum</b> Date
U. Köhler	20.10.2008

Referenzgeräte Reference Equipment	Typ Type	Serien-Nr. Serial No.
Gebrauchsnormal Working Standard	Kistler 7005-350	634580
Ladungsverstärker Charge Amplifier	Kistler 5011A	572386
Ladungskalibrator Charge Calibrator	Kistler 5395A	530633

<b>Umgebungstemperatur</b> Ambient Temperature	<b>Relative Feuchte</b> Relative Humidity
°C	%
23	41

## Messergebnisse Results of Measurement

Kalibrierter Bereich Calibrated Range	Empfindlichkeit Sensitivity	Linearität Linearity
bar	pC / bar	≤ ± %FSO
0 ... 250	-80,60	0,11
0 ... 25	-79,49	0,04
0 ... 2,5	-79,22	0,04

**Messverfahren**      **Kontinuierliche Kalibrierung, Vergleichsverfahren**  
Measurement Procedure      Continuous Calibration, Comparison Method

## Bestätigung Confirmation

Die Geräte halten die Herstellertoleranzen gemäss Spezifikationen der Datenblätter ein. Wir bestätigen, dass das oben identifizierte Gerät nach den vorgeschriebenen Verfahren geprüft wurde. Alle Messmittel sind auf nationale Normale rückverfolgbar. Kistler betreibt die SCS (Swiss Calibration Service) Kalibrierstelle Nr. 049, akkreditiert nach ISO 17025. Das Kistler Qualitätsmanagement System ist nach ISO 9001 zertifiziert.

The equipment meets the manufacturing tolerances according to the specification data sheets. We confirm that the device identified above was tested by the prescribed procedures. All measuring devices are traceable to national standards. The SCS (Swiss Calibration Service) Calibration Laboratory No. 049 is operated by Kistler and accredited per ISO 17025. The Kistler Quality Management System is certified per ISO 9001.

**Kistler Instrumente AG**  
Eulachstrasse 22      Tel. +41 52 224 11 11      ZKB Winterthur BC 732      IBAN: CH67 0070 0113 2003 7462 8  
PO Box      Fax +41 52 224 14 14      Swift: ZKBKCHZZ80A      VAT: 229 713  
CH-8408 Wintherthur      info@kistler.com      Account: 1132-0374.628      ISO 9001 certified

[www.kistler.com](http://www.kistler.com)

Seite page 1 / 1

## E.4 Pressure transducers

**KISTLER**  
measure. analyze. innovate.

### Kalibrierschein DRUCK Calibration Certificate PRESSURE

Type **701A**

Serial No. **1740584**

<b>Kalibriert durch</b> Calibrated by	<b>Datum</b> Date		
U. Köhler	20.10.2008		
<b>Referenzgeräte</b> Reference Equipment	<b>Typ</b> Type	<b>Serien-Nr.</b> Serial No.	
<b>Gebrauchsnorm</b> Working Standard	Kistler 7005-350	634580	
<b>Ladungsverstärker</b> Charge Amplifier	Kistler 5011A	572386	
<b>Ladungskalibrator</b> Charge Calibrator	Kistler 5395A	530633	
<b>Umgebungstemperatur</b> Ambient Temperature	<b>Relative Feuchte</b> Relative Humidity		
°C	%		
23	41		

### Messergebnisse Results of Measurement

<b>Kalibrierter Bereich</b> Calibrated Range	<b>Empfindlichkeit</b> Sensitivity	<b>Linearität</b> Linearity
bar	pC / bar	≤ ± %FSO
0 ... 250	-82,92	0,37
0 ... 25	-82,79	0,08
0 ... 2,5	-82,61	0,06

**Messverfahren**      **Kontinuierliche Kalibrierung, Vergleichsverfahren**  
Measurement Procedure      Continuous Calibration, Comparison Method

### Bestätigung Confirmation

Die Geräte halten die Herstellertoleranzen gemäss Spezifikationen der Datenblätter ein. Wir bestätigen, dass das oben identifizierte Gerät nach den vorgeschriebenen Verfahren geprüft wurde. Alle Messmittel sind auf nationale Normale rückverfolgbar. Kistler betreibt die SCS (Swiss Calibration Service) Kalibrierstelle Nr. 049, akkreditiert nach ISO 17025. Das Kistler Qualitätsmanagement System ist nach ISO 9001 zertifiziert.

The equipment meets the manufacturing tolerances according to the specification data sheets. We confirm that the device identified above was tested by the prescribed procedures. All measuring devices are traceable to national standards. The SCS (Swiss Calibration Service) Calibration Laboratory No. 049 is operated by Kistler and accredited per ISO 17025. The Kistler Quality Management System is certified per ISO 9001.

**Kistler Instrumente AG**  
Eulachstrasse 22  
PO Box  
CH-8408 Wintherthur

Tel. +41 52 224 11 11  
Fax +41 52 224 14 14  
info@kistler.com

ZKB Winterthur BC 732  
Swift: ZKBKCHZZ80A  
Account: 1132-0374.628

IBAN: CH67 0070 0113 2003 7462 8  
VAT: 229 713  
ISO 9001 certified

www.kistler.com

Seite page 1 / 1

## E.5 Charge amplifier

# KISTLER

measure. analyze. innovate.

## Kalibrierschein Ladung Calibration Certificate Charge

Type 5073A221 Serial No. 1584688

<b>Kalibriert durch</b> Calibrated by	<b>Datum</b> Date	
S. Mancikilar	19.10.2007	
<b>Referenzgeräte</b> Reference Equipment	<b>Typ</b> Type	<b>Serien-Nr.</b> Serial-No.
<b>Ladungskalibrator</b> Charge Calibrator	5395A1	530626
<b>Umgebungstemperatur</b> Ambient Temperature	<b>Relative Feuchte</b> Relative Humidity	
°C	%	
24	40	

<b>Geräteinstellungen</b> Instrument settings	
<b>LP Filter</b> LP Filter	<b>Ausgangsbereich FS</b> Output Range FS
kHz	V
off	± 10

### Messergebnisse Results of Measurement

<b>Kanal</b> Channel		<b>1</b>	<b>2</b>
<b>Nullpunktabweichung</b> Offset Voltage	mV	-6,1	4,9
<b>Reset-Operate-Sprung</b> Reset-Operate Step	pC	0,35	-0,61
<b>Drift (Bereich = 100 pC)</b> Drift (Range = 100 pC)	pC/s	-0,01	-0,02
<b>Bereich</b> Range	<b>Abweichung</b> Deviation		
pC 100	%	0,1	0,1
pC 10000	%	0,0	0,0
pC 10085	%	-0,2	-0,2
pC 100000	%	0,2	0,2

### Bestätigung Confirmation

Wir bestätigen, dass das oben identifizierte Gerät nach den vorgeschriebenen Verfahren geprüft wurde. Alle Messmittel sind auf nationale Normale rückverfolgbar. Kistler betreibt die SCS (Swiss Calibration Service) Kalibrierstelle Nr. 049, akkreditiert nach ISO 17025. Das Kistler Qualitätsmanagement System ist nach ISO 9001 zertifiziert.

We confirm that the device identified above was tested by the prescribed procedures. All measuring devices are traceable to national standards, the SCS (Swiss Calibration Service) Calibration Laboratory No. 049 is operated by Kistler and accredited per ISO 17025. The Kistler Quality Management System is certified per ISO 9001.

#### Kistler Instrumente AG

Eulachstrasse 22  
PO Box  
CH-8408 Winterthur

Tel. +41 52 224 11 11  
Fax +41 52 224 14 14  
info@kistler.com

ZKB Winterthur BC 732  
Swift: ZKBKCHZ80A  
Account: 1132-0374.628

IBAN: CH67 0070 0113 2003 7462 8  
VAT: 229 713  
ISO 9001 certified

www.kistler.com

## References

- Kalvatn, I. (2009). EXPERIMENTAL INVESTIGATION OF THE OPTICAL MEASUREMENT METHOD FOR DETECTING DUST AND GAS FLAMES IN A FLAME ACCELERATION TUBE. Department of physics and technology. Bergen, University of Bergen. **Master Sc.**
- Opsvik, H. E. Z. (2010). Experimental investigation of the influence of mechanical and corrosion damage of gap surfaces on the efficiency of flame gaps in flameproof apparatus. Department of physics and technology. Bergen, University of Bergen. **Master Sc.**